

University of Nottingham
UK | CHINA | MALAYSIA

Novel Biocatalytic Routes for the Synthesis of Small Cyclic Chiral Molecules

Eimear Hegarty

Supervisor:
Prof. Francesca Paradisi

A thesis submitted to the University of Nottingham for the degree of Doctor of Philosophy in Organic Chemistry

September 2019

Table of Contents

Abstract……1

Abbreviations……...2

Chapter 1 Introduction……6

1.1 Enzymes as biocatalysts……9

1.2 Key enzymes in biocatalysis……..9

1.2.1 Aminotransferases……7

1.2.2 Acyltransferases……13

1.2.3 Oxidoreductases……16

1.3 Improving biocatalysts through protein engineering……19

1.4 Enzyme immobilisation……22

1.5 Flow biocatalysis……25

1.6 Small cyclic molecules: the challenges……..……27

Aims & Objectives……..…...…….37

Chapter 2 Materials & Methods……...39

2.1 Reagents……40

2.2 Bacterial strains……40

2.3 Plasmids……41

2.4 Culture medium……42

2.5 General procedures……..42

2.5.1 Preparation of chemically competent cells……42

2.5.2 Preparation of electrocompetent cells……43

2.5.3 Transformation of chemically competent cells……...43

2.5.4 Protein quantification……..44

2.5.5 SDS-PAGE……..45

2.6 Characterisation of *He*WT mutants……...45

2.6.1 Expression and purification of *He*WT and mutant variants...45

2.6.2 Enzymatic activity assay……..…..47

2.6.3 pH effect on enzyme activity and stability……47

2.6.4 Temperature effect on enzyme activity and stability……..48

2.6.5 10 mM scale biotransformations……...48

2.6.6 Kinetic parameters……..49

2.6.7 Evaluation of enantioselectivity……49

2.7 Synthesis of small cyclic molecules……50
2.7.1 Expression and purification of KRED1-*Pglu*……..…50
2.7.2 KRED1-*Pglu* activity assay……52
2.7.3 Expression and purification of *Bm*GDH……..……...52
2.7.4 BnGDH activity assay……..…….53
2.7.5 10 mM scale biotransformations for the preparation of small cyclic alcohols……..53
2.7.6 Expression and purification of *Ms*AcT……..……..54
2.7.7 *Ms*AcT activity assay……..……...56
2.7.8 20 mM scale biotransformations for the preparation of small cyclic amides……....56
2.8 Preparation of biocatalysts for application in continuous flow…56
2.8.1 Activation of enzyme carriers……56
2.8.2 Immobilisation of biocatalysts……..……57
2.8.3 Preparation of DEX50……..……57
2.8.4 Determination of the stabilisation of the quaternary structure of multimeric enzymes…….……58
2.8.5 Surface coating with DEX50……..…..58
2.8.6 Functionalisation of Sepharose CL-6B……...58
2.8.7 Activity of immobilised *He*WT…….....58
2.8.8 Activity of immobilised *Ms*AcT…….……...58
2.8.9 Continuous flow biotransfrormations…….…….59
Chapter 3 Characterisation of *Halomonas elongata* ω -transaminse (*He*WT) mutants……62
3.1 Introduction……..……..63
3.2 Characterisation of *He*WT mutants evolved towards substituted acetophenones……..…63
3.3 Characterisation of *He*WT mutants evolved towards small cyclic ketones……..…73
3.4 Conclusions……78
Chapter 4 The Synthesis of Small Cyclic Molecules: Alcohols, Amines & Amides……81
4.1 Introduction……82
4.2 Results and discussion……83

4.2.1 Exploring the substrate scope of KRED1-*Pglu*……...83
4.2.2 Pseudomonas fluorescens ω -transaminse as an alternative to *He*WT for the synthesis of small cyclic chiral amines……..…86
4.2.3 Biocatalytic performance of *He*WT at high substrate loadings……..……91
4.2.4 Immobilisation of HeWT……..93
4.2.5 Flow synthesis of small cyclic amines……..94
4.2.6 Acyltransferase substrate scope evaluation……96
4.2.7 Acyltransferase immobilisation and optimisation……99
4.2.8 Flow synthesis of small cyclic amides……..…..104
4.3 Conclusion……106
Chapter 5 The Development of a Biocatalytic Cascade for the Synthesis of Small Cyclic Amides……110
5.1 Introduction……..111
5.2 Results and discussion……..112
5.2.1 One-pot cascade in batch……112
5.2.2 Optimisation of a stepwise cascade in continuous flow..…116
5.2.3 Immobilisation of *He*WT on epoxy activated agarose…….119
5.2.4 Continuous flow synthesis of a model small cyclic amide..121
5.3 Conclusions……122
Chapter 6 Conclusions & future outlook……..125
Appendix Exploring the Production of Enzymes of Industrial Interest in *Haloferax volcanii*…..…129
Introduction……130
1.1 The discovery of Archaea……..…….130
1.2 Characterisation of Archaea…….…131
1.3 *Haloferax vlocanii*…….....132
1.4 Overexpression and purification of halophilic proteins in *Haloferax volcanii*……..……..134
1.5 Common expression systems in the biotech industry…….136
1.6 The application of *Haloferax volcanii* as an alternative expression system for enzymes of industrial interest……...139
Aims & Objectives……..…140
Material & Methods……..……..141

2.1 Reagents, strains & culture conditions……..141
2.2 Construction of the pTA963-*spuC* expression vector…..…...141
2.3 Transformation of *Haloferax volcanii* H1895……..……..142
2.4 Expression of *He*WT in *Haloferax volcanii* H1895……..…….142
2.5 Purification of *He*WT from *Haloferax volcanii* H1895……..143
2.6 Synthetic gene design and syntheses……..…….144
2.7 Construction of the pTA963-HLADH expression vector…..…144
2.8 Expression of HLADH in *Haloferax volcanii* H1895 and H1325……..……..144
2.9 Alcohol Dehydrogenase activity assay……..……145
2.10 Construction of the pTA963-*spuC* expression vector……...146
2.11 Expression of *He*WT in *Haloferax volcanii* H185 & H1325..147
2.12 Purification of *He*WT from *Haloferax volcanii*……...147
Results & Discussion……149
4.1 Expression of *He*WT in *Haloferax volcanii*……..……..149
4.2 Codon optimization of genes……..……153
4.3 Construction of the pTA963-HLADH expression vector…..…154
4.4 Construction of the pTA963-*spuC-Opt* expression vector….155
4.5 Expression of synthetic genes in *Haloferax volcanii*……..….156
Conclusions……159
Acknowledgements…… 164

Abstract

The catalytical asymmetric reduction of small cyclic prochiral ketones with the formation of optically pure alcohols and amines is a fundamentally important reaction in synthetic organic chemistry. However, achieving selectivity using traditional synthetic methodology is challenging, particularly when the prochiral ketone has minimal discrimination between the two side chains. In light of this, new biocatalytic strategies for the enantioselective preparation of small cyclic molecules starting from readily available and inexpensive prochiral ketones was explored.

To this aim, initial efforts focussed on the use of an established and highly efficient solid phase screening methodology for the screening of aminotransferase (ATs) variants. The screen was successfully applied to an AT from *Halomonas elongata* (*He*WT*)*, evolved through rounds of random mutagenesis towards a series of 4 small cyclic ketones, which lead to the identification of a variant with modest improvements in activity (ca. 2-fold) (Chapter 3). The substrate scope of a ketoreductase from *Pichia glucozyma* (KRED1-*Pglu*) and a structurally different AT from *Pseudomonas fluorescens* (*Pf*TA) was subsequently probed using the same panel of small cyclic ketones. Under the reaction conditions tested, KRED1-*Pglu* failed to produce the target alcohols with a synthetically useful optical purity, while *He*WT presented itself as a much more robust biocatalyst for the synthesis of the target amines, with respect to *Pf*TA. To increase the complexity of the system, the development of a tandem enzymatic reaction, combing *He*WT with a second biocatalyst, an acyltransferase from *Mycobacterium smegmatis* (*Ms*AcT), for the synthesis of optically active amides was explored (Chapter 4). Finally, a multi-enzymatic cascade in continuous flow, featuring the immobilised *He*WT and *Ms*AcT is presented, demonstrating a fully intensified and industrially relevant biocatalytic process for the synthesis of small cyclic chiral molecules (Chapter 5).

Abbreviations

(S)-MBA	(S)-α-methylbenzylamine
EDC	1-Ethyl-3-(3- dimethylaminopropyl)carbodiimide
ATA	Aminotransferase
Aq.	Aqueous
CDI	Carbony diimidazole
DNA	Deoxyribonucleic acid
DEX50	Dextran aldehyde (50% oxidised)
DCC	Dicyclohexylcarbodiimide
DSF	Differential scanning fluorimetry
DMS	Dimethyl sulfide
DMSO	Dimethylsulfoxide
DTT	Dithiothreitol
e.e.	Enantiomeric excess
E. caballus	*Equus caballus*
E. coli	*Escherichia coli*
EtOH	Ethanol
EtOAc	Ethyl acetate
EDTA	Ethylenediaminetetraacetic acid
FID	Flame ionisatization detector
GC	Gas chromatography
GDH	Glucose dehydrogenase
H. volcanii	*Haloferax volcanii*
HHDH	Halohydrin dehydrogenase
H. elongata	*Halomonas elongata*
*He*WT	*Halomonas elongata* ω-transaminase
HPLC	High performace liquid chromatography
HLADH	Horse liver alcohol dehydrogenase
HCl	Hydrocloric acid
IDA	Iminodiacetic acid
IPTG	Isopropyl-β-D-thiogalactopyranoside
IPA	Isopropylamine
KRED	Ketoreductase
kDa	Kilo daltons
LEH	Limonene epoxide hydrolase
LB	Lysogeny broth
MW	Molecukar weight
MWCO	Molecular weight cut off
MAO-N	Monoamine oxidase
TEMED	N,N,N',N'-Tetramethylethylenediamine
NAD+	Nicotinamide adenine dinucleotide (oxidized form)

NADH	Nicotinamide adenine dinucleotide (reduced form)
NAD(P)H	Nicotinamide adenine dinucleotide phosphate (reduced form)
ω-TA	Omega transaminse
Org.	Organic
PBR	Packed bed reactor
Pd	Palladium
KRED1-*Pglu*	*Pichia glucozyma* ketoreductase
PEG	Polyethylene glycol
PS-BZA	Polymer supported benzylamine
PCR	Polymerase chain reaction
PTM	Post translational monidication
T3P	Propylphosphonic acid anhydride
PDB	Protein data bank
*Pf*TA	*Pseudomonas fluorescens ω-transaminase*
PLP	Pyridoxal 5'-phosphate
PMP	Pyridoxamine 5'-phosphate
Rh	Rhodium
Ru	Ruthenium
SDR	Short chain dehydrogenase/reductase
SDS-PAGE	Sodium dodecyl sulfate polyacrylamide gel elecrophoresis
NaOH	Sodium hydroxide
SPS	Solid-phase screening
STY	Space time yield
SOB	Super optimal broth
TB	Terrific broth
THF	Tetrahydrofuran
TLL	*Thermomyces lanuginosus* lipase
TEA	Triethylamine
TFA	Trifluoroacetic acid
TCSM	Triple code saturation mutagesesis
TAE	Tris-acetate-EDTA
UV	Ultraviolet
WT	Wild type

Amino acids

A	Ala	Alanine
C	Cys	Cysteine
D	Asp	Aspartic acid
E	Glu	Glutamic acid
F	Phe	Phenylalanine
G	Gly	Glycine
H	His	Histidine
I	Ile	Isoleucine
K	Lys	Lysine
L	Leu	Leucine
M	Met	Methionine
N	Asn	Asparagine
P	Pro	Proline
Q	Gln	Glutamine
R	Arg	Arginine
S	Ser	Serine
T	Thr	Threonine
V	Val	Valine
W	Trp	Tryptophan
Y	Tyr	Tyrosine

Nucleotides

A	Adenine
C	Cytosine
G	Guanine
T	Thyamine
U	Uracil

Units of measure

bp	Base pair
g	Gram
mol	Mole
Da	Dalton
L	Litre
h	Hour
s	Second
min	Minute
M	Molarity
rpm	Revolutions per minute

Introduction

Introduction

1.1 Enzymes as biocatalysts

Nature is capable of synthesising a diverse range of highly functionalised and complex molecules starting from a limited set of building blocks. In all but a handful of cases these reactions are catalysed by enzymes, which mediate these transformations with unparalleled selectivity. In 1858, Louis Pasteur demonstrated the resolution of racemic tartaric acid through fermentation with a variety of microorganisms, providing the first example of modern biocatalysis.[1] In these experiments, (+)-tartaric acid was consumed much faster than (−)-tartaric acid, allowing for isolation of the latter. Towards the end of the 19th century, Emil Fischer proposed the “lock and key” model for enzyme catalysis and Buchner demonstrated that cell-free extracts were capable of catalysing fermentation processes.[2,3] Following these seminal developments, biocatalysis has emerged as one of the most promising technologies to enable the green and sustainable synthesis of a wealth of high value compounds.[4]

Today industries, in particular chemical and pharmaceutical industries are under significant pressure to adopt more environmentally benign and sustainable methods when carrying out chemical syntheses. In this context, the concept of Green Chemistry was developed in 1998 by the chemists Paul Anastas and John Warner, who defined the term green chemistry as the “utilization of a set of principles that reduces or eliminates the use or generation of chemical products”.[5] Enzyme catalysed reactions conform to these principles in many ways to the extent that biocatalysts are now being considered as an option when designing synthetic routes to target organic molecules, particularly in cases when it is important to achieve some type of selectivity whether it is stereo-, regio- or chemoselectivity. The use of biocatalysts as an alternative to chemical reagents and catalysts can also provide benefits in terms of a reduced number of synthetic steps, lower cost of goods, reduced use of harmful solvents and overall improved safety profiles.[6,7]

Together these benefits can lead to a more sustainable process with lower overall environmental impact.

Table 1| The impact of biocatalysis on the 12 green chemistry principles.[8]

Green chemistry principle	Biocatalysis
1. Prevent waste	Biocatalyisis can enable more sustainable routes to drugs, reducing the levels of waste
2. Atom economy	Biocatalysis often enables more efficient synthetic routes due to higher selectivity
3. Less hazardous synthesis	Enzymes are generally of low toxicity, replacing more toxic reagents
4. Design benign chemicals	No impact
5. Benign solvents & auxiliaries	Enzymatic reactions are often performed in water and low hazard organic solvents.
6. Design for energy efficiency	Enzymatic reactions are usually performed at or slightly above room temperature, making them energy efficient
7. Use of renewable feedstocks	Enzymes are renewable
8. Reduce derivatives	Enzymes have high selectivity (chemo-, regio-, and stereo-) typically avoiding the need for protecting groups
9. Catalysis (vs. stoichiometric)	Enzymes are catalytic
10. Design for degradation	No impact on the design of products (although enzymes are biodegradable)
11. Real-time analysis for pollution prevention	No impact
12. Inherently benign chemistry for accident prevention	Enzymatic reactions are generally performed under mild conditions, where the risk of explosions or run-away reactions is very small, making them inherently safe

Our ability to discover new biocatalysts and subsequently engineer them to expand their substrate scope or perform new reaction chemistry is rapidly increasing due to advances in technologies such as metagenomics, genome sequencing, protein engineering, directed evolution and high-throughput screening. As a result tailored biocatalysts can now be applied for the synthesis of non-natural target molecules. This is particularly true for the synthesis of chiral alcohols, amines, carboxylic acids, esters and amides for which there are now several biocatalytic systems available. In the following sections, an overview of key enzymes within the field, and particularly relevant to this thesis, is presented together with the various tools and technologies that have led to the industrial viability of biocatalytic prosses.

1.2 Key enzymes in biocatalysis

1.2.1 Aminotransferases

Aminotransaminases (ATAs) have attracted considerable attention for the production of compounds containing chiral amino groups, which are widespread in the pharmaceutical, agrochemical and fine chemical industry.[9,10] These enzymes belong to fold types I and IV of pyridoxal 5'-phosphate (PLP) dependent enzymes and catalyse the transfer of an amino group to a suitable amino acceptor.[11] Two types of PLP-dependent TAs have been identified and are grouped according to the type of substrate they convert.[12] α-TAs, for example, exclusively convert α-amino and α-keto acids**.** Of particular interest, in terms of synthetic applications, are the ω-transaminases (ω-TAs), (*R*)- or (*S*)-selective enzymes that are capable of aminating carbonyls (both aldehydes and ketones) in the absence of a neighbouring carboxylic group.

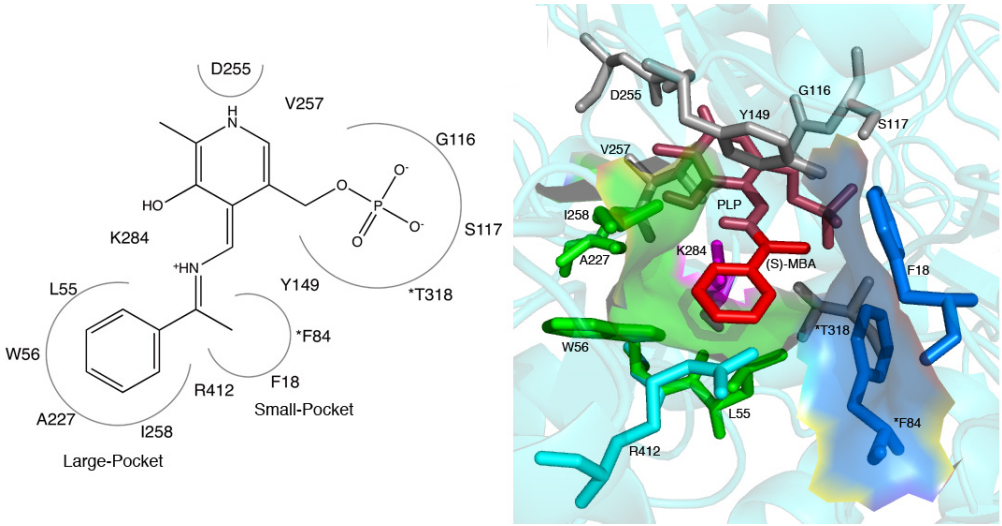
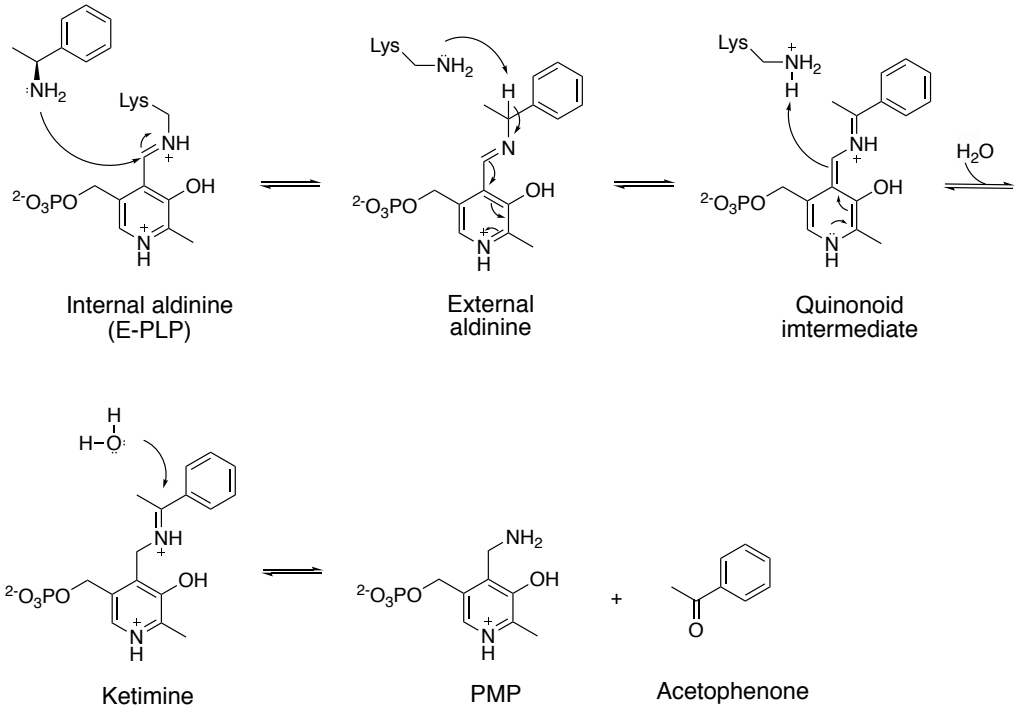


Figure 1| Representation of the *Halomoans elongata* ω-transaminase (*He*WT) catalytic active-site.

Transaminases typically follow a ping-pong reaction mechanism in which the enzyme bounces back from its intermediate form to its standard state, thereby regenerating the PLP cofactor in the process.[13] The first step of the reaction typically involves the formation of an external aldimine between the PLP cofactor and the amino donor. Formation of this aldimine adduct dramatically increases the acidity of the α-proton. The catalytic lysine residue that has been released from binding PLP acts as a base and deprotonates the acidic α-hydrogen of the external aldimine. This forms the quinonoid intermediate (Figure 1). The quinonoid is re-protonated adjacent to the heterocyclic ring to generate the ketimine intermediate. This intermediate is then hydrolysed to release PMP and the free product, thus completing the first half of the reaction in the transaminase mechanism. The second half of the reaction involves carrying out the reverse transamination on the amino acceptor substrate. The substrate is bound via a ketimine linkage, which is isomerised to the aldimine intermediate. Displacement of the aldimine linkage by lysine and hydrolyses releases the amine product and importantly, regenerates the PLP form of the cofactor (Scheme 1).

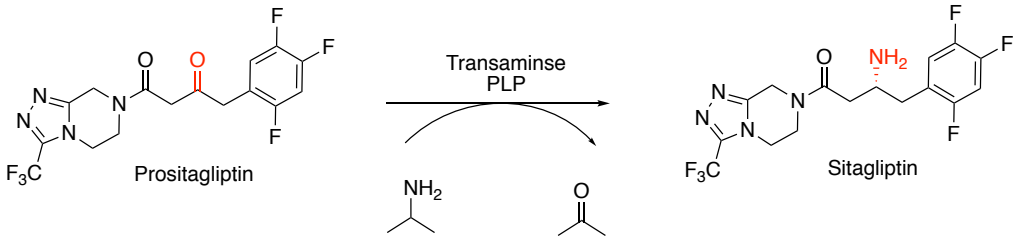


Scheme 1| First half-reaction catalysed by transaminases, where the amino donor ((*S*)-MBA) is converted into the corresponding ketone (acetophenone), while PLP is transformed to PMP.

Despite the enormous potential of TAs, the widespread application of these biocatalysts in their wild type form is hindered by a number of challenges including limited substrate specificities, substrate and product inhibition and unfavourable reaction equilibria.[14] To this aim considerable effort has been directed to addressing these challenges. While the substrate scope of TAs can be considered relatively broad, as they are capable of catalysing the amination of a broad range of aldehydes and ketones, the active site of these enzymes contain a small and large binding pocket.[15,16] Therefore wild-type enzymes are generally restricted to ketones bearing at least one small substituent.[17,18] Considerable effort has been directed towards increasing the capacity of the small binding pocket to enable these enzymes to accept ketones with two bulky substituents.

A particularly notable achievement within this context was the redesign of an (*R*)-selective ω-TA for the industrial scale synthesis of sitagliptin.[19] Starting from an enzyme that had the appropriate catalytic machinery but

lacked any activity towards the prositagliptin substrate, a weakly active transaminase for the target reaction was created by computational modelling and substrate walking. Subsequent optimization via multiple rounds of mutagenesis yielded a variant with a 25,000-fold improvement in catalytic activity. The resulting biocatalyst is now used in the final step of the synthesis of the API replacing an equivalent step in which a rhodium catalyst was used to achieve the same overall conversion.



Scheme 2| Enzymatic synthesis of sitagliptin. The biocatalytic process using an engineered transaminase affords higher overall yields and stereoselectivity while reducing total waste and manufacturing costs, compared with the previously utilized rhodium-catalysed process.

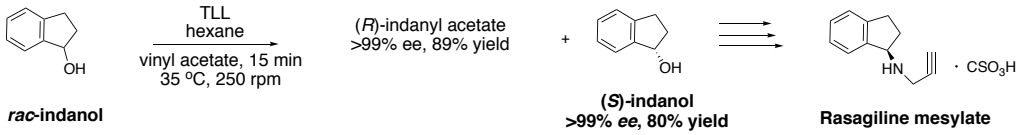
Bornscheuer and co-workers have also made significant progress in developing TAs that accept substrates with two sterically demanding substituents. They reported an (*S*)-selective ω-TA variant from *Rugeria* sp. TM1040 (3FCR) that is capable of converting bulky ketones to the corresponding chiral amines with good to excellent yields and enantiomeric excess.[20] Despite the impressive activity of the variant towards bulky substrates, modest substituent changes were not well tolerated by the mutant.

Recently, our group reported on the isolation and characterisation of an interesting ω-TA from the moderate halophile *Halomonas elongata* (*He*WT) that is able to withstand the presence of a variety of organic solvents and accommodate a broad range of substrates.[21] However, the enzyme was weakly active towards substituted acetophenones. The steric effects of the substituents were probed through a series of rationally engineered variants which led to a better understanding of the key residues in the active site, but produced only minimal improvements

in activity, which further highlight the challenges associated with developing TAs with broad activity.[22]

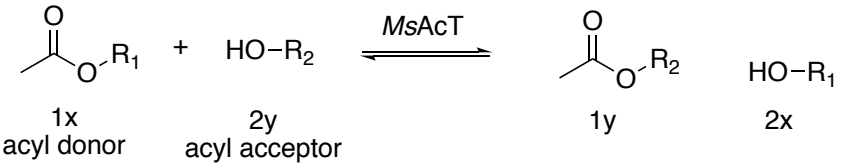
1.2.2 Acyltransferases

In addition to transamination, transesterification and transamidation are key reactions in many biotechnological applications. Esterases and lipases, for example are extensively used on an industrial scale because they exhibit board substrate scopes.[23,24] In addition, a number of lipases are available that catalyse acyl transfer reactions of a diverse range of substrates.[25] For example, an immobilised lipase from *Thermomyces lanuginosus* (TLL) was found to be an efficient biocatalyst for the kinetic resolution of *rac*-indanol in the chemoenzymatic synthesis of Rasagiline mesylate (Scheme 3), which is used in the treatment of Parkinson disease.[26] This reaction is performed in an organic solvent and in the absence of water to circumvent hydrolysis of the acyl donor.



Scheme 3| Enzymatic kinetic resolution of *rac*-indanol in the chemoenzymatic synthesis of Ragagiline mesylate.

Within this context, the acyltransferase from *Mycobacterium smegmatis* (*Ms*AcT), has gained significant attention for its ability to catalyse a series of transesterifications and transamidation reactions in aqueous solution (Scheme 4). [27–30]



Scheme 4| Transesterification reaction catalysed by *Ms*AcT. x,y indicate the R and R_1 group, respectively. x,y are from a-e. R, R_1 = a: Et, b: -CH_2Ph, c: H, d: Ph, e: -CH=CH_2.

*Ms*AcT is composed of eight identical subunits and shares common features with the SGNH superfamily of serine hydrolases, including the catalytic triad and the oxyanion hole (Figure 2).[27,31] Interestingly, the tunnel leading to the active site exhibits extensive hydrophobic character, creating a microenvironment which disfavours the ingress of water into the active site. This unique feature has been suggested to contribute to the ability of the enzyme to perform transesterifications reactions in aqueous solution.

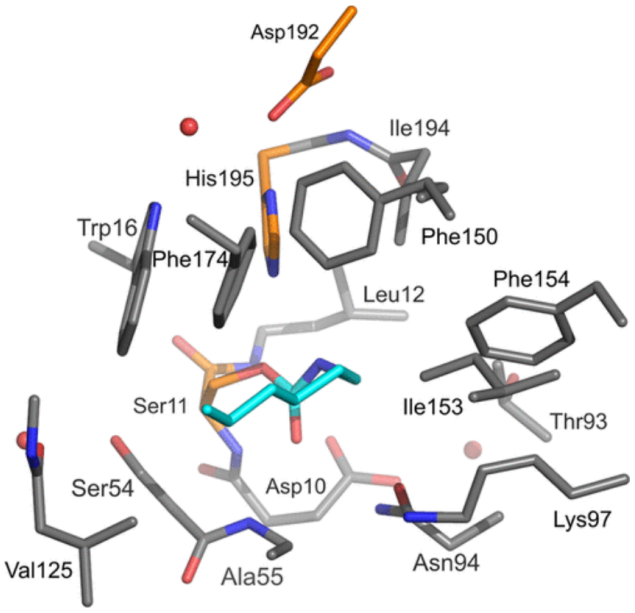
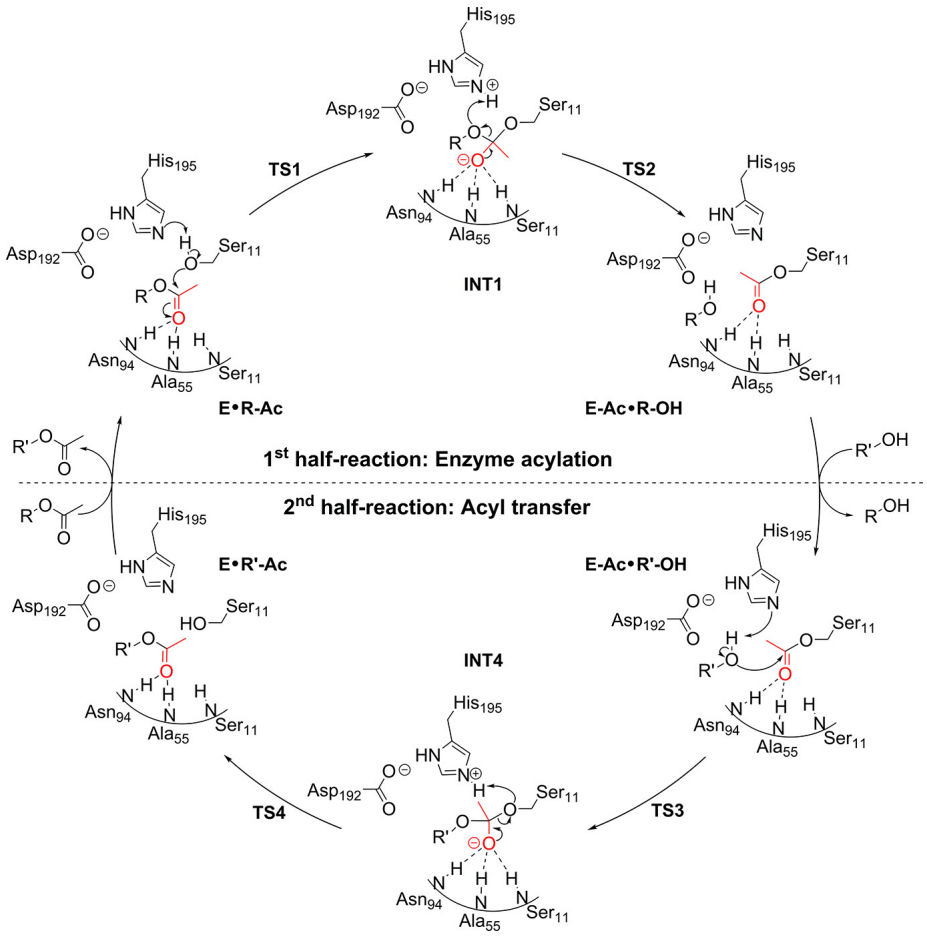


Figure 2| Crystal structure of the *Ms*AcT active site with the covalently bound inhibitor. The catalytic triad is depicted in orange and the inhibitor is highlighted in cyan.[31] (PDB code: 2QOS)

Similar to esterases and lipases, the transesterification reaction catalysed by *Ms*AcT consists of two half reactions in which the enzyme is first acylated by an acyl donor. The acyl group is then transferred to the substrate in the second half of the reaction.[32] In a previous study, Kazemi *et al*, demonstrated that the first step of the enzyme acylation half-reaction involves the nucleophilic attack of the carbonyl carbon of the acyl donor by Ser11 which leads to the formation of a negatively charged tetrahedral intermediate. The negative charge of the intermediate is stabilized by hydrogen bonds to the oxyanion hole while the positive charge of the protonated His195 is stabilized by the carboxylate of Asp192. The tetrahedral intermediate subsequently collapses to form an acylated enzyme in complex with the alcohol substrate (Scheme 5)



Scheme 5| Mechanism of *Ms*AcT catalysed transesterification.[31]

A second negatively charged tetrahedral intermediate is formed in the first step of the second half-reaction which is followed by nucleophilic attack of the carbonyl carbon by the hydroxyl group of the substrate and concomitant proton transfer to the His195. Collapse of the tetrahedral intermediate in this case generates the ester product. The transition state of this step involves C−O bond cleavage with concurrent proton transfer from His195 to Ser11.

While the full potential of *Ms*AcT has yet to be realised, this phenomenal enzyme offers a viable route for the preparation of valuable esters and amides in aqueous solution, which alone is a significant milestone in the field of biocatalysis.

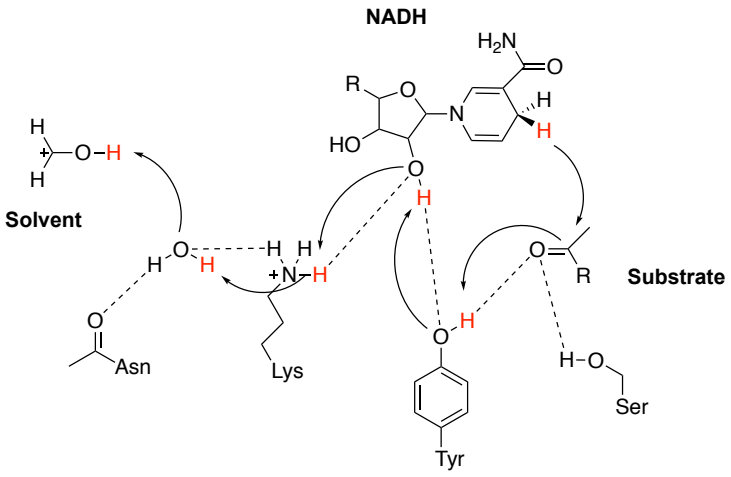
1.2.3 Oxidoreductases

Another group of enzymes which have gained significant interest within the field of biocatalysis are oxidoreductases, specifically alcohol dehydrogenases (ADHs) and ketoreductases (KREDs). While both enzymes are ubiquitous in all domains of life, ADHs exclusively catalyse the interconversion of alcohols to carbonyl functional groups such as aldehydes and ketones using stochiometric amounts of nicotinamide adenine dinucleotide (NAD+) or its phosphorylated analogue NADP+ as cofactor.[33] Of particular interest from a synthetic perspective is the reverse reaction, which synthetically is extremely useful as the reduction of a ketone directly yields a chiral alcohol by selective asymmetric hydrogenation with concomitant consumption of NAD(P)H.[34]

Recently a NADPH-dependent benzil reductase (KRED1-*Pglu*) was identified from the genome of the non-conventional yeast *Pichia glucozyma* CBS 5766. [35] This enzyme belongs to the superfamily of short chain dehydrogenases/reductases (SDRs). These enzymes span several E.C. classes, from oxidoreductases and lyases to isomerases, with NADPH-dependent oxidoreductases constituting the majority of forms. The pairwise sequence identity between different members of the SDR family is low, typically 15-30%. However, all available structures

exhibit a highly similar α/β folding pattern, including a Rossmann fold which comprises a central β -sheet flanked by α -helices.[36] The majority of SDR enzymes have a core structure of approximately 250-350 residues, where conserved sequence regions include a variable N-terminal Gly-X-Gly-X-X-Gly motif which forms part of the nucleotide binding region, as well as the active site with a tetrad of catalytically important Asn, Ser, Tyr and Lys residues.[37]

As shown in scheme 6, catalysis is initiated by proton transfer from the Tyr hydroxyl group to the carbonyl of the substrate. This is followed by hydride transfer from the cofactor molecule. The ε-amino group of the Lys residue is involved in the binding of the nicotinamide ribose group, whereas the role of the Ser residue is to stabilize the substrate. The main chain carbonyl group of the Asn residue ligates a conserved water molecule in hydrogen bonding distance from the catalytic lysine. In this manner a proton relay system is established that connects the bulk solvent to the catalytic Tyr residue.[38]



Scheme 6| SDR (3β/17 β-HDS) mechanism. The Tyr residue fixes the catalytic base, the Ser residue fixes the substrate, while the Lys residue forms a hydrogen bond with NADH.

KRED1-*Pglu* has successfully been applied for the enantioselective preparation of bulky aromatic alcohols and hydroxy ketones, demonstrating the broad scope and variety of substrates accepted by this class of enzymes.[35] Within this context, KREDs have been used extensively for the synthesis of enantiopure alcohols. One prominent example, is the application of a KRED for the synthesis of a key side chain in the drug molecule atorvastatin (Figure 3).[39] Different chemical methods have been used, ranging from asymmetric hydrogenation to oxidative cleavage of sugar derivatives. However these methodologies require the use of hydrogen at high pressures or hydrogen peroxide, which in most cases are not preferred by process chemists.[40] The biocatalytic approach involves the use of an inexpensive and readily available substrate, 4-chloroacetoacetate ethylester , which undergoes bioreduction mediated by a KRED to afford the (*S*)-4-chloro-3-hydroxy-butyrate ester.[39] Furthermore the use of a glucose dehydrogenase (GDH) for in situ cofactor regeneration exemplifies that the cost of cofactor can be negligible.

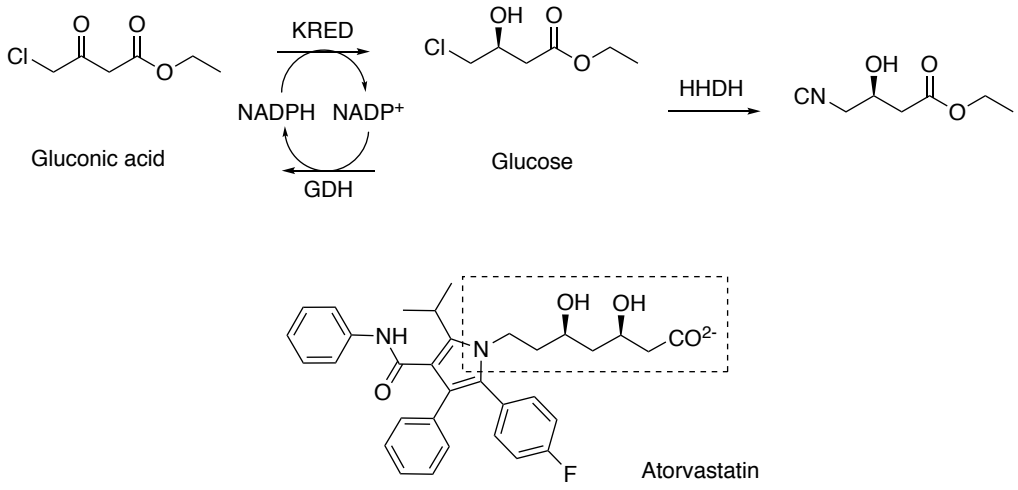


Figure 3| Enzyme mediated synthesis of the key side chain of atorvastatin using a ketoreductase (KR) and halohydrin dehalogenase (HHDH).

1.3 Enzyme engineering and screening

Protein engineering by rational design and directed evolution have played a major role in addressing the limitations of biocatalysis.[41–43] Evolutionary strategies in particular, which involves subjecting a gene to iterative rounds of mutagenesis are ideally suited to the optimisation of the physical properties of enzymes, as well as enabling fine-tuning of substrate and stereochemical preferences. The success of this approach has made it possible to consider enzymes alongside more traditional catalysts when designing synthetic routes to complex molecules. For example, the evolution of ATAs by Codexis and Merck[44,45] pioneered subsequent engineering efforts for the production of highly specialised ATAs for chiral amine synthesis.[46–48]

Even though a fully randomised approach to mutagenesis, targeting the whole length of the protein, has become less common, directed evolution requires high-throughput screening methods to evaluate variable size libraries of engineered variants. The generation of smaller, libraries designed by rational approaches such as CASTing,[49] or saturation mutagenesis of specific residues identified *in silico*, still yield a sizable number of clones to screen. The identification of hits within live cells is advantageous for library screening because it prevents culturing of large number of clones followed by assays with cell extracts, which, in the absence of robotics, is very time-consuming.[50] Recently, microfluidic screening,[51,52] in addition to the application of desorption electrospray ionisation mass spectrometry[53] on whole colonies, have emerged as powerful tools for screening large libraries, however, the equipment required in both cases is highly specialised and expensive, therefore they are not yet suitable for widespread implementation. Solid-phase screening (SPS), on the other hand, is a much simpler approach that facilitates the screening of a medium-large number of mutant variants based on colorimetric changes that are easily observed by the naked eye.[54] SPS was successfully applied in the evolution of monoamine oxidase (MAO-N) enzymes, using two libraries that were fully saturated at two positions each (400 variants).[55]

SPS methods applicable to ATA mutant libraries are currently limited to a few strategies to screen the possible amino donors. Wu and co-workers, for example, reported the use of SPS for libraries of approximately 100 000 ATA variants for reduced inhibition towards methoxyisopropylamine.[56] Later, Bornscheuer and colleagues applied SPS to evolve an ATA towards suitable amino donors (screening *ca.* 4600 colonies), however this required co-expression of a second enzyme as a coupled reporting system, increasing the complexity of the system.[57,58] Similarly, Turner and co-workers evolved SPS for ATA library screening, specifically to identify either (*R*)- or (*S*)-selective ATAs (screening *ca.* 1000 colonies). This methodology required multiple reporting enzymes, as well as flash-freezing in liquid nitrogen, to improve the cell permeability increasing time and cost associated with the methodology.[59]

Screening strategies for varying carbonyl acceptors, which are key substrates for ATAs to produce chiral amine products, appear to be more challenging. *ortho*-Xylylenediamine and 4-nitrophenethylamine have recently been reported as amine donors in proof of concept studies to rapidly generate coloured by-products upon transamination. Both these strategies suffer from strong background interference in live cells due to endogenous pyruvate which is nearly always an excellent substrate for ATAs; in a mutant library screening, the number of false positives is certain to be significant without an efficient system to deplete background. Pyruvate is a primary metabolite, essential for cell growth, therefore knock-out strategies are not feasible, making it inherently difficult to minimise the background noise in SPS.

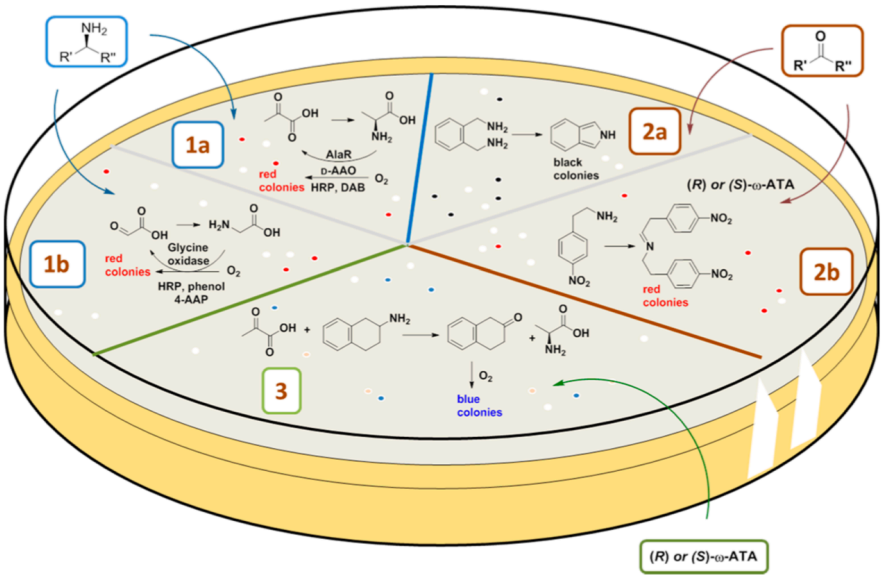


Figure 4| Solid-phase assays allowing for the screening of transaminases and various amine substrates (**1a-1b**), transaminases and various ketone substrates (**2a-2b**) and transaminases in the presence of a fixed set of substrates (**3**).[60]

The development of a versatile colony-based assay that allows high-throughput screening of transaminase libraries for activity towards ketone substrates was recently reported by Planchestainer *et al.* Key to the success of the assay is a preincubation step with (*S*)-(−)-α-methylbenzylamine, which acts as a background depletion agent to eliminate interference from endogenous pyruvate produced within bacterial cells.[61] The reaction is catalysed by the expressed transaminase to produce alanine and acetophenone with an extremely favourable equilibrium, effectively removing pyruvate as a non-specific acceptor from the environment. The background depletion step is straightforward and reliable, and can be applied to other screening methods where endogenous pyruvate interferes with detection making the evolution of ATAs a much less challenging task. This will be further discussed in Chapter 3.

1.4 Enzyme immobilisation

While biocatalysis has emerged as an important technology for the green and sustainable synthesis of pharmaceuticals, agrochemicals, flavours and fragrances and other fine chemicals, the uptake of biocatalysis at an industrial level has been significantly impeded by the lack of long-term operational stability and difficult recovery and re-use of the enzyme.[62] The development of effective immobilisation techniques however has played a key role in overcoming some of these challenges.

Immobilised enzymes generally exhibit enhanced stability under both storage and operational conditions.[63–65] This enhanced stability is typically the direct result of a decrease in the flexibility of the enzyme molecule upon immobilisation, thus reducing the tendency to denature by unfolding in the presence of harsh reaction conditions. An additional benefit of immobilised enzymes is that they can easily be removed from the reaction medium, thereby minimising the risk of protein contamination and simplifying downstream processing.[66] Moreover immobilisation facilitates the efficient recovery and re-use of the enzyme which is essential for the cost-efficient application and intensification of enzymatic processes.

Immobilisation involves binding the enzyme to a prefabricated carrier, such as an organic resin or entrapment in a polymeric matrix which is formed in the presence of the enzyme.[66] The goal is to deliver a biocatalyst that has a superior operational performance and is more cost effective compared to the free enzyme. Over the last number of years, an array of techniques to immobilise enzymes have been developed. A general overview of each is presented below (Figure 5).

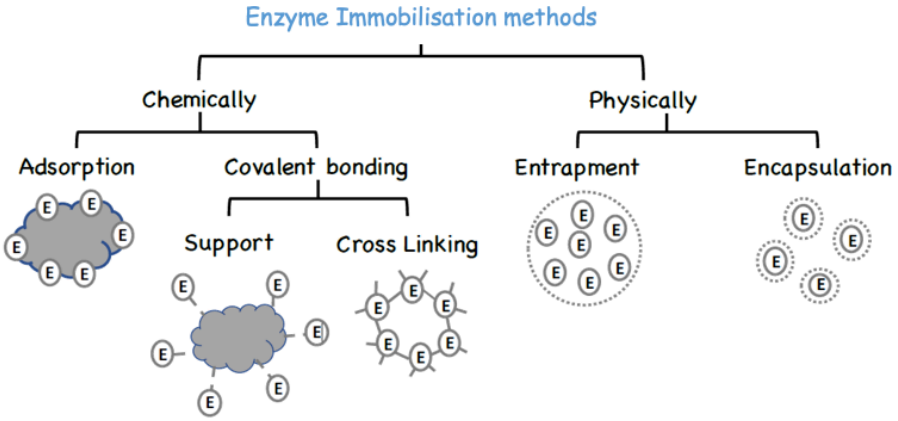


Figure 5| Scheme of the various immobilisation methodologies available.

Methodologies for enzyme immobilisation:

- Physical adsorption: Perhaps the most straightforward technique used in protein immobilisation is nonspecific adsorption, in which the protein is attached to the carrier via a number of physiochemical interactions including hydrogen bonding, van der Waals forces, hydrophobic interactions or ionic bonding. [67] The nature of the forces involved in noncovalent immobilization result in a process that can be reversed by changing the conditions that influence the strength of the interaction.[68] This technique is mild, easy to perform and usually preserves the catalytic activity of the enzyme. Such methods are therefore economically attractive, but may suffer from problems such as leaching when the interactions are relatively weak.

- Covalent binding: In the case of covalent attachment, reactive groups (epoxides, aldehydes, etc.) on the surface of the support form covalent bonds with lysine groups on the surface of the protein.[69] Given the stable nature of the bonds formed between enzyme and matrix, covalent binding offers benefits in terms of operational stability and reuse which are crucial for industrial biocatalytic processes.[70] Furthermore, the enzyme is not released

into the solution upon use. As a result, covalent binding is the most commonly used strategies for enzyme immobilisation.

- Entrapment: The entrapment method is based on the encapsulation of an enzyme within a polymeric network that allows the substrate and products to pass through but retains the enzyme.[71,72] This method differs from the coupling methods described above, in that the enzyme is not bound to the matrix or membrane. The practical use of these methods however is limited by mass transfer limitations through membranes or gels.

- Crosslinked aggregates: Cross linked enzyme aggregates (CLEAs) are prepared by first aggregating the enzyme. The addition of precipitants such as ammonium sulphate, organic solvents (acetone, butanol or ethanol) or other precipitating agents is followed by a crosslinker, typically glutaraldehyde.[73] Instead of anchoring the enzyme to a carrier, the enzyme acts as its own carrier in this case. Despite the appeal of a simple, carrier free enzyme immobilisation, the optimisation of the aggregation and cross-linking procedure can be tedious and often results in poor recovery of enzyme activity.[69]

While immobilisation enables the packing of biocatalysts in continuous flow reactors, it is important to note that most enzymes do not retain their *in vitro* activity upon immobilisation. A significant amount of optimisation is therefore required to obtain acceptable performance, which is further discussed in Chapters 4 & 5.

1.5 Flow biocatalysis

The uptake of biocatalysis as a useful tool for asymmetric synthesis has led to the development of a number of complementary technologies that have enabled the intensification of industrially relevant biocatalytic processes. In particular, the transfer of enzyme based processes into continuous flow is currently the focus of growing attention.[74]

Compared to batch processes, performing reactions in continuous flow mode offer the following benefits: excellent control of temperature, pressure and mixing; in situ product separation and/or recycling of unreacted reagents; real-time online optimisation of reaction conditions to maximise efficiency; real-time in-line monitoring that enables the detection and correction of process condition deviations, resulting in less of the batch being at risk of being discarded.[75] Specifically with respect to biocatalytic transformations, continuous flow can also offer additional benefits such as reduced enzyme inhibition through continuous product removal and facile downstream processing.[76]

While flow biocatalysis can be performed using immobilised whole-cells or cell-free enzymes, some excellent examples of cell-free enzymatic reactions in continuous flow have appeared in the literature in recent years. For example, our group has recently described the use of *He*WT in continuous flow (Figure 6).[77] The enzyme, which was covalently immobilised onto a commercially available metal derivatized epoxy resin, proved to be highly stable in a packed bed reactor (PBR) at high flow rates for the synthesis of a panel of amines. An in-line purification protocol was used, in which basification of the reaction stream and extraction with EtOAc, afforded the desired amine product. Traces of unreacted aldehyde substrate in the organic phase was effectively trapped using a benzylamine functionalized resin. In addition excellent conversions and reaction times were achieved compared to those obtained in batch. More recently, the Paradisi group reported on the conversion of a series primary amines to aldehydes catalysed by the same immobilised *He*WT system.[78] In-line acidification of the reaction

stream followed by liquid−liquid extraction using a Zaiput separator facilitated the separation of the aldehyde. Notably, this system afforded up to 5-fold improvements in productivity when compared to the equivalent batch process.

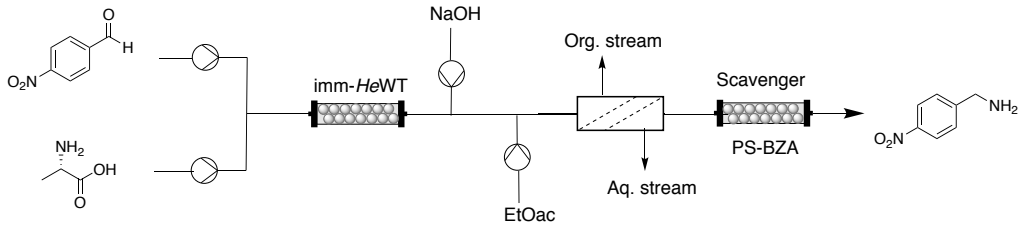


Figure 6| Synthesis of amines using the immobilised *He*WT incorporating a two-step *in situ* product removal system.

In addition, the group has also demonstrated the use of an immobilised acyltransferase from *Mycobacterium smegmatis* (*Ms*AcT) for the multigram synthesis of melatonin in continuous flow mode.[79] The design of this system very elegantly facilitated the recovery of all materials involved in the biosynthesis, including the waste water containing any unreacted amine. This system represents one of the most efficient examples of biocatalysis in continuous flow reported to date.

Dall'Oglio and colleagues described the enantioselective reduction of bulky ketones in continuous flow by combining the ketoreductase from *Pichia glucozyma* with a glucose dehydrogenase from *Bacillus megaterium* for co-factor regeneration.[80] The stereoselective reduction of the bulky substrate, ethyl secodione using this system gave a recovered yield of 60 mg of the hydroxy ketone over 15 days of continuous operation (STY = 4.8 g L−1 day−1). Remarkably, the biocatalysts remained catalytically active for several weeks despite the presence of 20% DMSO.

1.6 Small cyclic molecules: the challenges

The asymmetric reduction of prochiral ketones with the formation of enantiomerically pure molecules is a fundamentally important reaction in synthetic organic and medicinal chemistry. These architectures find application in a wide range of fields, as well as serving as key intermediates in the synthesis of several pharmaceutical compounds. For example, the enantiopure chiral alcohol derived from tetrahydrofuran-3-one, is used in the synthesis of the HIV inhibitor amprenavir and its prodrug form fosamprenavir, while the amine analogue forms an integral structural feature in selective high affinity adenosine A1 receptor agonists, which have received considerable attention for their antiarrhythmic activity.[81,82]

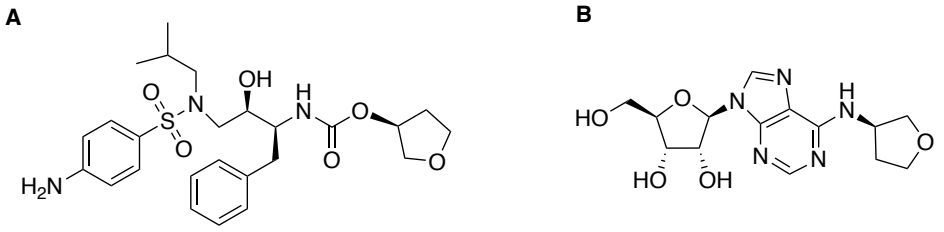


Figure 7| A. HIV Inhibitor, Amprenavir. **B.** Selective high affinity adenosine A1 receptor agonist, Tecadenoson.

Chiral manmade transition metal catalysts and certain organocatalysts have been applied successfully in ketone reductions.[83,84] However, in all of these approaches, high enantioselectivity can be achieved only when the α- and α'- substituents flanking the carbonyl functionality differ sterically. Spatially symmetrical ketones, such as tetrahydrofuran-3-one and related substrates, are particularly challenging in this regard, with asymmetric reductions typically resulting in poor enantioselectivities irrespective of the catalyst. To overcome these challenges, Pfizer developed a five-step process to obtain the chiral alcohol (*R*)-tetrahydrothiophene-3-ol, which is a key component in the potent antibiotic sulopenem (Figure 8). [85]

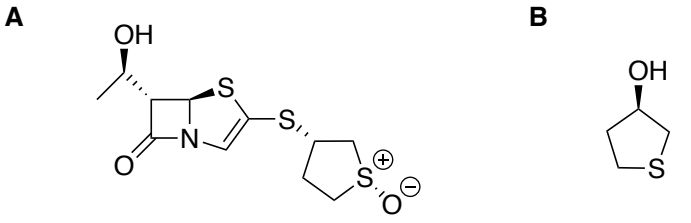
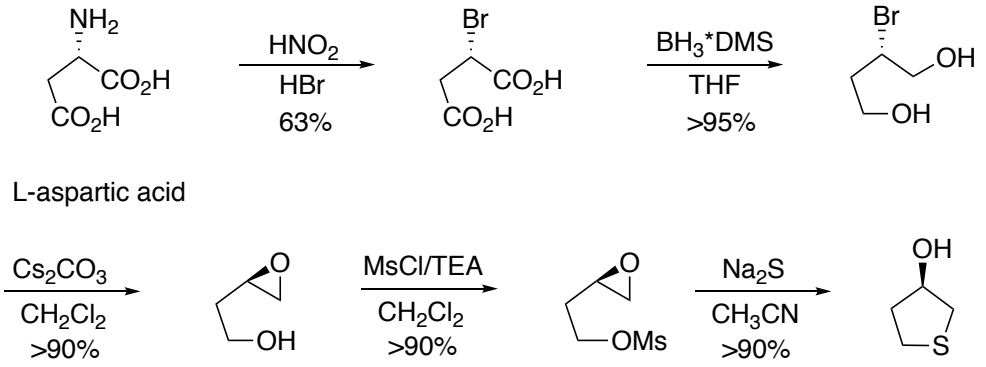


Figure 8| A. Sulopenem, a potent antibiotic. **B. (***R*)-tetrahydrothiophene-3-ol.

While the desired alcohol is generally obtained in good yields and high optical purity (96-98% *e.e.*) using this approach, the synthesis involves hazardous conditions (diazotization in step 1), a sensitive reagent (BH_3·dimethylsulfide in step 2), high energy intermediates (epoxides in steps 3 and 4) and a noxious reagent (Na_2 in step 5) (Scheme 7).



Scheme 7| Synthesis of (*R*)-tetrahydrothiophene-3-ol starting from L-aspartic acid.

Another key challenge in organic chemistry laboratories is the green and sustainable synthesis of amides. Strategies for amide synthesis, as outlined in Figure 8, typically involves the activation of a carboxylic acid, using either toxic chlorinating agents, or atom inefficient coupling reagents.[86] It therefore comes as no surprise that amide bond formation avoiding poor atom economy was voted as a top challenge for the organic chemists in 2007.[87]

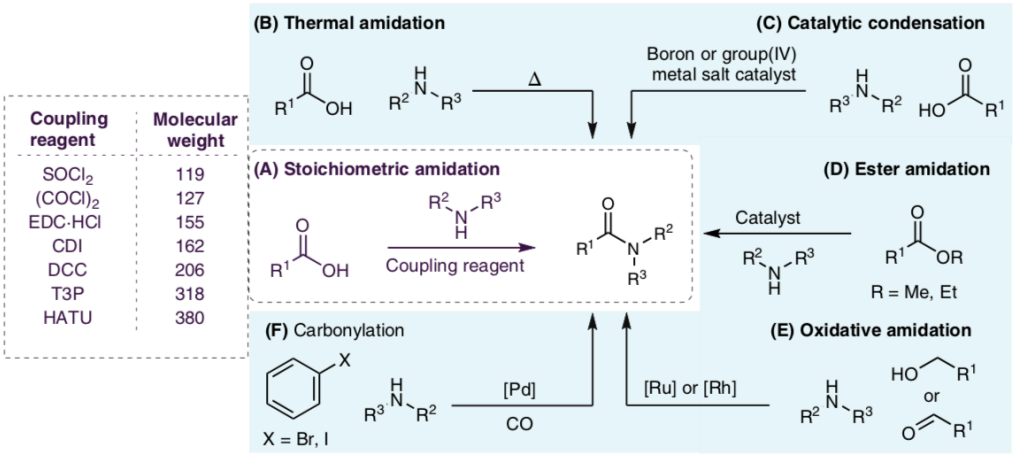


Figure 8| Methods for amide synthesis. Common stoichiometric amide coupling reagents and the various catalytic amidation strategies employed in organic chemistry laboratories.[86]

Biocatalysis is a tool at the disposal of synthetic organic chemists that continues to expand in scope as new enzymes are discovered and engineered. Such enzyme based processes can potentially open up new strategic routes to high value molecules, like those outlined above, that are difficult to produce using traditional chemical methods.

References

1. Pasteur, L. Mémoire sur la fermentation de l'acide tartrique. *CR Séances Acad. Sci*. **46**, 615–618 (1958).

2. Fischer, E. Einfluss der Configuration auf die Wirkung der Enzyme. *Ber. Dtsch. Chem. Ges.* **27**, 2985–2993 (1894).

3. Buchner, E. & Rapp, R. Alkoholische Gährung ohne Hefezellen. *Berichte der Dtsch. Chem. Gesellschaft*. **32**, 2086–2094 (1899).

4. Hughes, G. & Lewis, J. C. Introduction: Biocatalysis in Industry. *Chem. Rev.* **118**, 1–3 (2018).

5. Anastas, P. T. & Warner, C. J. *Green Chemistry: Theory and Practice*. (Oxford University Press, New York, 1998).

6. Sheldon, R. A. & Woodley, J. M. Role of Biocatalysis in Sustainable Chemistry. *Chem. Rev.* **118**, 801–838 (2018).

7. Sheldon, R. A. & Brady, D. Broadening the Scope of Biocatalysis in Sustainable Organic Synthesis. *ChemSusChem*. **12**, 2859–2881 (2019).

8. Turner, N. J. & Humphreys, L. *Biocatalysis in Organic Synthesis: The Retrosynthesis Approach*. (Royal Society of Chemistry, London, 2018).

9. Slabu, I., Galman, J. L., Lloyd, R. C. & Turner, N. J. Discovery, Engineering, and Synthetic Application of Transaminase Biocatalysts. *ACS Catal.* **7**, 8263–8284 (2017).

10. Fuchs, M., Farnberger, J. E. & Kroutil, W. The Industrial Age of Biocatalytic Transamination. *European J. Org. Chem.* **2015**, 6965–6982 (2015).

11. Mehta, P. K., Hale, T. I. & Christen, P. Aminotransferases: demonstration of homology and division into evolutionary subgroups. *Eur. J. Biochem.* **214**, 549–561 (1993).

12. Steffen-Munsberg, F. et al. Bioinformatic analysis of a PLP-dependent enzyme superfamily suitable for biocatalytic applications. *Biotechnol. Adv.* **33**, 566–604 (2015).

13. Guo, F. & Berglund, P. Transaminase biocatalysis: Optimization and application. *Green Chem.* **19**, 333–360 (2017).

14. Gomm, A. & O'Reilly, E. Transaminases for chiral amine synthesis. *Curr. Opin. Chem. Biol.* **43**, 106–112 (2018).

15. Sayer, C. et al. Structural studies of Pseudomonas and

Chromobacterium ω- aminotransferases provide insights into their differing substrate specificity. *Acta Crystallogr. Sect. D Biol. Crystallogr.* **69**, 564–576 (2013).

16. Humble, M. S. et al. Crystal structures of the Chromobacterium violaceumω-transaminase reveal major structural rearrangements upon binding of coenzyme PLP. *FEBS J.* **279**, 779–792 (2012).

17. Shin, J. S. & Kim, B. G. Exploring the active site of amine:pyruvate aminotransferase on the basis of the substrate structure-reactivity relationship: How the enzyme controls substrate specificity and stereoselectivity. *J. Org. Chem.* **67**, 2848–2853 (2002).

18. Park, E. S., Kim, M. & Shin, J. S. Molecular determinants for substrate selectivity of ω-transaminases. *Appl. Microbiol. Biotechnol.* **93**, 2425–2435 (2012).

19. Savile, C. K. et al. Biocatalytic Asymmetric Synthesis of Chiral Amines from Ketones Applied to Sitagliptin Manufacture. *Science (80-.).* **329**, 305–310 (2010).

20. Weiß, M. S. et al. Amine Transaminase Engineering for Spatially Bulky Substrate Acceptance. *ChemBioChem.* **18**, 1022–1026 (2017).

21. Cerioli, L. et al. Characterization of a novel amine transaminase from Halomonas elongata. *J. Mol. Catal. B Enzym.* **120**, 141–150 (2015).

22. Contente, M. L. et al. Stereoelectronic effects in the reaction of aromatic substrates catalysed by: Halomonas elongata transaminase and its mutants. *Org. Biomol. Chem.* **14**, 9306–9311 (2016).

23. Jaeger, K. E. & Reetz, M. T. Microbial lipases form versatile tools for biotechnology. *Trends Biotechnol.* **16**, 396–403 (1998).

24. Schmid, R. D. & Verger, R. Lipases: Interfacial Enzymes with Attractive Applications. *Angew. Chemie Int. Ed.* **37**, 1608–1633 (1998).

25. Subileau, M., Jan, A. H. & Dubreucq, E. *Lipid Modification by Enzymes and Engineered Microbes*. (Academic Press and AOCS, 2018).

26. De Mattos, M. C. et al. Chemoenzymatic synthesis of rasagiline mesylate using lipases. *Appl. Catal. A Gen.* **492**, 76–82 (2015).

27. Mathews, I. et al. Structure of a novel enzyme that catalyzes acyl transfer to alcohols in aqueous conditions. *Biochemistry* **46**, 8969–8979 (2007).

28. de Leeuw, N. et al. Ester Synthesis in Water: Mycobacterium smegmatis Acyl Transferase for Kinetic Resolutions. *Adv. Synth. Catal.* **360**, 242–249 (2018).

29. Szymańska, K. et al. MsAcT in siliceous monolithic microreactors enables quantitative ester synthesis in water. *Catal. Sci. Technol.* **6**, 4882–4888 (2016).

30. Contente, M. L. et al. Biocatalytic N-Acylation of Amines in Water Using an Acyltransferase from Mycobacterium smegmatis. *Adv. Synth. Catal.* **360**, 4814–4819 (2018).

31. Kazemi, M., Sheng, X., Kroutil, W. & Himo, F. Computational Study of Mycobacterium smegmatis Acyl Transferase Reaction Mechanism and Specificity. *ACS Catal.* **8**, 10698–10706 (2018).

32. Kazemi, M., Sheng, X. & Himo, F. Origins of Enantiopreference of Mycobacterium smegmatis Acyl Transferase: A Computational Analysis. *Chem. – A Eur. J.* **25**, 1–11 (2019).

33. Xu, F. Applications of oxidoreductases: Recent progress . *Ind. Biotechnol.* **1**, 38–50 (2005).

34. de Souza, R. O. M. A., Miranda, L. S. M. & Bornscheuer, U. T. A Retrosynthesis Approach for Biocatalysis in Organic Synthesis. *Chem. - A Eur. J.* **23**, 12040–12063 (2017).

35. Contente, M. L. et al. Stereoselective reduction of aromatic ketones by a new ketoreductase from Pichia glucozyma. *Appl. Microbiol. Biotechnol.* **100**, 193–201 (2016).

36. Oppermann, U. et al. Short-chain dehydrogenases/reductases (SDR): The 2002 update. *Chem. Biol. Interact.* **143**–**144**, 247–253 (2003).

37. Kavanagh, K. L. et al. Medium and short-chain dehydrogenase/reductase gene and protein families: The SDR superfamily: Functional and structural diversity within a family of metabolic and regulatory enzymes. *Cell. Mol. Life Sci.* **65**, 3895–3906 (2008).

38. Filling, C. et al. Critical residues for structure and catalysis in short-chain dehydrogenases/reductases. *J. Biol. Chem.* **277**, 25677–25684 (2002).

39. Ma, S. K. *et al.* A green-by-design biocatalytic process for atorvastatin intermediate. *Green Chem.* **12**, 81–86 (2010).

40. Butler, D. et al. Process for the synthesis of (5*R*)-1, 1-dimethylethyl-6-cyano-5-hydroxy-3-oxo-hexanoate. *US. Pat*, US5155251, (1992).

41. Romero, P. A. & Arnold, F. H. Exploring protein fitness landscapes by directed evolution. *Nat. Rev. Mol. Cell Biol.* **10**, 866–876 (2009).

42. You, L. & Arnold, F. H. Directed evolution of subtilisin E in Bacillus subtilis to enhance total activity in aqueous dimethylformamide. *Protein Eng.* **9**, 77–83 (1996).

43. Arnold, H. Engineering proteins for nonnatural environments. *Faseb J.* **7**, 744–749 (1993).

44. Savile, C. K. et al. Biocatalytic asymmetric synthesis of chiral amines from ketones applied to sitagliptin manufacture. *Science* **329**, 305–9 (2010).

45. Limanto, J. et al. A Highly Efficient Asymmetric Synthesis of Vernakalant. *Org. Lett.* **16**, 2716–2719 (2014).

46. Yun, H. et al. Use of enrichment culture for directed evolution of the Vibrio fluvialis JS17 omega-transaminase, which is resistant to product inhibition by aliphatic ketones. *Appl. Environ. Microbiol.* **71**, 4220–4224 (2005).

47. Pavlidis, I. V. et al. Identification of (S)-selective transaminases for the asymmetric synthesis of bulky chiral amines. *Nat. Chem.* **8**, 1076–1082 (2016).

48. Martin, A. R. et al. Improved activity and thermostability of (S)-aminotransferase by error-prone polymerase chain reaction for the production of a chiral amine. *Biochem. Eng. J.* **37**, 246–255 (2007).

49. Reetz, M. T. et al. Expanding the substrate scope of enzymes: Combining mutations obtained by CASTing. *Chem. - A Eur. J.* **12**, 6031–6038 (2006).

50. Xiao, H., Bao, Z. & Zhao, H. High throughput screening and selection methods for directed enzyme evolution. *Ind. Eng. Chem. Res.* **54**, 4011–4020 (2015).

51. Obexer, R. et al. Emergence of a catalytic tetrad during evolution of a highly active artificial aldolase. *Nat. Chem.* **9**, 50–56 (2017).

52. Longwell, C. K., Labanieh, L. & Cochran, J. R. High-throughput screening technologies for enzyme engineering. *Curr. Opin. Biotechnol.* **48**, 196–202 (2017).

53. Yan, C. et al. Real-Time Screening of Biocatalysts in Live Bacterial Colonies. *J. Am. Chem. Soc.* **139**, 1408–1411 (2017).

54. Arnold, F. H. & Georgiou, G. *Directed enzyme evolution : screening and selection methods*. (Humana Press, New Jersey, 2003).

55. Rowles, I. et al. Directed Evolution of the Enzyme Monoamine Oxidase (MAO-N): Highly Efficient Chemo-enzymatic Deracemisation of the Alkaloid (±)-Crispine A. ChemCatChem. **4**, 1259–1261 (2012).

56. Matcham, G. et al. Enzyme and Reaction Engineering in Biocatalysis: Synthesis of (S)-Methoxyisopropylamine (= (S)-1-Methoxypropan-2-amine). *Chim. Int. J. Chem.* **53**, 584–589 (1999).

57. Weiß, M. S. et al. Protein-engineering of an amine transaminase for the stereoselective synthesis of a pharmaceutically relevant bicyclic amine. *Org. Biomol. Chem.* **14**, 10249–10254 (2016).

58. Weiß, M. S. et al. Glycine oxidase based high-throughput solid-phase assay for substrate profiling and directed evolution of (R)- and (S)-selective amine transaminases. *Anal. Chem.* **86**, 11847–11853 (2014).

59. Willies, S. C. et al. A stereospecific solid-phase screening assay for colonies expressing both (R)- and (S)-selective ω-aminotransferases. *Philos. Trans. R. Soc. A Math. Phys. Eng. Sci.* **374**, 20150084 (2016).

60. Slabu, I. et al. Discovery, Engineering, and Synthetic Application of Transaminase Biocatalysts. *ACS Catal.* **7**, 8263–8284 (2017).

61. Planchestainer, M. et al. Widely applicable background depletion step enables transaminase evolution through solid-phase screening. *Chem. Sci.* **10**, 5952–5958 (2019).

62. Sheldon, R. A. *Biocatalysis: An Industrial Perspective*. (Royal Society of Chemistry, London, 2018).

63. Sheldon, R. A. Enzyme immobilization: The quest for optimum performance. *Adv. Synth. Catal.* **349**, 1289–1307 (2007).

64. Hanefeld, U., Gardossi, L. & Magner, E. Understanding enzyme immobilisation. *Chem. Soc. Rev.* **38**, 453–468 (2009).

65. Garcia-Galan, C. et al. Potential of different enzyme immobilization strategies to improve enzyme performance. *Adv. Synth. Catal.* **353**, 2885–2904 (2011).

66. Sheldon, R. A. & van Pelt, S. Enzyme immobilisation in biocatalysis: Why, what and how. *Chem. Soc. Rev.* **42**, 6223–6235 (2013).

67. Jesionowski, T., Zdarta, J. & Krajewska, B. Enzyme immobilization by adsorption: A review. *Adsorption.* **20**, 801–821 (2014).

68. Mateo, C. et al. Reversible enzyme immobilization via a very strong and nondistorting ionic adsorption on support-polyethylenimine composites. *Biotechnol. Bioeng.* **68**, 98–105 (2000).

69. Thompson, M. P. et al. Biocatalysis Using Immobilized Enzymes in Continuous Flow for the Synthesis of Fine Chemicals. *Org. Process Res. Dev.* **23**, 9–18 (2019).

70. Guisán, J. M. *Immobilization of enzymes and cells*. (Humana Press, New Jersey, 2000).

71. Reetz, M. T. *Immobilization of Enzymes and Cells*. (Humana Press, New Jersey, 2013).

72. Sassolas, A., Hayat, A. & Marty, J.-L. *Immobilization of enzymes in cells*. (Humana Press, New Jersey, 2013).

73. Sheldon, R. A. Cross-linked enzyme aggregates as industrial biocatalysts. *Org. Process Res. Dev.* **15**, 213–223 (2011).

74. Tamborini, L., Fernandes, P., Paradisi, F. & Molinari, F. Flow Bioreactors as Complementary Tools for Biocatalytic Process Intensification. *Trends Biotechnol.* **36**, 73–88 (2018).

75. Devine, P. N. *et al.* Extending the application of biocatalysis to meet the challenges of drug development. *Nat. Rev. Chem.* **2**, 409–421 (2018).

76. Britton, J., Majumdar, S. & Weiss, G. A. Continuous flow biocatalysis. *Chem. Soc. Rev.* **47**, 5891–5918 (2018).

77. Planchestainer, M. et al. Continuous flow biocatalysis: Production and in-line purification of amines by immobilised transaminase from Halomonas elongata. *Green Chem.* **19**, 372–375 (2017).

78. Contente, M. L. et al. Highly Efficient Oxidation of Amines to Aldehydes with Flow-based Biocatalysis. *ChemCatChem*. **9**, 3843–3848 (2017).

79. Contente, M. L. et al. Flow-based enzymatic synthesis of melatonin and other high value tryptamine derivatives: A five-minute intensified process. *Green Chem.* **21**, 3263–3266 (2019).

80. Dall'Oglio, F. et al. Flow-based stereoselective reduction of ketones using an immobilized ketoreductase/glucose dehydrogenase mixed bed system. *Catal. Commun.* **93**, 29–32 (2017).

81. Sun, Z. et al. Catalytic Asymmetric Reduction of Difficult-to-Reduce Ketones: Triple-Code Saturation Mutagenesis of an Alcohol Dehydrogenase. *ACS Catal.* **6**, 1598–1605 (2016).

82. Elzein, E. et al. N6-Cycloalkyl-2-substituted adenosine derivatives as selective, high affinity adenosine A1 receptor agonists. *Bioorganic Med. Chem. Lett.* **17**, 161–166 (2007).

83. Noyori, R. Asymmetric Catalysis: Science and Opportunities (Nobel lecture). *Angew. Chemie - Int. Ed.* **41**, 2008–2022 (2002).

84. Corey, E. J. & Helal, C. J. Reduction of Carbonyl Compounds with Chiral Oxazaborolidine Catalysts: A New Paradigm for Enantioselective Catalysis and a Powerful New Synthetic Method. *Angew. Chemie - Int. Ed.* **37**, 1986–2012 (1998).

85. Liang, J. et al. Highly enantioselective reduction of a small heterocyclic ketone: Biocatalytic reduction of tetrahydrothiophene-3-one to the corresponding (*R*)-Alcohol. *Org. Process Res. Dev.* **14**, 188–192 (2010).

86. Sabatini, M. T. et al. A green chemistry perspective on catalytic amide bond formation. *Nat. Catal.* **2**, 10–17 (2019).

87. Constable, D. J. C. et al. Key green chemistry research areas - A perspective from pharmaceutical manufacturers. *Green Chem.* **9**, 411–420 (2007).

Aims & Objectives

Aims & Objectives

The principle aim of this research project is to investigate novel biocatalytic routes for the synthesis of small cyclic chiral molecules, with a particular focus on chiral alcohols, amines and amides. Within this contest, the development of an efficient biocatalytic system to generate small chiral alcohols and amines starting from readily available and inexpensive ketone precursors was investigated. To achieve this goal, the following steps will be taken:

- The substrate scope of a ketoreductase from *Pichia glucozyma* and an ω-transaminase from the moderate halophilic bacterium *Halomonas elongata* will be screened for activity towards more complex ketone substrates. The application of these enzymes for the asymmetric reduction of these substrates would further demonstrate the value of these biocatalysts in chemical synthesis.

- In addition, a tandem enzymatic reaction will be implemented ti combine the transaminase with a second biocatalysts, an acyltransferase from Mycobacterium smegmatis, which was used to merge the newly synthesised chiral amines with different acyl donors to form optically active amides. Finally, the scalability and intensification of these biocatalytic processes were accessed by applying the reactions in a continuous flow reactor.

- The project will also involve the screening of transaminase libraries generated by random mutagenesis to evaluate the validity of a newly developed solid phase screen.

The results obtained during the course of this project are presented herein.

Chapter 2

Material and Method

2.1 Reagents

Commercially available reagents and solvents were purchased from ACROS Organics, Fluorochem, Sigma Aldrich and Thermo Fisher Scientific unless otherwise stated. Unstained protein standard, broad range (10-200 kDa) was purchased from New England Biolabs. Pierce Prestained Protein Molecular Weight Marker (20-120 kDa) was purchased from ThermoFisher Scientific. Transparent 96-well plates and 1 mL cuvettes were purchased from Corning and Sigma Aldrich, respectively. Separose CL-6B was purchased from Sigma Aldrich. Sepabeads EC-EP/S, Relizyme EP403 and Relizyme HFA403 were kindly donated by Resindion.

2.2 Bacterial strains

- *E. coli* XL10-Gold (Agilent) for construct replication and extraction. Genotype: *endA1 glnV44 recA1 thi-1 gyrA96 relA1 lac Hte Δ(mcrA)183 Δ(mcrCB-hsdSMR-mrr)173 tet^R F'[proAB lacI^{q}ZΔM15 Tn10(Tet^R Amy Cm^R)]*.
- *E.coli* BL21 (DE3)STAR (ThermoFisher Scientific) for standard protein expression. Genotype: F$^-$ *omp*T *hsd*S$_B$ (r_B^-, m_B^-) *galdcmrne*131 (DE3

2.3 Plasmids

Table 1| List of plasmids encoding the enzymes featured in thesis. The function and origin of the enzyme are presented, together with the respective vectors and the original source of cloning.

Name of Plasmid	Backbone	Function	Organism	Source
pMP89a-*He*WT	pRSETb	ω-TA	*Halomonas elongata*	Dr. Matteo Planchestainer – Paradisi Research Group
pMP89a-*He*WT-A1	pRSETb	ω-TA	*Halomonas elongata*	
pMP89a-*He*WT-B1	pRSETb	ω-TA	*Halomonas elongata*	
pMP89a-*He*WT-B2	pRSETb	ω-TA	*Halomonas elongata*	
pMP89a-*He*WT-C1	pRSETb	ω-TA	*Hamononas elongata*	
pET28b-*Pf*TA	pET28b	ω-TA	*Pseudomonas fluorescence*	Mutti Research Group[1]
pET26b-KRED1	pET26b	KRED	*Pichia glucozyma*	Molinari Research Group[2]
pET26b-*Ms*AcT	pET26b	AcT	*Mycobacterium smegmatis*	Dr. Martina Letiza Contente – Paradisi Research Group

2.4 Culture medium

Mediums for cell culture were prepared in-house as described below. All components were purchased from Sigma Aldrich.

- LB medium: N-Z amine (10 g), yeast extract (5 g), NaCl (10 g) and distilled H_2O (1 L).
- LB agar plates: N-Z amine (10 g), yeast extract (5 g), NaCl (10 g), agar (15 g) and distilled H_2O (1 L).
- SOB medium: N-Z amine (5 g), yeast extract (1.25 g), NaCl (0.25 g), KCl (0.05 g), $MgCl_2$ $6H_2O$ (0.5 g), $MgSO_4$ $6H_2O$ (0.6 g) and distilled H_2O (250 mL).
- TB medium: N-Z amine (12 g), yeast extract (24 g), glycerol (5 g), K_2HPO_4 (2.2 g) and KH_2PO_4 (9.4 g) and distilled H_2O (1 L).
- ZYP-5052 auto-induction media: N-Z-Amine (3 g), yeast extract (1.5 g), 1M K_2HPO_4 (15 mL), 1M KH_2PO_4 (15 mL), 1M $(NH_4)_2SO_4$ (7.5 mL); 1 M $MgSO_4$ (0.6 mL); 1000x trace element solution (0,6 mL); 50x 5052 solution (6 mL); dH_2O (to 300 mL).
- 1000x trace element solution: $FeCl_2$ (50 mM), $CaCl_2$ (20 mM), $MnCl_2$ (10 mM), $ZnSO_4$ (10 mM), $CoCl_2$ (2 mM), $CuCl_2$ (2 mM), $NiCl_2$ (2 mM), HCl (60 mM), Na_2MoO_4 (2 mM), Na_2SeO_4 (2 mM) and H_3BO_3 (2 mM), dH_2O to 100 mL (sterilized using a 0.22 μm syringe filter).
- 50x 5052 solution: glycerol (25 g), glucose (2.5 g), α-lactose monohydrate (10 g), dH_2O (to 100 mL).

2.5 General Procedures

2.5.1 Preparation of chemically competent cells:

A single colony of the desired *E. coli* strain was inoculated into LB medium (100 mL) and grown at 37ºC, 150 rpm to an OD_{600} between 0.35-0.4. The culture was placed on ice for 30 minutes and subsequently harvested by centrifugation at 3000 *g* for 15 minutes at 4 ºC. The cells were resuspended in 50 mL of an ice-cold 100 mM magnesium chloride solution and harvested again (2000 g, 15

minutes, 4 ºC). The pellet was resuspended in 25 mL of an ice-cold solution of 100 mM calcium chloride and incubated in ice for at least 20 minutes. After a final centrifuge (2000 *g*, 10 minutes, 4ºC), the pellet was resuspended in 1 mL of ice cold 85 mM calcium chloride containing 15 % v/v glycerol. 40 µL aliquots were prepared in sterile 1.5 mL microcentrifuge tubes and stored at -80ºC.

2.5.2 Preparation of electro competent cells:

A single colony of the desired *E. coli* strain was inoculated into LB medium (50 mL) and grown at 37ºC, 150 rpm to an OD_{600} of approximately 0.4. The cells were chilled on ice for 20 minutes and then harvested by centrifugation at 3 000 rpm, 15 minutes at 4 ºC. The pellet was then carefully resuspended in ice cold sterilised water followed by centrifugation using the same conditions as before. The wash step was repeated with 25 mL of water and then 15 mL of water containing 10 % v/v glycerol. The pellet was finally resuspended in 0.5 mL of water containing 10 % v/v glycerol. The cell were aliquoted (50 µL) in 1.5 mL microcentrifuge tubes and routinely stored at -80ºC.

2.5.3 Transformation of chemically competent *E. coli* cells:

Under sterile conditions plasmid DNA (20-50 ng) harbouring the gene of interest was transferred to a tube containing chemically competent *E.coli* BL21(DE3)STAR cells (40 µL aliquot). The contents of the tube were mixed gently, incubated on ice for 30 min, heat-shocked at 42°C for 90 s and transferred back to ice for 5 min. LB medium (250 µL) was added to the tube and incubated at 37°C, 150 rpm for 1 h. The culture was then plated onto LB agar plates supplemented with the appropriate antibiotics. Plates were incubated overnight at 37°C and stored at 4 °C.

2.5.4 Protein quantification:

Determination of protein concentration was performed by measuring absorbance at 280 nm, based on the absorbance of the aromatic amino acids tryptophan and tyrosine and disulphide bonded cysteine residues in the protein solutions. The protein concentration was then calculated using the Beer-Lambert law. Molar extinction coefficients for each protein, was estimated by ProtPram (Table 1). All absorbance readings were carried our using a BioTek Take3 Microplate reader.

Table 1| Extinction coefficient and molecular mass used for the calculation of protein concentration using a BioTekTake3 microplate reader in combination with an Epoch 2.

Protein	Extinction coefficient (mM^{-1} cm^{-1})	Molecular mass (kDa)
*He*WT	62.8	54.0
KRED1-*Pglu*	20.4	29.0
*Bm*GDH	28.4	29.0
*Ms*AcT	28.1	25.6

2.5.5 SDS-PAGE:

SDS-PAGE was performed using the following procedure. The running gel (12%: 4.93 mL of Tris HCl 1 M pH 8.8, 4.92 mL acrylamide 30%, 2.14 mL of dH_2O, 150 µL SDS 10%, 150 µL ammonium persulfate 10% (w/v) and 15 µL TEMED) was prepared and loaded in between the two glass pieces, adding a few drops of isopropanol on top to avoid the formation of a meniscus. After the gel was polymerised, the stacking gel was prepared and loaded (1 mL 0.5 M Tris pH 6.8, 0.68 mL acrylamide 30%, 2.27 mL dH_2O, 40 µL SDS 10%, 40 µL ammonium persulfate 10% (w/v) and 6 µL TEMED). Before loading, the samples were heated at 90 ºC for at least 10 minutes after mixed with an equal volume of the 2x loading buffer (5 mL 1 M Tris-HCl buffer pH 6.8, 2.5 mL β-mercaptoethanol, 2 g SDS, 20 mL glycerol, 50 mg bromophenol blue and 7.5 mL dH_2O). The gel was run at 30 mA, 300V for 70 minutes. The protein marker, unstained protein standard, Broad range (10-200 kDa, New England Biolabs) was loaded as a comparison. The gel was then removed from the mould and either stained with comassie blue staining solution (2% Comassie brilliant blue R-250 in aqueous solution 50% methanol and 10% acetic acid) for 15-30 minutes following destaining with the destaining solution (aqueous solution 7.5% methanol and 10% acetic acid) overnight or with InsantBlue (Expedion) solution overnight. All reagents used were purchased from Sigma Aldrich unless otherwise stated.

2.6 Characterization of *He*WT mutants

2.6.1 Expression and purification of *He*WT and mutant variants

*He*WT biocatalysts were prepared as previously reported.[3] Chemically competent *E.coli* BL21(DE3)STAR cells were transformed with the pMP89a vector containing either the wild-type or variant gene. Transformants were selected by growth on LB agar plates supplemented with 100 µg/mL ampicillin. A single colony was used to inoculate 300 mL of auto-induction medium supplemented with 100

µg/mL ampicillin. The cultues were then incubated at 37 °C, 150 rpm. After 24 hours the cells were harvested by centrifugation at 4 000 rpm, 4 °C for 20 min. The resulting pellet was resuspended in loading buffer (50 mM potassium phosphate buffer, pH 8.0 containing 100 mM NaCl, 30 mM imidazole and 0.1 mM PLP), employing 5 mL per gram of cell pellet. The cells were disrupted by sonication (10 cycles, 30s sonication followed by 30s of cooling on ice, 40% amplitude). After centrifugation (14 000 rpm, 4°C, 45 min), the supernatant was clarified by filtration (0.45 µm filter). Purification of *He*WT and mutant variants was carried out by affinity chromatography using an ÄKTA Start chromatography system (GE Heathcare). A 5 mL Ni-NTA Superflow Cartridge (Qiagen) precharged with 0.1 M $NiSO_4$ was employed for the purification. In brief, the system was equilibrated with loading buffer and the filtered cellular extract loaded. The column was then washed with 20 column volumes of the same buffer at a flow rate of 1 mL/min followed by an intermediate step with 10% of elution buffer (50 mM potassium phosphate buffer, pH 8.0 containing 100 mM NaCl, 300 mM imidazole and 0.1 mM PLP) to remove non-specifically bound proteins. An isocratic elution step using elution buffer was then applied to collect the His-tagged protein. Samples of the pellet, crude extract and fractions collected were analysed by SDS PAGE using a 12% polyacrylamide gel stained with Instant Blue. A broad range protein marker was used to determine relative molecular weight. The fractions showing the presence of a band corresponding to the expected molecular weight of the His-tagged protein (54 kDa) were pooled, dialyzed overnight against 50 mM potassium phosphate buffer pH 8.0 containing 0.1 mM PLP. The purified protein was routinely stored at 4 °C in 50 mM potassium phosphate buffer pH 8.0 containing 0.1 mM PLP . Protein yields: WT 80 mg/L of media, A1 6 mg/L, B1 7 mg/L, B2 15 mg/L, B3 35 mg/L, C1 28 mg/L. The protein concentration was determined by absorbance at 280 nm using a calculated molar extinction coefficient of 62.8 $mmol^{-1}$ cm^{-1} for a single subunit with a molecular weight of 54 kDa (Xpasy Protparam).

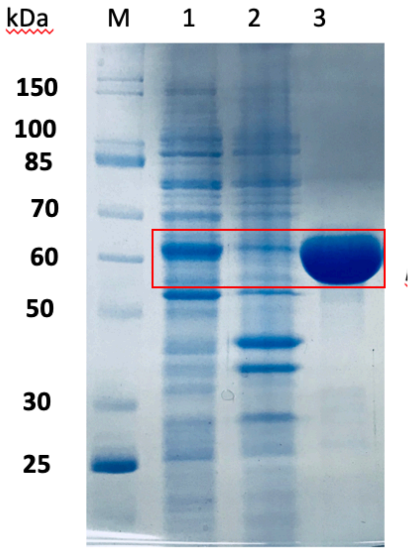


Figure 1| SDS-PAGE of *He*WT purification.
M: Unstained Protein Standard Broad Range (10-200 kDa); **1:** Crude extract **2:** Insoluble fraction **3:** Pure *He*WT

2.6.2 Enzymatic activity

Activity measurements were performed spectrophotometrically at 245 nm by determining the production of acetophenone at 25 °C in a 1.5 mL cuvette (total volume 1 mL) for 5 min.[4] One unit (U) of activity is defined as the amount of enzyme required for the production of 1 µmol of acetophenone per min under reference conditions: 2.5 mM (*S*)-MBA, 2.5 mM pyruvate, 0.25% DMSO, 0.1mM PLP and an appropriate amount of enzyme in 50 mM potassium phosphate buffer pH 8.0, ε = 12.6 mM^{-1} cm^{-1}.

2.6.3 pH effect on enzyme activity and stability

Experiments to investigate the optimum pH for enzyme activity were performed using the spectrophotometric assay outlined above with some modifications. In this case, a universal buffer (25 mM citric acid, 25 mM KH_2PO_4, 25 mM Tris, 12.5 mM $Na_2B_4O_7$, and 25 mM KCl) was used instead of potassium phosphate buffer to cover a broad range of pH values (from pH 6-12).[5] Similarly, pH stability experiments were performed in universal buffer. The purified enzyme was first diluted in

universal buffer at the desired pH and stored at 4 °C for 60 minutes. After the incubation period, the residual enzyme activity was measured using the spectrophotometric assay described above.

2.6.4 Temperature effect on enzyme activity and stability

Experiments to investigate the optimum temperature for enzyme activity were performed using the spectrophotometric assay outlined above across a range of temperatures (from 25 °C to 60 °C). For the stability experiment, the enzyme was stored in potassium phosphate buffer 50 mM pH 8 in the presence of pyridoxal 5'-phosphate (PLP) 1 mM and incubated at the desired temperature for up to 24 hours. After the incubation period, the residual enzyme activity was measured using the spectrophotometric assay described above.

2.6.5 10 mM scale biotransformations

For the substituted acetophenone substrates (**1a** to **2a**), batch reactions were performed in potassium phosphate buffer (50 mM, pH 8.0, 10% v/v DMSO), containing 10 mM of the ketone substrate, 50 eq. of L-alanine, 0.1 mM PLP and 0.1 mg/mL (1.9 µM) of *He*WT, in a total reaction volume of 200 µL. Similarly, for the small cyclic ketone substrates (**3a** to **6a**), batch reactions were performed in potassium phosphate buffer (50 mM, pH 8.0, containing 10 mM of the ketone substrate, 1 eq. of (*S*)-MBA, 0.1 mM PLP and 1 mg/mL of *He*WT, in a total reaction volume of 1 mL.10 % v/v DMSO was used in the case of 3a to improve solubility. The reactions were incubated at 37 °C with gentle shaking for up to 24 hours. Samples (100 µL aliquots) were quenched with 0.2% HCl every 15 min for the first 60 min of reaction, followed by sampling after 2 h, 4 h, 6h and 24 h, respectively. All samples were analysed using a HPLC equipped with a Waters X-Bridge column (C18, 3.5 µm, 2.1 mm x 30.0 mm). The aromatic substrates and products were detected using a UV detector at 210 nm, 250 nm or 280 nm following a gradient run (A: 0.01 % Ammonia in water, B: Acetonitrile. Gradient: 0 min 5 % A 95 % B; 3.10 min 0 % A 100 % B; 3.50 min 0% A 100 % B; 3.51 min 95 % A 5% B; 4.50 min 95 % A 5% B) at 40 °C. The flow rate was maintained at 0.8 mL/min. The retention times

in minutes were confirmed by comparison with commercially available compounds (Table 2). and conversions determined using a calibration curve.

Table 2| HPLC retention times of ketones and amines

Ketones	Retention time (min)	Amines	Retention time (min)
Acetophenone	2.0	(*S*)-(−)-α-methylbenzylamine	1.9
para-NO_2-acetophenone	2.1	(*S*)-*para*-NO_2-phenylethanamine	1.9
para-CN-acetophenone	1.8	(*S*)-*para*-CN-phenylethanamine	1.6

2.6.6 Kinetic parameters

The kinetic parameters for the small cyclic ketones were obtained by measuring the initial velocities of the enzymatic reaction and curve fitting according to the Michaelis-Menten equation using GraphPad Prism 5 software (GraphPad Software, Inc). For ketones 3a to 6a, the activity assay was performed at pH 8.0, 30 °C, in the presence of 5 mM (*S*)-1-phenylethylamine, 0.1 mM PLP, various concentrations of the ketone (0.5 to 75 mM), 0.1 mM PLP, 0.5% v/v DMSO, and an appropriate amount of enzyme (0.1-0.5 mg/mL). The activity was determined by measuring the production of acetophenone at 245 nm (ε = 12.6 mM^{-1} cm^{-1}). All experiments were conducted in triplicate.

2.6.7 Evaluation of enantioselectivity

For the determination of enantioselectivity, batch reactions (1 mL total volume), were carried out as described in the biotransformation methods. After 24 hours, the reactions were basified with the addition of 5 M NaOH (100 µL), followed by extraction with ethyl acetate (900 µL). To facilitate enantiomeric separation and allow for GC analysis, the amine products were acetylated with the addition of triethylamine (5 µL) and acetic anhydride (5 µL). For analysis of the small cyclic amines, the reaction mixtures were saturated with NaCl prior to basification and extracted with a 3:1 mixture of isopropanol and chloroform (2 × 500 µL). The amine products were then acetylated as described above. The samples were

analysed by GC-FID using a Thermo Scientific™ Trace™ 1310 GC equipped with an Agilent CHIRASIL-DEX CB (25 m x 0.25 mm x 0.25 mm) column. The following method was used: injector temperature 230 °C, split ratio 1:10, continuous flow 1.7 mL/min: 40 °C for 2 min, 20 °C/min to 150 °C, hold for 5 min, then 30 °C/min to 225 °C, then hold for 8 min, FID temperature 250 °C. Helium was used as carrier gas. The retention times in minutes are presented in Table 3. The enantiomeric purity was determined by comparison with commercially available compounds.

Table 3| GC retention of aromatic and small cyclic amines

Amine	Retention time (min)
(*S*)-*para*-NO_2-phenylethanamine	20.893
(*R*)- *para*-NO_2-phenylethanamine	21.098
(*S*)-*para*-CN-phenylethanamine	18.150
(*R*)-*para*-CN-phenylethanamine	18.277
(*S*)-tetrahydrothiophen-3-amine	13.473
(*R*)-tetrahydrothiophen-3-amine	10.135
(*S*)-tetrahydrofuran-3-amine	10.215
(*S*)-1-methylpyrrolidin-3-ylamine	10.032
(*R*)-1-methylpyrrolidin-3-ylamine	10.240
(S)-1-methyl-piperidin-3-ylamine	10.840
(R)-1-methyl-piperidin-3-ylamine	11.150

2.7 Syntheses of small cyclic molecules: alcohols, amines and amides

2.7.1 Expression and purification of KRED1-*Pglu*

KRED1-*Pglu* was prepared as previously reported.[2] *E.coli* BL21(DE3)STAR cells were transformed with the pET26b(+) vector containing the gene encoding for KRED1-*Pglu*. Transformants were selected by growth on LB agar plates supplemented with 25 μg/mL

kanamycin. A single colony was used to inoculate 50 mL of LB containing 25 µg/mL kanamycin. The starter culture was left to grow overnight at 37 °C, 150 rpm. The seed culture was then diluted into 300 mL of Terrific Broth to an initial OD_{600} of 0.05. When the OD_{600} reached 0.8, the cultures were induced for 20 h with the addition of isopropyl-β-thiogalactopyranoside (IPTG) to a final concentration of 0.5 mM. The cells were then harvested by centrifugation at 4 000 rpm for 20 min. The resulting pellet was resuspended in loading buffer (50 mM Tris HCl, 100 mM NaCl, 6 mM imidazole, pH 8.0), employing 5 mL per gram of cell pellet. The cells were disrupted by sonication (10 cycles, 30s sonication followed by 30s cooling on ice, 40% amplitude). After centrifugation (14 000 rpm, 4°C, 45 min), the supernatant was clarified by filtration (0.45 µm filter). Purification of KRED1-*Pglu* was carried out by affinity chromatography using an ÄKTA Start chromatography system. A 1 mL HisTrap FF column precharged with 0.1 M $NiSO_4$ was employed for the purification. In brief, the system was equilibrated with loading buffer and the filtered sample loaded. The column was then washed with 20 column volumes of the same buffer at a flow rate of 1 mL/min followed by an intermediate step with 10 % of elution buffer (50 mM, Tris HCl buffer, pH 8.0 containing 100 mM NaCl and 250 mM imidazole) to remove non-specifically bound proteins. An isocratic elution step using elution buffer was then applied to collect the His-tagged protein. Samples of the pellet, crude extract and fractions collected were analysed by SDS PAGE using a 12 % polyacrylamide gel stained with Instant Blue. A broad range protein marker was used to determine relative molecular weight. The fractions showing the presence of a band corresponding to the expected molecular weight of the His-tagged protein (29 kDa) were pooled, dialyzed overnight against 50 mM Tris HCl buffer, pH 8.0 and routinely stored at -20 °C.

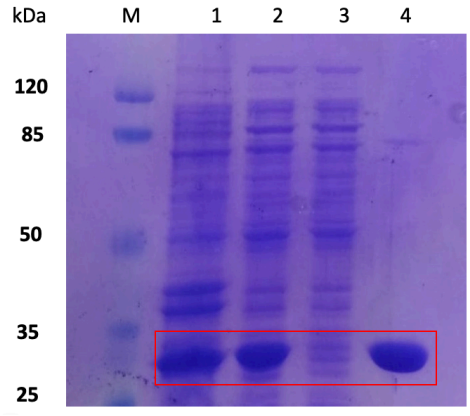


Figure 2| SDS-PAGE of KRED1-*Pglu* purification.
M: Pierce prestained protein molecular weight maker (20 -120 kDa) (ThermoFisher Scientific); **1:** Crude extract; **2:** Insoluble fraction; **3:** Flow through**; 4:** Pure KRED1-*Pglu*

2.7.2 KRED1-*Pglu* activity assay

Activity measurements were performed spectrophotometrically at 340 nm by determining the consumption of NAD(P)H at 25 °C in a 1.5 mL microcuvette (total volume 1 mL) for 5 min.[2] One unit of activity is defined as the amount of enzyme which catalyses the consumption of 1 µmol of NAD(P)H per minute under reference conditions: 0.25 mM NAD(P)H 0.47 mM benzil as substrate (added as concentrated DMSO solution; final DMSO concentration in cuvette amounts to 0.1 %), and an appropriate amount of enzyme in 50 mM Tris HCl buffer, pH 8.0, ε = 6.22 mM^{-1} cm^{-1}.

2.7.3 Expression and purification of *Bm*GDH

*Bm*GDH was prepared as previously reported.[2] *E.coli* BL21(DE3)STAR cells were transformed with plasmid containing the gene encoding for *Bm*GDH. Transformants were selected by growth on LB agar plates supplemented with 100 µg/mL ampicillin. A single colony was used to inoculate 50 mL of LB containing 100 µg/mL kanamycin. The seed culture was then diluted into 300 mL of Terrific Broth to an initial OD_{600} of 0.05. When the OD_{600} reached 0.4-0.5, the cultures were induced for 5-6 h with the addition of IPTG to a final concentration of 0.1 mM (50

ng/mL of anhydrotetracycline was also added). The cells were then harvested by centrifugation at 4 000 rpm for 30 min. The wet cell pellet was weighted and stored at -20 °C. The pellet was thawed and resuspended in 50 mM Tris HCl, 100 mM NaCl, 6 mM imidazole, pH 8.0, employing 5 mL per gram of pellet. The cells were disrupted by sonication (10 cycles of 30 s sonication followed by 30 s cooling on ice). After centrifugation (14 000 rpm, 4°C, 45 min), the supernatant was clarified by filtration (0.45 µm filter). Purification of *Bm*GDH was performed using the same procedure outlined for KRED1-*Pglu*.

2.7.4 *Bm*GDH Activity Assay

Activity measurements were performed spectrophotometrically at 340 nm by determining the production of NAD(P)H at 25 °C in a 1.5 mL microcuvette (total volume 1 mL) for 5 min.[2] One unit of activity is defined as the amount of enzyme which catalyses the production of 1 µmol of NAD(P)H per minute under reference conditions: 40 mM glucose, 1 mM NAD^+ and an appropriate amount of enzyme in 50 mM Tris HCl buffer, pH 8, ε = 6.22 mM^{-1} cm^{-1}.

2.7.5 10 mM scale biotransformations for the preparation of small cyclic alcohols

1 mL batch reactions were performed in Tris-HCl buffer (50 mM, pH 8.0), containing 10 mM ketone substrate, 40 mM glucose, 0.1 mM $NADP^+$. 20 mU/mL KRED1-*Pglu* and 1 U/mL GDH. The reactions were incubated at 30 °C with gentle shaking for up to 24 hours. To prepare samples for GC analysis, the reaction mixtures were saturated with NaCl prior to basification and extracted with a 3:1 mixture of isopropanol and chloroform (2 × 500 µL). The alcohol product was then derivatized with the addition of 20 µL of acetic anhydride and 20 µL of pyridine followed by heating at 70 °C for 20 min. The samples were analysed by GC-FID using a Thermo Scientific™ Trace™ 1310 GC equipped with an Agilent CHIRASIL-DEX CB (25 m x 0.25 mm x 0.25 mm) column. The following method was used: injector temperature 230 °C, split ratio 1:10,

continuous flow 1.7 mL/min: 40 °C for 2 min, 20 °C/min to 150 °C, hold for 5 min, then 30 °C/min to 225 °C, then hold for 8 min, FID temperature 250 °C. Helium was used as carrier gas. The retention times in minutes are presented in Table 4. Molar conversions were determined by comparison to commercially available standards.

Table 4| GC retention of aromatic and small cyclic amines

Alcohol	Retention time (min)
(*R*)-Tetrahydrofuran-3-ol	6.250
(*S*)-Tetrahydrofuran-3-ol	6.480

2.7.6 Expression and purification of *Ms*AcT

*Ms*AcT was prepared as previously reported.[6] *E.coli* BL21(DE3)STAR cells were transformed with the pET26b vector containing the gene encoding for *Ms*AcT. Transformants were selected by growth on LB agar plates supplemented with 25 µg/mL kanamycin. A single colony was used to inoculate 50 mL of LB containing 25 µg/mL kanamycin. The starter culture was left to grow overnight at 37 °C, 150 rpm. The starter culture was in turn used to inoculate 300 mL of TB to an initial OD_{600nm} of 0.1. Cultivation was carried out 37 °C, 150 rpm until the OD_{600nm} reached a value of 0.5. The expression of *Ms*AcT was induced with the addition of isopropyl-β-d-thiogalactopyranoside (IPTG) to a final concentration of 0.1 mM. Expression was carried out at 25 °C, 150 rpm. After 16 h the cells were then harvested by centrifugation at 4 000 rpm, 4 °C for 20 min. The resulting pellet was resuspended in loading buffer (100 mM potassium phosphate buffer, pH 8.0 containing 100 mM NaCl, and 6 mM imidazole), employing 5 mL per gram of cell pellet. The cells were disrupted by sonication (10 cycles of 30 s sonication followed by 30 s cooling on ice). After centrifugation (14 000 rpm, 4°C, 45 min), the supernatant was clarified by filtration (0.45 µm filter). Purification of *Ms*AcT was carried out by affinity chromatography using an ÄKTA Start chromatography system. A 1 mL HisTrap FF column precharged with 0.1

M NiSO4 was employed for the purification. In brief, the system was equilibrated with loading buffer and the filtered cellular extract loaded. The column was then washed with 20 column volumes of the same buffer at a flow rate of 0.5 mL/min followed by an intermediate step with 10% of elution buffer (100 mM potassium phosphate buffer, pH 8.0 containing 100 mM NaCl and 250 mM imidazole) to remove non-specifically bound proteins. An isocratic elution step using elution buffer was then applied to collect the His-tagged protein. Samples of the pellet, crude extract and fractions collected were analysed by SDS PAGE using a 12% polyacrylamide gel stained with Instant Blue. A broad range protein marker was used to determine relative molecular weight. The fractions showing the presence of a band corresponding to the expected molecular weight of the His-tagged protein (25.6 kDa) were pooled and the buffer was exchanged to 100 mM potassium phosphate buffer pH 8.0 using a Vivaspin 20 (MWCO 30 000 Da). The purified protein was routinely stored at 4 °C.

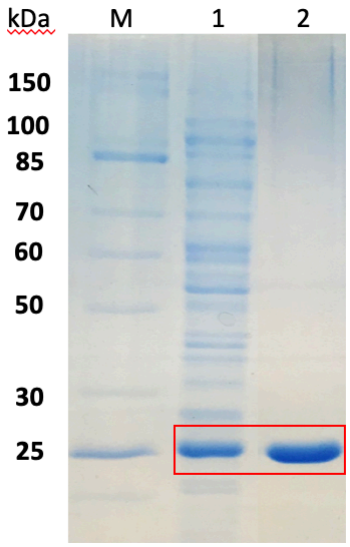


Figure 2| SDS-PAGE of *Ms*AcT purification.
M: Unstained Protein Standard Broad Range (10 -200 kDa); **1:** Crude extract
2: Pure *Ms*AcT.

2.7.7 *Ms*AcT activity assay

Activity measurements were performed spectrophotometrically at 400 nm by determining the formation of *para*-nitrophenol at 25 °C (total volume 1 mL) for 2 min.[6] One unit of activity is defined as the amount of enzyme which catalyzes the consumption of 1 µmol of *para*-nitrophenyl acetate per minute under reference conditions, namely 0.1 mg/mL *para*-nitrophenyl acetate, 0.1 % v/v EtOH, and an appropriate amount of *Ms*AcT in 100 mM phosphate buffer, pH 8.0. ε = 15.0 mM^{-1} cm^{-1}.

2.7.8 10 mM scale biotransformations

1 mL batch reactions were performed in phosphate buffer (100 mM, pH 8.0), containing 20 mM amine substrate, 10 % v/v acyl donor and 1 mg/mL *Ms*AcT. The reactions were incubated at 25 °C with gentle shaking for up to 24 hours. Control reactions, to which no enzyme was added was carried out in parallel. Reaction progress was monitored every 15 min for the first 60 min of reaction, followed by sampling after 2 h, 4 h, 6h and 24 h, respectively. For analysis, the reaction mixtures were saturated with NaCl prior to basification and extracted with a 3:1 mixture of isopropanol and chloroform (2 × 500 µL). Molar conversions were determined by following the depletion of the amine substrate using GC-FID equipped with a Thermo Scientific™ Trace™ 1310 GC equipped with an Agilent CHIRASIL-DEX CB (25 m x 0.25 mm x 0.25 mm) column. The following method was used: injector temperature 230 °C, split ratio 1:10, continuous flow 1.7 mL/min: 40 °C for 2 min, 20 °C/min to 150 °C, hold for 5 min, then 30 °C/min to 225 °C, then hold for 8 min, FID temperature 250 °C. Helium was used as carrier gas. The retention times in minutes for the amine substrates are presented in Table 3.

2.8 Preparation of biocatalysts for application in continuous flow

2.8.1 Activation of enzyme carriers

Briefly, 1 g of resin was treated with 2 mL of modification buffer (100 mM sodium borate and 2 M iminodiacetic acid in 50 mM phosphate

buffer pH 8.5) under gentle agitation for 2 hours at room temperature. The resin was filtered and washed with distilled water. 5 mL of metal buffer (1 M NaCl and 5 mg/mL $CoCl_2$ in 50 mM phosphate buffer pH 6.0) was applied and incubated with the resin for 2 h under gentle agitation at room temperature. Finally the resin was filtered, washed extensively with distilled water and stored at 4 ºC until ready for further use.

2.8.2 Immobilization of biocatalysts

10 mL of enzyme solution, containing the desired amount of protein, was added to 1 g of carrier and incubated under orbital shaking at room temperature. The activity of the supernatant was monitored periodically. When no activity remained, the solution was filtered off and the resin was washed with distilled water. 3 mL of desorption buffer (50 mM EDTA, 0.5 M NaCl in 20 mM phosphate buffer pH 7.2) was added to eliminate the metal before the addition of blocking buffer (3M glycine in 50 mM phosphate buffer pH 8.5). The mixture was left shaking for 20 h and finally filtered and washed with H_2O and the biocatalyst was stored in the appropriate storage buffer.[7]

2.8.3 Preparation of DEX50

1.67 g dextran was suspended in 50 mL of distilled water. To oxidise 50%, 1.98 g $NaIO_4$ was added and incubated for 90 min at room temperature under gentle agitation. The solution was dialyzed against 1 L dH_2O. After 1 h, the dialysis buffer was changed and again after another hour. It was then left overnight. The next morning, another buffer change was made and it was incubated for a further 8 h. The pH was adjusted to pH 8.5 with concentrated sodium bicarbonate buffer.[8]

2.8.4 Surface coating with DEX50

After protein immobilization, a solution of DEX50 (10 mL/g resin) was incubated with the resin for 16 h under gentle agitation at room temperature. Following this, solid sodium borohydride was added to a final concentration of 1 mg/mL and incubated for 30 min under the

same conditions.[8] After the reduction step, the resin was washed with distilled water, followed by the desorption and blocking steps as outlined in the standard immobilization procedure above.

2.8.5 Determination of the stabilisation of the quaternary structure of multimeric enzymes

50 mg of the immobilised protein preparation was incubated in 100 µl of 4 % (w/v) sodium dodecyl sulfate (SDS), in the presence of 10 % mercaptoethanol. The suspension was boiled for 30 min at 99 ºC to promote the release of any non-covalently immobilised protein.[7] Samples of the supernatant were then analysed by SDS-PAGE following standard protocols.

2.8.6 Functionalization of Sepharose CL-6B

10 g of agarose was suspended in 44 mL of dH_2O, 16 mL of acetone, 3.28 g NaOH, and 0.2 g $NaBH_4$. 11 mL of epichlorhydrine was added dropwise on ice. The suspension was stirred under gentle agitation for 16 h and washed with an excess of dH_2O. [9]

2.8.7 Activity of immobilized *He*WT

The activity of immobilized *He*WT was determined by mixing 25-50 mg of biocatalyst and 10 mL of reaction mixture (2.5 mM pyruvate, 2.5 mM S-MBA and 0.25 % DMSO in 50 mM phosphate buffer pH 8 containing 0.1 mM PLP) in a 15 mL reaction tube cap.[10] The final reaction mixture was incubated at room temperature under orbital shaking. The absorbance at 245 nm was measured along the time as single readings. One unit of ω-transaminase activity was defined as the amount of enzyme required for the production of 1 µmol of acetophenone per minute.

2.8.8 Activity of immobilized *Ms*AcT

The activity of immobilized *Ms*AcT was determined by mixing 25-50 mg of biocatalyst and 10 mL of reaction mixture (0.1 mg/mL *para*-nitrophenyl acetate, 0.1 % v/v EtOH in 100 mM phosphate buffer pH 8.0) in a 15 mL

reaction tube cap.[11] The final reaction mixture was incubated at room temperature under orbital shaking. The absorbance at 400 nm was measured along the time as single readings. One unit activity was defined as the amount of enzyme which catalyzes the consumption of 1 µmol of *para*-nitrophenyl acetate per min .

2.8.9 Continuous flow biotranformations

The continuous flow biotransformations were performed using a R2+/R4 flow reactor commercially available from Vapourtec equipped with an Omnifit glass column (6.6 mm i.d x 100 mm length) filled with 1.5 - 2 g of biocatalyst. A first washing step with buffer was performed at flow rate of 0.4 mL x min^{-1} for 30 minutes. Substrate solutions were prepared as outlined in the relevant chapters and mixed in a T-tube when appropriate. The resulting flow stream was directed to the packed-bed reactor with the biocatalyst, maintained at the desired temperature. The flow rate was varied in order to obtain the desired residence time. Finally the product were analysed by HPLC or GC.

References:

1. Knaus, T., Böhmer, W. & Mutti, F. G. Amine dehydrogenases: Efficient biocatalysts for the reductive amination of carbonyl compounds. *Green Chem.* **19**, 453–463 (2017).

2. Dall'Oglio, F. *et al.* Flow-based stereoselective reduction of ketones using an immobilized ketoreductase/glucose dehydrogenase mixed bed system. *Catal. Commun.* **93**, 29–32 (2017).

3. Cerioli, L., Planchestainer, M., Cassidy, J., Tessaro, D. & Paradisi, F. Characterization of a novel amine transaminase from Halomonas elongata. *J. Mol. Catal. B Enzym.* **120**, 141–150 (2015).

4. Schätzle, S., Höhne, M., Redestad, E., Robins, K. & Bornscheuer, U. T. Rapid and sensitive kinetic assay for characterization of ω-transaminases. *Anal. Chem.* **81**, 8244–8248 (2009).

5. Davies, M. . A universal buffer solution for use in ultra-violet spectrophotometry. *Analyst* **84**, 248–251 (1959).

6. Contente, M. L., Pinto, A., Molinari, F. & Paradisi, F. Biocatalytic N-Acylation of Amines in Water Using an Acyltransferase from Mycobacterium smegmatis. *Adv. Synth. Catal.* **360**, 4814–4819 (2018).

7. Guisán, J. M. *Immobilization of enzymes and cells*. (Human Press, 2000).

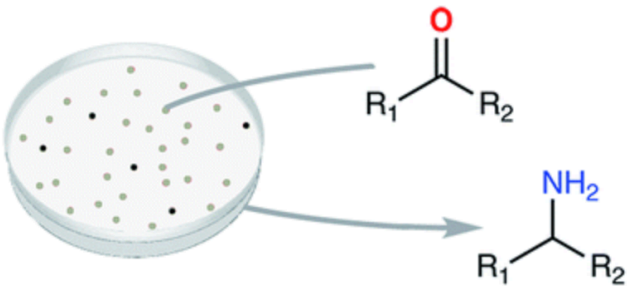
8. Pessela, B. C. *et al.* Stabilization of the quaternary structure of a hexameric alpha-galactosidase from Thermus sp. T2 by immobilization and post-immobilization techniques. *Process Biochem.* **43**, 193–198 (2008).

9. Guisan, J. M. *et al.* Improvement of Enzyme Properties with a Two-Step Immobilizaton Process on Novel Heterofunctional Supports. *Biomacromolecules* **11**, 3112–3117 (2010).

10. Planchestainer, M. *et al.* Continuous flow biocatalysis: Production and in-line purification of amines by immobilised transaminase from Halomonas elongata. *Green Chem.* **19**, 372–375 (2017).

11. Contente, M. L., Farris, S., Tamborini, L., Molinari, F. & Paradisi, F. Flow-based enzymatic synthesis of melatonin and other high value tryptamine derivatives: A five-minute intensified process. *Green Chem.* **21**, 3263–3266 (2019).

Chapter 3: Characterisation of Halomonas elongata ω-transaminase (*He*WT) mutants



Acknowledgements
The work presented in this chapter was a collaborative effort between the doctoral candidate (EH) and Dr. Matteo Planchestainer (MP) under the supervision of Prof. Francesca Paradisi. MP was responsible for the design of the solid-phase screen, the generation of the mutant libraries by error-prone PCR, and the screening of the isolated mutants for activity towards the substituted acetophenones. EH was responsible for the full characterization of all isolated mutants and the evaluation of enantiomeric excess in the case of the substituted acetophenones. All experiments regarding the small cyclic ketones were performed by EH.

3.1 Introduction

The prevalence of chiral amines in natural products, (agro)chemicals and active pharmaceutical ingredients has led to enormous interest in the engineering and evolution of amine transaminases (ATAs) for the production of high-value compounds.[1–3] The success of this approach however, relies heavily on efficient screening methodologies to allow for the detection of improved variants. In an effort to overcome some of the challenges associated with well-established methodologies, our group recently reported on a simple and reliable solid phase screening method, that utilises (*S*)-(-)-α-methylbenzylamine as a background depletion agent to eliminate interference from endogenous pyruvate produced within the bacterial cells.[4]

In this chapter, the newly developed SPS was applied for the high-throughput evaluation of a fully randomised mutant library of the (*S*)-selective ATA from *Halomonas elongata* (*He*WT) towards two structurally distinct ketone substrates: i) *para*-nitro acetophenone and ii) tetrahydrothiophen-3-one. To test the validity of the screen, the isolated mutants were assessed in terms of kinetic parameters, which revealed modest improvements in activity towards the target substrates. To support these findings, the effects of the various mutations are discussed based on structural analysis of the *He*WT crystal structure. Finally the isolated mutants were further characterized to determine the impact of the mutations on catalytic activity at different temperature and pH-values. These changes are difficult to predict based on structural analysis alone and were therefore verified experimentally.

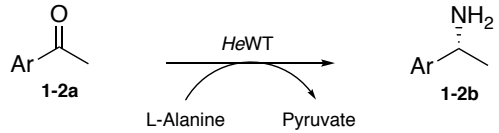
3.2 Characterization of *He*WT mutants evolved towards substituted acetophenones

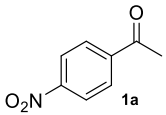
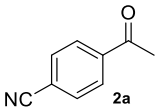
*He*WT has previously been characterized as an incredibly robust biocatalyst, demonstrating a very broad substrate scope and excellent tolerance in a wide range of organic solvents.[5] Cerioli *et al.* previously demonstrated the conversion of a comprehensive range of aldehydes, α-ketoacids and amines into their respective products, however like many

known ATAs, *He*WT showed poor activity towards aromatic and aliphatic ketones.[6,7] In the case of ketones, particularly aromatic ones, the carbonyl carbon is often not sufficiently electrophilic, resulting in a slow and thermodynamically unfavourable reaction.[7] Within this context, *He*WT was subjected to directed evolution using error-prone PCR, to generate a completely randomised mutant library with a high number of mutations. The enzyme has minimal activity towards the aromatic substrate *para*-nitroacetophenone (**1a**) and this was selected as amino acceptor for the initial screening, using *ortho*-xylylenediamine as amino donor. DMSO (10 % v/v) was required for substrate solubility and enhanced cell-permeability.

The discrimination between wild-type and an improved variant relies on the rapidity with which the enzyme converts the substrate *in vivo*. Screening of *ca.* 15 000 colonies provided two variants with enhanced activity towards *para*-nitroacetophenone. To test the validity of the SPS, the two new variants, referred to as A1 and B1, were over-expressed and purified for further characterization. Using the standard expression and purification procedure reported for the wild-type enzyme, significantly lower protein yields were obtained (WT:50mg/L culture; A1:6mg/L culture; B1:7mg/L culture). The specific activity of the mutants was also lower when assessed using the standard acetophenone assay (WT: 4.5 U/mg; A1 0.8 U/mg/ and 1.3 U/mg).[8] Perhaps most notable, however, was the 2-fold increase in turnover frequency (TOF) displayed by the A1 and B1 mutants towards the target substrate *para*-nitroacetophenone with respect to the wild-type enzyme. Encouraged by these results, the performance of the variants was next examined in batch. Biotransformations were performed on a 10 mM scale using 50 equivalents of L-alanine as the amino donor (total reaction volume: 1 mL). By monitoring the production of (*S*)-*para*-NO_2-phenylethanamine and the depletion of *para*-nitroacetophenone by HPLC, higher molar conversions were achieved by the mutants without any loss in enantioselectivity (Table 1).

Table 1| *He*WT evolution towards substituted acetophenones.



	WT			A1			B1			B2		
Substrate	**TOF (10^{-3} s^{-1})**	**m.c. (%)**	***e.e.* (%)**	**TOF (10^{-3} s^{-1})**	**m.c. (%)**	***e.e.* (%)**	**TOF (10^{-3} s^{-1})**	**m.c. (%)**	**e.e (%)**	**TOF (10^{-3} s^{-1})**	**m.c. (%)**	***e.e.* (%)**
 **1a**	36 ± 6	4	>99 (*S*)	66 ± 9	6	>99 (*S*)	65 ± 26	6	>99 (*S*)	92 ± 5	7	>99 (*S*)
 **2a**	4 ± 1	9	87 (*S*)	50 ± 7	11	94 (*S*)	127 ± 5	12	>99 (*S*)	229 ± 7	11	>99 (*S*)

Turnover frequencies (TOF) measured at 10 mM carbonyl concentration, 24 h molar conversions (m.c.) and enantiomeric excess (*e.e.*) for wild-type *He*WT and isolated variants towards *para*-nitroacetophenone (**1a**) and *para*-cyanoacetophenone (**2a**). Biotransformations were performed with 10 mM ketones, 500 mM L-Alanine, 0.1 mM PLP, 0.1 mg/mL enzyme in 50 mM phosphate buffer pH 8 and 10 % *(v/v)* DMSO at 37 °C (see experimental). All experiments were conducted in triplicate and the standard error is reported accordingly. Mutations; A1: W56C, V435A; B1: W56C, L211V, L306M; B2: W56C, L211V, L306M, V361A, Q388R, P453L.

Sequencing of the mutants identified two amino acid changes in the A1 variant, (W56C, V435A), while the B1 variant displayed three amino acid changes (W56C, L211V, L306M). Interestingly, both mutants harbour a tryptophan to cysteine substitution at position 56, which is located in the active site (Figure 1a). This residue has previously been identified as a hotspot in *in silico* rational design studies.[9,10] In this case, removing the large indole ring and replacing it with the smaller cysteine side chain may allow for easier substrate binding. Furthermore, the thiol can promote hydrogen bonding with the aromatic substituent and stabilise *para*-nitroacetophenone. The L306M mutation is peripheral and not conserved with regards to the sequence, and is therefore somewhat more difficult to rationalise. It is possible that the longer side chain of methionine may form more stabilising hydrophobic interactions with surrounding hydrophobic residues (M126, V302 and F313) (Figure 1b). This hydrophobic cluster may in turn stabilise regions of the protein that mediate dimerization.

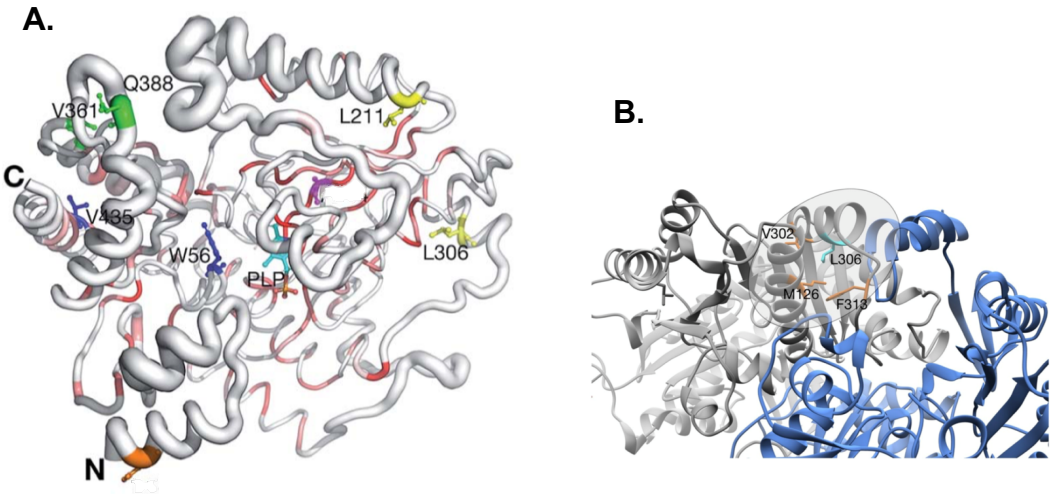


Figure 1| A. *He*WT 3D structure and mutant residue positions. The crystal structure was determined at a resolution of 2 Å, as described by Planchestainer et al. Atomic coordinates and structure factors have been deposited in the Protein Data Bank under PDB accession code 6GWI. Mutated residues in variants A1 (blue), B1 (yellow), and B2 (green) are shown as sticks. P453 from the B1 variant is not present in the model. The *N*- and *C*- *termini* are indicated and PLP is shown in sticks. (PDB code: **B. Location of the L306M mutation on the *He*WT crystal structure.** Mutation L306 to methionine may result in the formation of additional hydrophobic interactions with neighbouring hydrophobic residues (orange sticks). This hydrophobic cluster would may stabilise the dimer interface. This figure was generated using Chimera.

Both variants were subjected to a second round of error-prone PCR and the libraries screened as before with **1a**. Interestingly, in this case the positive colonies were isolated after a significantly shorter incubation period (2–15 minutes compared to 25 minutes for the parental colony). While the A1 template did not provide any significant hits, an improved variant was isolated from the B1 library. Upon expression and purification (Protein yield: 15 mg/L culture; Specific activity: 1.3 U/mg), the new mutant, identified as B2, afforded comparable molar conversion after 24 hours and a further 1.5-fold increase in turn-over frequency (Table 1). The *e.e.* measured at 24 h was in all cases >99 %. A third round of mutagenesis, using the B2 variant as a template failed to identify better variants. The second round of evolution introduced three additional mutations (V361A, Q388R, P453L) in the B2 variant, which are also located outside of the active site and all are exposed to the solvent, thus their side-chains do not make any significant stabilizing intramolecular interactions (Figure 1a).

A second substrate, *para*-cyanoacetophenone (**2a**), was also investigated. *He*WT wild-type has negligible activity towards this molecule, even lower than the nitro substitution, with a turnover frequency of 4×10^{-3} s^{-1}. While the activity of all 3 isolated variants was investigated towards this substrate, the B2 mutant was the best performing, displaying an impressive 60-fold increase in turn-over frequency (229×10^{-3} s^{-1}), and enhanced stereoselectivity, affording >99 % of the (*S*)-enantiomer (Table 1).

While these results effectively demonstrate the applicability of the screening methodology in ATA evolution towards target substrates, further rounds of mutagenesis failed to identify more active variants as the colour change was too rapid and did not allow sufficient discrimination between parental activity and mutant. Tuning the screening conditions to slow the reaction, however may extend the screening window.[4] In addition, through modulation of the parental activity by regulating the expression levels, this screening method could

be a very useful tool in further rounds of evolution for the identification of more active variants.[11]

In addition to the experiments carried out thus far, it is essential following any mutagenesis project to experimentally identify changes, if any, in the temperature and pH requirements of mutants with respect to the wild-type enzyme. Considering the structure of an enzyme is highly instrumental in its biological function, creating subtle changes in the sequence of amino acids that makes up an enzyme can improve properties such as activity or pH and temperature stability. The opposite however also applies. Taking this into consideration each of the isolated variants were characterised in terms of activity and stability at different pH values and temperatures. The influence of pH on the activity of the variants was investigated using pyruvate as the amino acceptor and (*S*)-MBA as the amino donor in universal buffer across a pH range of 6-12.[12] A pH profile was generated (see Figure 2) which shows that the maximum activity was reached at a pH value of 10, with each mutant showing little activity at values less than 7 or higher than 11. Interestingly, variants A1, B1 and B2 displayed activity across a broader range of pH values respect to the wild-type enzyme.

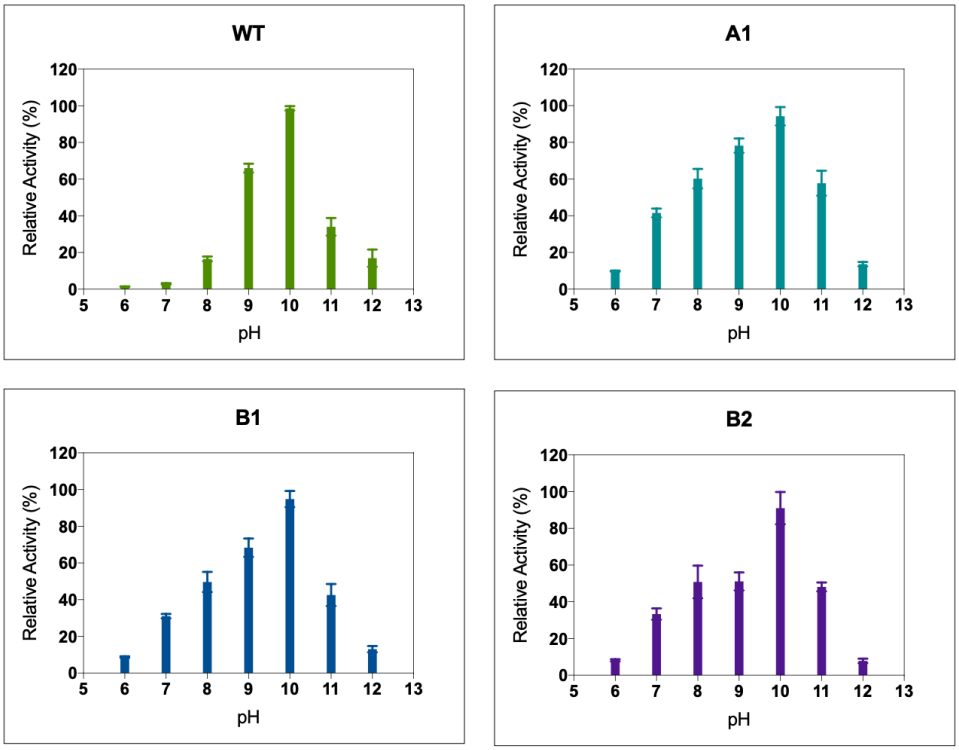


Figure 2 | pH effect on enzyme activity. Activity experiments were performed in universal buffer at the desired pH (from pH 6 – 12) according to the standard transaminase activity assay described in the experimental. The formation of acetophenone was quantified at 245 nm. 100 % activity corresponds to 4.0 U/mg, 0.98 U/mg, 1.2 U/mg and 1.3 U/mg respectively. All measurements were performed in triplicate.

In terms of stability, all variants were highly stable across the range of values investigated (Figure 3). While the highest activity was reached at pH 10, the wild type and mutants displayed optimal stability at pH 9.

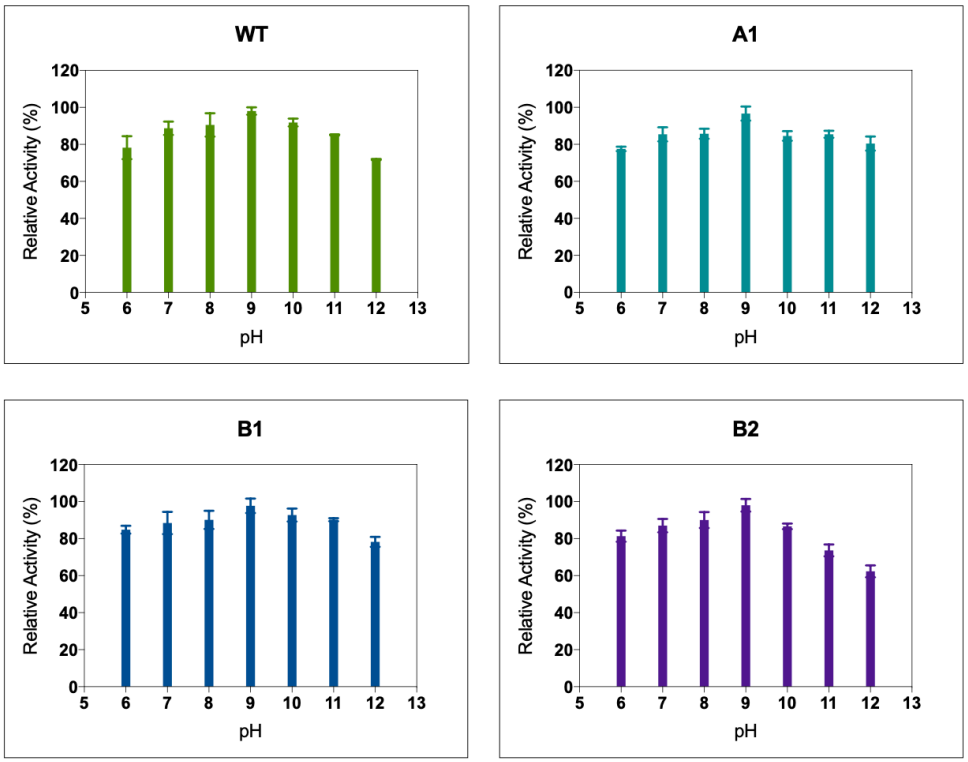


Figure 3 | pH effect on enzyme stability. Purified enzyme was diluted with universal buffer at the desired pH (from pH 6 – 12) and stored at 4 ℃ for 60 min. After incubation, the residual activity was determined using the standard enzyme activity assay described above. The formation of acetophenone was quantified at 245 nm. 100 % activity corresponds to 1.3 U/mg, 0.86 U/mg, 1.06 U/mg and 0.73 U/mg respectively. All measurements were performed in triplicate.

The temperature effect on enzyme activity is displayed in Figure 4. The temperature at which each variant displayed its highest activity was found to be 50 °C, which is consistent with the wild-type enzyme. The variants also demonstrated excellent stability at temperatures up to 45 °C (Figure 5). These findings indicate that the mutants generated do not exhibit any significant alterations when compared to the wild-type enzyme.

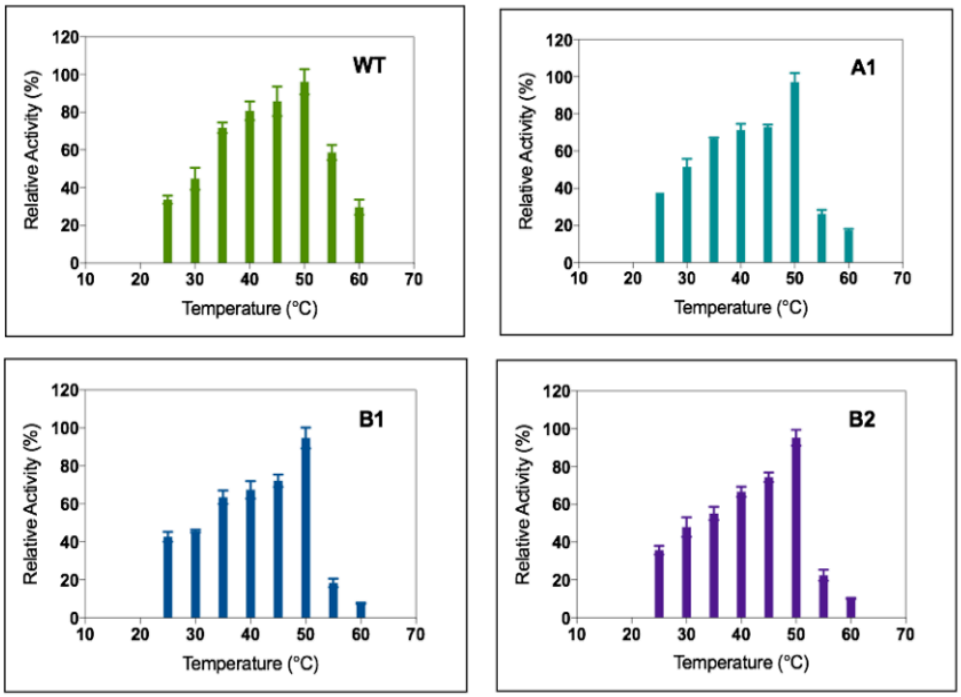


Figure 4 | Temperature effect on enzyme activity. The activity was determined using the standard activity assay performed at the indicated temperature (from 25 °C – 60 °C). 100 % activity corresponds 4.8 U/mg, 2.35 U/mg, and 2.5 U/mg respectively. All measurements were performed in triplicate.

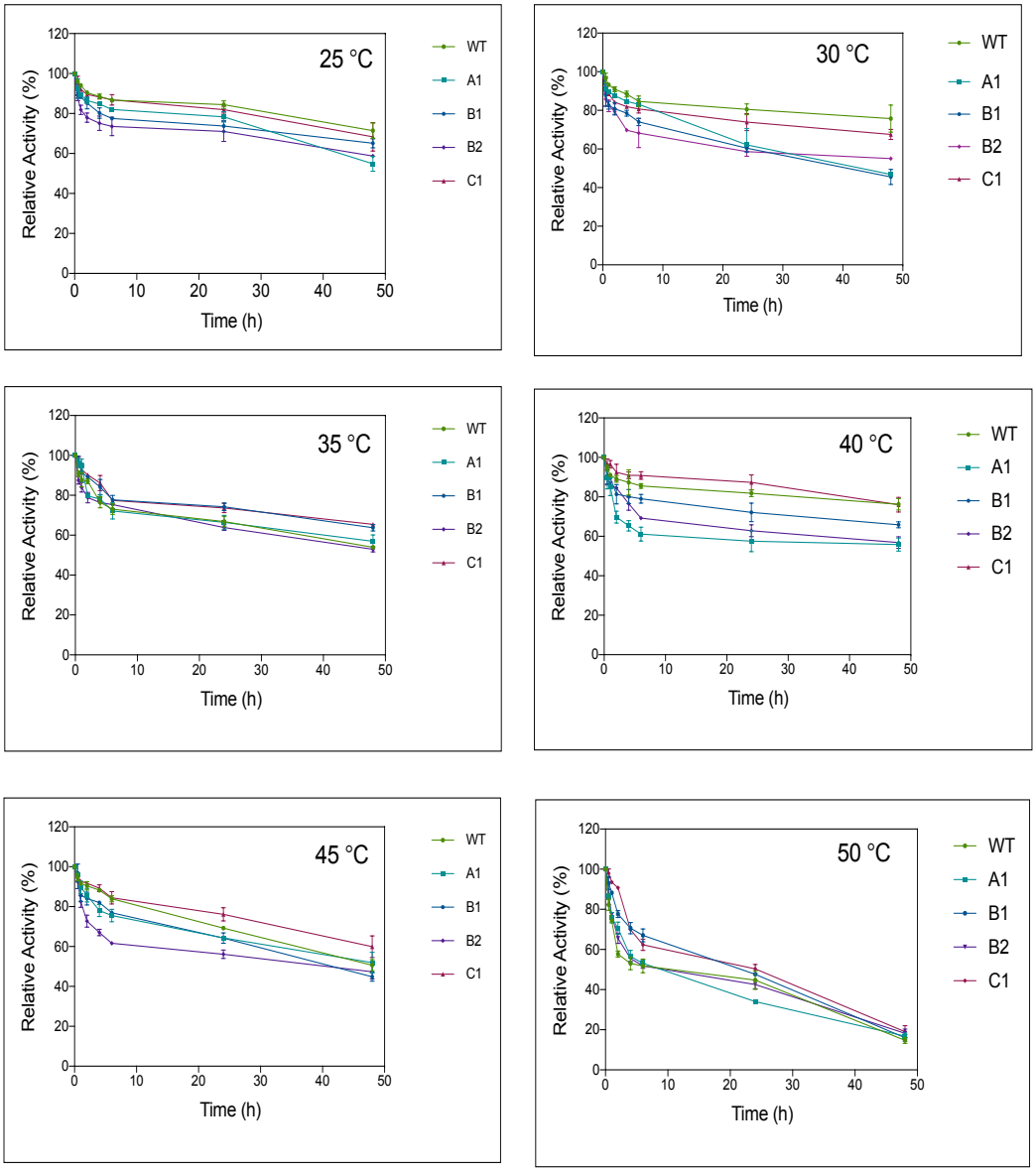


Figure 5| Temperature effect on enzyme stability. For the stability experiment, the enzyme was stored in phosphate buffer (50 mM pH 8.0) in the presence of pyridoxal 5'-phosphate (PLP) 1 mM and incubated at the desired temperature for up to 48 hours. The residual activity was determined using the standard activity assay. Acetophenone formation was quantified at 245 nm. 100% activity corresponds to 4.0 U/mg, 0.8 U/mg, 1.3 U/mg, 1.3 U/mg and 4.5 U/mg respectively (see section 3.3 for further discussion on the C1 mutant). All measurements were performed in triplicate

3.3 Characterization of *He*WT mutants towards small cyclic ketones

The original mutant library was subsequently screened against a structurally different substrate, tetrahydrothiophene-3-one (**3a**), a small cyclic ketone which if successfully aminated yields a chiral amine that has potential use as a building block for active pharmaceutical ingredients. In particular, this moiety features in compounds (Figure 6) that act as CXCR2 receptor antagonists, which inhibit the infiltration and activation of inflammatory cells involved in chronic obstructive pulmonary disease (COPD), providing symptomatic relief and reduced disease progression.[13]

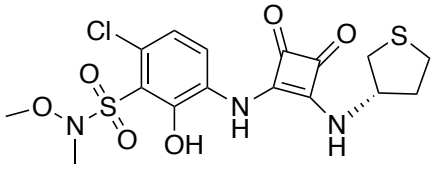
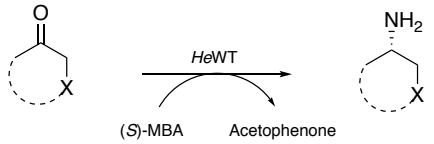


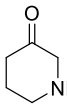
Figure 6 | A. CXCR2 receptor antagonist featuring the (*S*)-tetrahydro-3-thienylamine moiety.

In this case, the wild-type enzyme already possessed some activity towards the target substrate (**3a**), with a turnover frequency of 206 × 10^{-3} s^{-1} and complete molar conversion (>99 %) after 24 h using an equimolar amount of (*S*)-MBA as amino donor and a catalyst loading of 1 mg/mL. In keeping with previously reported data, the enzyme showed a clear preference for the (*S*)-enantiomer, however the overall enantiomeric excess was low at 66 %. Using the optimised solid phase screen with *ortho*-xylylenediamine, the original mutant library was screened towards the small cyclic ketone (**3a**), which enabled the identification of a variant (C1) showing a colour change after 18 minutes, compared to 30 minutes for the wild-type control. For further characterization, the mutant was expressed and purified following the same protocol as for the wild-type enzyme. While lower expression yields were obtained (28 mg/L culture), the activity of the mutant under standard conditions was comparable to that of the wild-type enzyme (4.5 U/mg).[8]

A full kinetic analysis of the new mutant revealed a 2-fold increase in turnover frequency (Table 2) and catalytic efficiency (*k*cat/*K*m) (Figure 7).

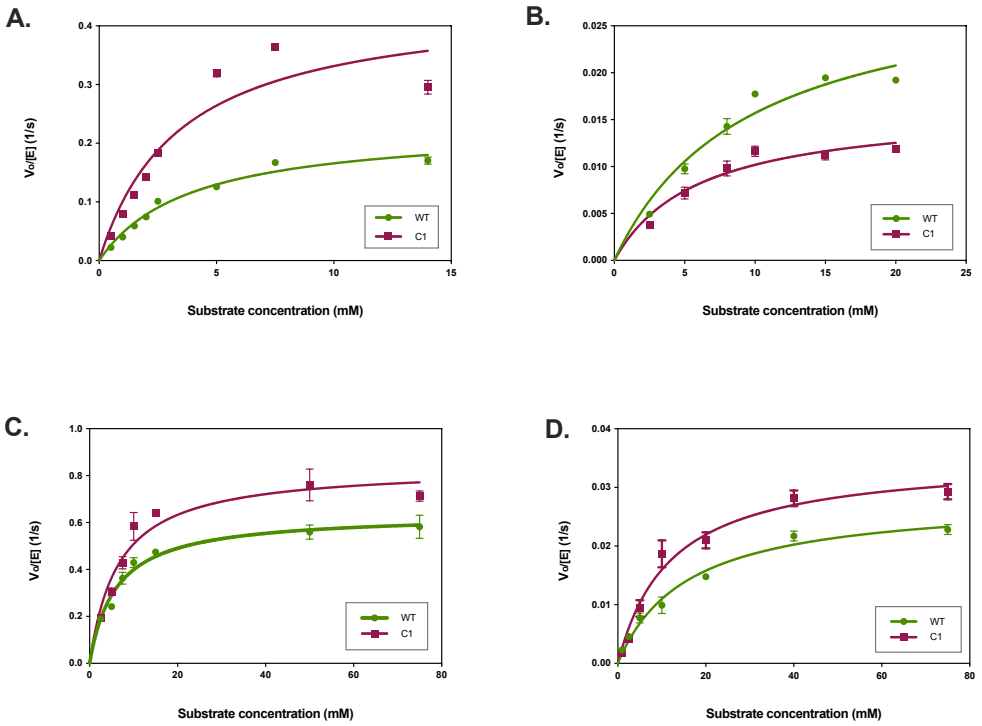
Table 2| *He*WT evolution towards small cyclic ketones



	WT			C1		
Substrate	**TOF (10^{-3} s^{-1})**	**m.c. (%)**	***e.e.* (%)**	**TOF (10^{-3} s^{-1})**	**m.c. (%)**	***e.e.* (%)**
 **3a**	206 ± 5	>99	66 (*S*)	460 ± 6	>99	66 (*S*)
 **4a**	430 ± 1	>99	70 (*S*)	580 ± 3	>99	70 (*S*)
 **5a**	18 ± 0.2	94	90 (*S*)	11.6 ± 0.3	94	90 (*S*)
 **6a**	10 ± 0.8	98	90 (*S*)	19 ± 0.8	98	90 (*S*)

Turnover frequencies (TOF) measured at 10 mM carbonyl concentration, molar conversions (m.c.), and enantiomeric excess (*e.e.)* for wild-type *He*WT and isolated variants towards tetrahydrothiophene-3-one (**3a**), tetrahydrofuran-3-one (**4a**), 1-methylpyrrolidin-3-one (**5a**) and 1-methyl-piperidin-3-one (**6a**). Final conversion was obtained within 2 h of reaction. Biotransformations were performed with 10 mM ketones, 10 mM (*S*)-MBA 0.1 mM PLP, 1 mg/mL enzyme in 50 mM phosphate buffer pH 8 at 37 °C (See experimental) 10 % (*v/v*) DMSO was used in the case of **3a** to improve solubility. All experiments were conducted in triplicate and the standard error is reported accordingly. Mutation in C1: D5E..

Based on these favourable results, the C1 variant was subsequently screened against a panel of representative small cyclic ketones (Table 2, Substrates **4a**, **5a**, **6a**). While the C1 mutant was in fact slower with 1-methylpyrrolidin-3-one (**5a**) (Figure 7) a notably lower Km with respect to the wild type was observed. This may be explained by subtle changes in the topology of the active site that favour substrate binding



Substrate	WT			C1		
	***K*m** (mM)	***K*cat** (10^{-3} s^{-1})	***k*cat/*K*m** (10^{-3} s^{-1} mM^{-1})	***K*m** (mM)	***k*cat** (10^{-3} s^{-1})	***k*cat/*K*m** (10^{-3} s^{-1} mM^{-1})
3a	3.9 ± 0.4	206 ± 5	52.8 ± 6	3.4 ± 0.7	460 ± 6	135 ± 11
4a	5.6 ± 0.5	430 ± 1	76.5 ± 7	6.5 ± 0.9	580 ± 3	82.9 ± 12
5a	10 ± 2	18 ± 0.2	1.8 ± 0.4	6 ± 1	11.6 ± 0.3	1.9 ± 0.3
6a	16 ± 2	10 ± 0.8	0.6 ± 0.1	12 ± 2	19 ± 0.8	1.6 ± 0.3

Figure 7| Determination of kinetic parameters. Michaelis-Menten plot of **wild type enzyme** (circles) and C1 mutant (squares) for (**A**) tetrhydrothiophen-3-one, (**B**) tetrahydrofuran-3-one, (**C**) 1-methyl-3-pyrrolidinone and (**D**) 1-methyl-3-piperidinone; the initial velocities were measured at pH 8.0 and 30 °C using the standard ATA kinetic assay described in the experimental. Reactions were carried out in the presence of 5 mM (*S*)-MBA (saturating conditions), various concentrations of the carbonyl substrate (0.5 – 75 mM), 0.25 % DMSO, 0.1 mM PLP and an appropriate amount of the purified enzyme.

Sequencing of the C1 mutant identified a single mutation (D5E) positioned at the *N*-terminus of the protein (Figure 8). Although the mutation is somewhat peripheral to the active site an aspartate to glutamate mutation may alter the local protein dynamics that can indeed cause alterations in the topology of the active site and hence substrate specificity.

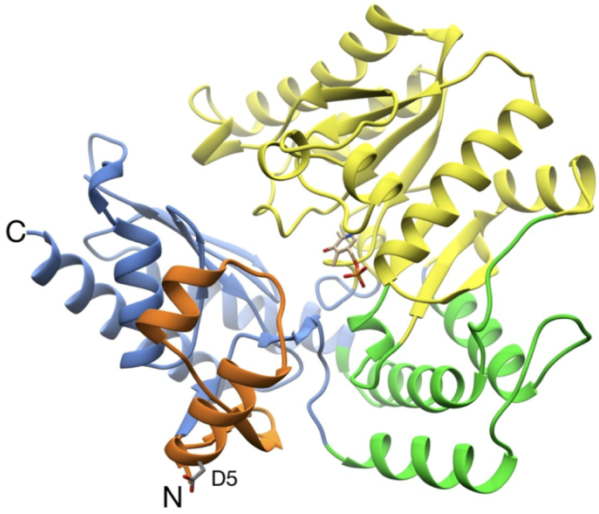
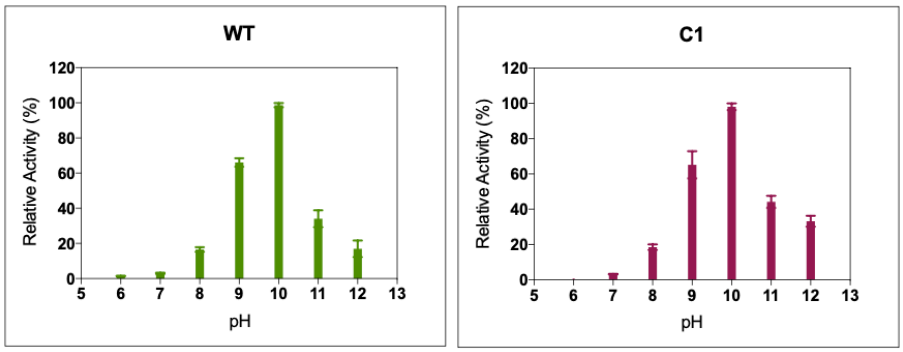


Figure 8| Location of the D5E mutation on the *He*WT crystal structure. The mutated residue in the C1 variant and PLP are shown in sticks. This figure was generated using Chimera.

The mutant was subsequently probed for changes in activity and stability. Similar to what was observed for the A1, B1 and B2 mutants, the C1 mutant behaved virtually the same as the wild-type enzyme, showing its optimal activity at pH 10 (see Figure 9a). The mutant was also highly stable following an incubation period at different pH values (pH 6 - 12), however the optimal stability was achieved at pH 10 (see Figure 9b), which is consistent with the wild-type.

A.



B.

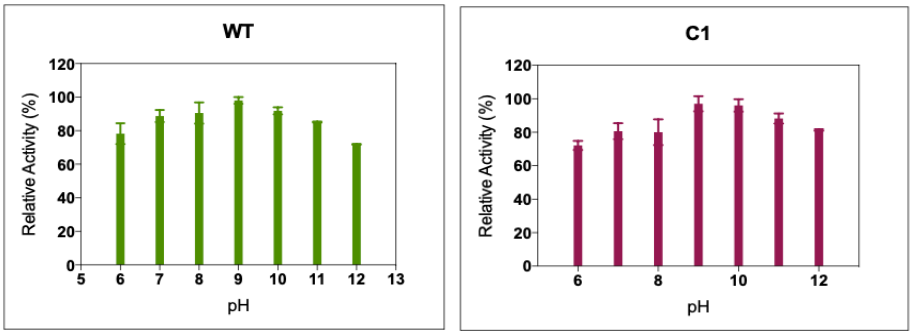


Figure 9 | A. pH effect on enzyme activity. Activity experiments were performed in universal buffer at the desired pH (from pH 6 – 12) according to the standard transaminase activity assay described in the experimental. The formation of acetophenone was quantified at 245 nm. 100 % activity corresponds to 4.0 U/mg and 6.6 U/mg respectively. All measurements were performed in triplicate. **B. pH effect on enzyme stability. .** Purified enzyme was diluted with universal buffer at the desired pH (from pH 6 – 12) and stored at 4 °C for 60 min. After incubation, the residual activity was determined using the standard enzyme activity assay described above. The formation of acetophenone was quantified at 245 nm. 100 % activity corresponds to 1.3 U/mg and 2.9 U/mg respectively. All measurements were performed in triplicate.

In terms of temperature, both wild-type and mutant displayed their highest activities at a temperature of 50 °C (see Figure 9). Perhaps most notable however is that the mutant displays significantly higher activities at lower temperatures (25 - 45 °C), although a significant loss in activity was encountered at temperatures exceeding 50 °C . Interestingly, this effect was not as pronounced for the wild-type enzyme.

While the screening methodology was successful in delivering a mutant with enhanced TOF and binding affinities towards the target substrates, both wild-type and mutant favoured the formation of (*S*)-3b and (*S*)-4b with only moderate selectivity (66 % and 70 % *e.e.* respectively). Further engineering efforts are therefore required to improve the stereoselectivity of the enzyme. Saturation mutagenesis (SM) at sites lining the binding pocket (CASTing) and iterative saturation mutagenesis (ISM) have emerged as efficient techniques in the directed evolution of stereoselective enzymes and could well be suited for the redesign of *He*WT as a better catalyst for the asymmetric reduction of the challenging ketones 3a and 4a.[14]

3.4 Conclusion

The introduction of an amine donor as a background depletion agent, which exploits the expressed ATA to quench endogenous pyruvate proved to be very effective in delivering an efficient screening platform for aminotransferase directed evolution. This high-throughput screening strategy was developed on the basis of the *ortho*-xylylenediamine assay described by O' Reilly and co-workers, and was a fundamental tool in the evolution of *He*WT towards a diverse set of aromatic and cyclic ketones.[4,15] After two rounds of directed evolution, a 2.5-fold increase in activity was obtained for *para*-nitroacetophenone, while with *para*-cyanoacetophenone the identified mutant exhibited a 60-fold higher turnover frequency coupled with a substantial improvement of the enantioselectivity with respect to the wild type. Furthermore, the evolution towards tetrahydrothiophen-3-one yielded a 2-fold increase in the overall catalytic efficiency. This enzyme also showed improved catalytic properties when screened against similarly challenging cyclic ketones. While further efforts are required to redesign this enzyme for better biocatalytic applicability, the insights gained by this work suggest that *He*WT is highly amendable for the synthesis of synthetically useful chiral amines. These result contribute favourably to the core research outcomes of this thesis.

References

1. Kohls, H., Steffen-Munsberg, F. & Höhne, M. Recent achievements in developing the biocatalytic toolbox for chiral amine synthesis. *Curr. Opin. Chem. Biol.* **19**, 180–192 (2014).

2. Gomm, A. & O'Reilly, E. Transaminases for chiral amine synthesis. *Curr. Opin. Chem. Biol.* **43**, 106–112 (2018).

3. Grogan, G. Synthesis of chiral amines using redox biocatalysis. *Curr. Opin. Chem. Biol.* **43**, 15–22 (2018).

4. Planchestainer, M. et al. Widely applicable background depletion step enables transaminase evolution through solid-phase screening. *Chem. Sci.* **10**, 5952–5958 (2019).

5. Cerioli, L. et al. Characterization of a novel amine transaminase from Halomonas elongata. *J. Mol. Catal. B Enzym.* **120**, 141–150 (2015).

6. Kaulmann, U. et al. Substrate spectrum of ω-transaminase from Chromobacterium violaceum DSM30191 and its potential for biocatalysis. *Enzyme Microb. Technol.* **41**, 628–637 (2007).

7. Shin, J. S. & Kim, B. G. Exploring the active site of amine:pyruvate aminotransferase on the basis of the substrate structure-reactivity relationship: How the enzyme controls substrate specificity and stereoselectivity. *J. Org. Chem.* **67**, 2848–2853 (2002).

8. Schätzle, S. et al. Rapid and sensitive kinetic assay for characterization of ω-transaminases. *Anal. Chem.* **81**, 8244–8248 (2009).

9. Cassimjee, K. E. et al. Chromobacterium violaceum ω-transaminase variant Trp60Cys shows increased specificity for (S)-1-phenylethylamine and 4′-substituted acetophenones, and follows Swain–Lupton parameterisation. *Org. Biomol. Chem.* **10**, 5466 (2012).

10. Nobili, A. et al. Simultaneous Use of in Silico Design and a Correlated Mutation Network as a Tool To Efficiently Guide Enzyme Engineering. *ChemBioChem.* **16**, 805–810 (2015).

11. Joseph, B. C. et al. An Overview of the Parameters for Recombinant Protein Expression in Esxherichia coli. *J. Cell Sci. Ther.* **6**, 221 (2015).

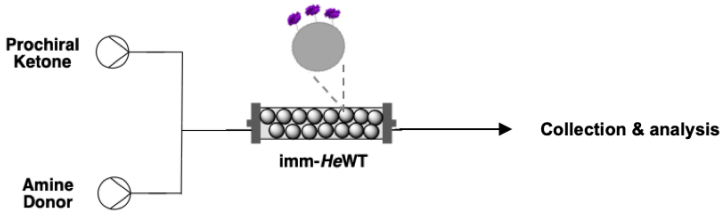
12. Davies, M. . A universal buffer solution for use in ultra-violet spectrophotometry. *Analyst* **84**, 248–251 (1959).

13. Baettig, U. et al. Cyclobutenylaminobenzenesulfonamides as CXCR2 receptor inhibitors and their preparation, pharmaceutical compositions and use in the treatment of CXCR2 receptor mediated diseases. *US Pat.,* US0100029670A11 (2010).

14. Qu, G. et al. Mothodology Development in Directed Evolution: Exploring options when applying Triple Code Saturataion Mutagenesis, *ChemBioChem*. **19**, 239-246 (2018)

15. Green, A. P., Turner, N. J. & O' Reilly, E. Chiral amine synthesis using ω-transaminases: An amine donor that displaces equilibria and enables high-throughput screening. *Angew. Chemie - Int. Ed.* **53**, 10714–10717 (2014).

Chapter 4: The Synthesis of Small Cyclic Molecules: Alcohols, Amines & Amides



4.1 Introduction

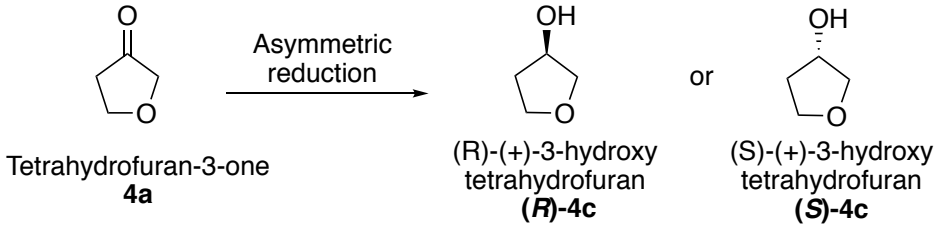
The growing toolbox of biocatalysts opens new opportunities to redesign synthetic strategies for the synthesis of target molecules. Synthetic transformations, in particular stereo- and regioselective transformations that are difficult to perform using transition metal catalysts or organocatalysts, have successfully been achieved by incorporating enzymatic steps into the synthesis.[1] In this chapter, a biocatalytic approach for the enantioselective preparation of a series of small cyclic chiral alcohols and amines is described. This approach is highly desirable as it allows for the direct, one-pot conversion of readily available prochiral ketones to stereodefined products which serve as key intermediates in the synthesis of several pharmaceutical compounds.[2–4] Enzymes from a diverse range of classes, with different reaction chemistries, cofactor requirements and reaction conditions were initially screened for activity towards the target substrates. Robust immobilization strategies were then applied so that the methodology could easily be transferred into continuous flow.

To increase the complexity of the system, it was envisaged that the newly synthesised compounds could be subjected to a second round of catalysis, using an acyltransferase from *Mycobacterium smegmatis* (*Ms*AcT), for the highly efficient and sustainable synthesis of chiral esters and amides in aqueous solution. This work offers an attractive alternative to other synthetic strategies for the preparation of a diverse set of molecules. The application of flow biocatalysis in this case is of particular importance, as it highlights how biocatalytic processes can effectively be scaled-up, while also maintaining very low environmental impact.

4.2 Results and discussion

4.2.1 Exploring the substrate scope of KRED1-*Pglu*

Ketoreductases (KREDs) have emerged as important enzymes for the synthesis of optically pure chiral alcohols starting from readily available prochiral ketones. [5] In light of this, it was envisaged that a KRED could be applied for the asymmetric reduction of tetrahydrofuran-3-one following the strategy outlined in Scheme 1. In this study, a ketoreductase from *Pichia glucozyma* (KRED1-*Pglu*) was selected to evaluate the methodology, due to its broad substrate specificity and high enantioselectivity in the synthesis of chiral alcohols, including bulky aromatic alcohols and hydroxyketones.[6]

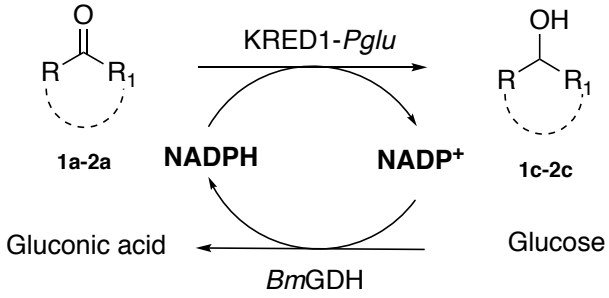


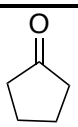
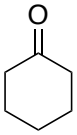
Scheme 1| Asymmetric reduction of tetrahydrofuran-3-one

Cyclopentanone and cyclohexanone were first screened to determine whether the enzyme had a preference for five or six membered rings. This would become important if other small cyclic substrates were to be assessed. Initial assays were carried out on a 10 mM scale in combination with a glucose dehydrogenase (GDH)/NADPH recycling system. The product alcohols **1c**-**2c** were detected by GC following extraction with ethyl acetate. While the five membered ring had negligible reactivity, cyclohexanone was better accepted by the enzyme, affording the corresponding alcohol with 26 % conversion (Table 1). Not discouraged by these results, the methodology was applied for the target synthesis of 3-hydroxytetrahydrofuran (**4c**). It was envisaged that the tetrahydrofuranyl ring oxygen may promote additional hydrogen bonding interactions which may in turn help anchor the substrate in the active site, thereby favouring catalysis. However, extraction of the highly water soluble alcohol product (**4c**) from the aqueous phase proved to be a

much more challenging task compared to cyclopentanol (**1c**) and cyclohexanol (**2c**).

Table 1| KRED1-*Pglu* mediated reduction of cyclic ketones 1a-2a in combination with a GDH for in situ cofactor recycling.



Entry	Substrate	Reaction time (h)	M.c. %
1a		**24**	**26**
2a		**24**	**n.d**

Molar conversions (m.c.) for KRED1-*Pglu* towards cyclopentanone (**1a**) and cyclohexanone (**2a**). Final Conversions were determined after 24 h of reaction. Biotransformations were performed with 10 mM ketones, 40 mM glucose, 0.1 mM $NADP^+$ 20 mU/mL KRED1-*Pglu* and 1 U/mL GDH in 50 mM Tris-HCl buffer pH 8 at 30 °C (See experimental). All experiments were conducted in triplicate. Shown are an average of the three experiments which were within 5 %.

Typical extraction methods involve multiple rounds of product extraction with solvents such as ethyl acetate, however in this case, ethyl acetate was not sufficiently polar to recover the alcohol from the aqueous phase. To optimize the extraction process, a 10 mM solution of the commercially available alcohol (**4c**) was prepared in 50 mM Tris-HCl, pH 8.0, effectively mimicking the biotransformation reaction conditions. Two rounds of extraction (2x 500 µL) with a 3:1 mixture of isopropanol and chloroform was subsequently applied. The switch to a highly polar organic solvent proved to be successful, enabling the detection of a peak by GC following acetylation of the alcohol with acetic anhydride and pyridine. Nevertheless, the efficiency of the extraction was still low. A

salting-out strategy was subsequently applied to further improve the extraction efficiency based on the assumption that dissolved anions with a high charge density can cause salting-out through a combination of electronic repulsion and enhancement of the hydrophobic effect (Figure 1).[7] An excess of NaCl was thus added to a buffered solution (50 mM Tris-HCl, pH 8.0) containing 10 mM of 3-hydroxytetrahydrofuran (**4c**). Liquid-liquid extraction was carried out as described above using a 3:1 mixture of isopropanol and chloroform. The organic phase was then subjected to GC analysis. In this case, a quantifiable peak corresponding the acetylated alcohol was detected.

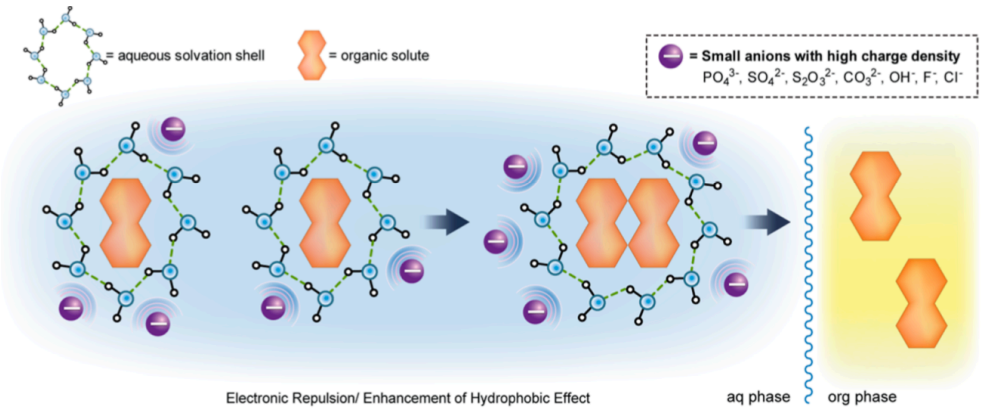


Figure 1| Molecular forces that dictate the aqueous solubility of organic compounds.[7]

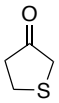
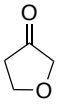
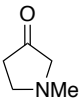
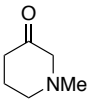
With a reliable analytical method in place, the biocatalytic reduction of tetrahydrofuran-3-one (**4a**) was examined. After 24 h, **4a** was converted to **4c** with 49% conversion, indicating that the tetrahydrofuranyl ring oxygen may well enhance substrate binding in the catalytic active site. No further conversion was detected after this time. Furthermore, the biocatalyst failed to produce the alcohol with a synthetically useful optical purity. It is thought that the binding orientation of the substrate with respect to NADPH determines which face of the C=O bond undergoes nucleophilic attack and consequently the stereochemistry of the product. The low stereoselectivity in this case suggests that reduction of the carbonyl can occur from either face.

While this work was being carried out, the group of Manfred Reetz very elegantly reported the application of triple code saturation mutagenesis (TCSM) as an advanced form of CASTing to the robust alcohol dehydrogenase from *Thermoethanolicus brockii* also using tetrahydrofuran-3-one as the target substrate.[2] Both (*R*)- and (*S*)-selective mutants were evolved leading to 95-99% *e.e.* at full conversion. Notably, the mutants were also active and selective for other challenging ketones. Based on these impressive results, and the fact that the KRED1-*Pglu* was in any case not stereoselective, attention was focused on the biocatalytic synthesis of the amine analogues which have not been well explored in the literature to date.

4.2.2 *Pseudomonas fluorescens* ω-transaminse (*Pf*TA) as an alternative to *He*WT for the synthesis of small cyclic chiral amines

In the previous chapter, *He*WT was successfully applied for the asymmetric reductive amination of a panel of small cyclic ketones (**3a**-**6a**), leading to the synthesis of chiral amines with potential application in the synthesis of pharmaceuticals.[3] While *He*WT was highly stereoselective in the synthesis of **5c** and **6c** (90% *ee* respectively), the *ee* was notably lower in the case of **3c** and **4c** (66% and 70% respectively) (Table 2).

Table 2| *He*WT mediated conversion of small cyclic prochiral ketones (3a-6a) to the corresponding amines.

Entry	Substrate	M.c. (%)	*e.e.* (%)
3a		>99	66 (*S*)
4a		>99	70 (*S*)
5a		94	90 (*S*)
6a		98	90 (*S*)

Molar conversions (m.c.), and enantiomeric excess (*e.e.)* for wild-type *He*WT towards tetrahydrofuran-3-one (3a), tetrahydrothiophene-3-one (4a), 1-methylpyrrolidin-3-one (5a) and 1-methyl-piperidin-3-one (6a). Molar conversions were obtained within 24 h of reaction. Biotransformations were performed with 10 mM ketones, 1 equiv. (*S*)-(-)-α-methylbenzylamine, 0.1 mM PLP, 1 mg/mL enzyme in 50 mM phosphate buffer pH 8 at 37 °C (See experimental) 10 % (*v/v*) DMSO was used in the case of 4a to improve solubility. All experiments were conducted in triplicate. Shown are an average of the three experiments which were within 5 %.

*He*WT is a homodimer, who's active site is positioned at the interface of the monomers and the substrate binding region is composed of a large and small binding pocket. This characteristic architecture typically limits the substrate scope of wild-type ω-TAs to ketones bearing at least one small substituent, not exceeding that of a methyl group. Docking studies have revealed that small cyclic ketones are particularly challenging for *He*WT as they do not display the well-defined small and large substituent areas that are characteristic for the transaminase biocatalytic mechanism.[8] Figure 2a, shows the docking of tetrahydrofuran-3-one (**4a**) in the active site of *He*WT. In this case, the tetrahydrofuranyl ring oxygen appears to form a hydrogen bond with the side chain of W56. This

interaction anchors the substrate in the active site such that the reductive amination of the carbonyl is favoured. In the case of 1-methyl-3-piperidinone (**6a**), the docking displaying the most favourable score places the substrate in a position that is further away from the PLP co-factor (3.23 Å) when compared to **4a** (2.70 Å) (Figure 2b). Interestingly, the substrate is positioned in the vicinity of the large binding pocket. The high stereoselectivity achieved by *He*WT in the case of **6c** suggests that this orientation favours the formation of the (*S*)-enantiomer.

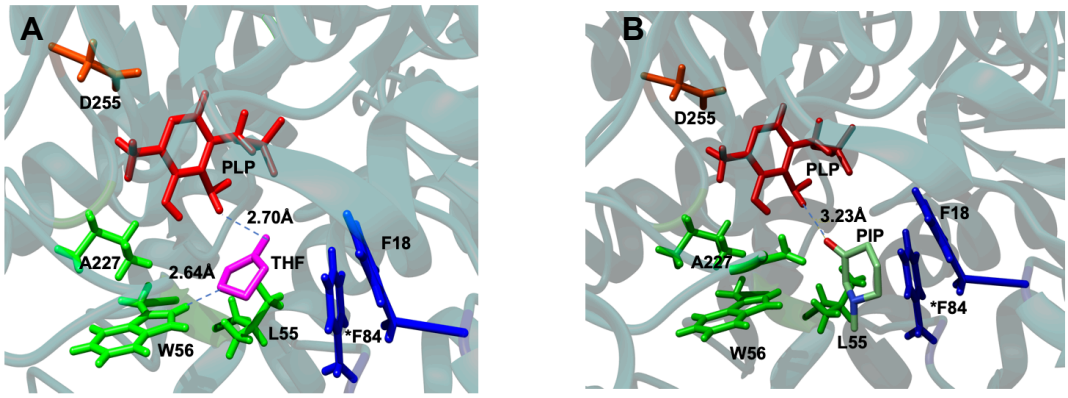
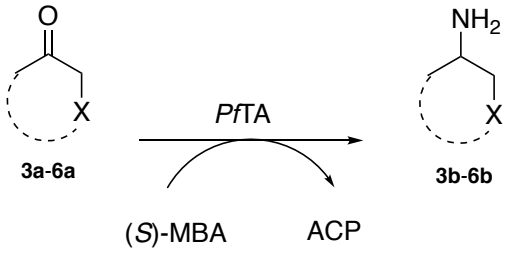


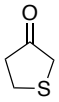
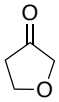
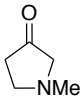
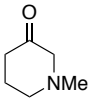
Figure 2| Docking poses for tetrahydrofuran-3-one (a) and 1-methyl-3-piperidinone (b) in the active site of *He*WT (PDB: 6GWI). Both figures were generated using Chimera.

Very recently, our group solved the crystal structure of an new ω-TA from the bacterium *Pseudomonas fluorescens* (*Pf*TA), the manuscript of which has just been accepted.[9] Notably, this enzyme was found to be a tetramer, composed of four identical subunits. In light of this, *Pf*TA was proposed as an alternative catalyst for the synthesis of small cyclic chiral amines. The ability of this enzyme to convert the selected ketones (**3a**-**6a**) to the corresponding amines (**3b**-**6b**) was initially evaluated by monitoring the production of acetophenone at 245 nm using a modified version of the transaminase activity assay previously reported by Schätzle *et al*.[10] Under these reaction conditions the enzyme showed moderate activity towards **3a** and **4a**, while no activity could be detected in the case of **5a** and **6a** (Table 3). 10 mM scale biotransformations were subsequently carried out using a range of (*S*)-MBA concentrations and a

high catalyst loading (1 mg/mL). The results presented in Table 3 suggest that the substrates were not well accepted by the enzyme. While *Pf*TA was highly selective in the synthesis of **6c**, producing the (*S*)-enantiomer with >99% *ee*, significantly lower molar conversions were observed in each case with respect to *He*WT. Notably, precipitation of the enzyme was observed within 2 h in the case of substrates **5a** and **6a.** Precipitation was even more prominent when 2 equivalents of (*S*)-MBA was applied. While the active site of *Pf*TA was found to be very similar to *He*WT, the rigidity imposed by the additional subunits makes it more difficult for the enzyme to orientate these substrates correctly in the active site. Furthermore, the tetramer showed significant instability under the reaction conditions tested, which suggests that the *He*WT dimer interface is much more stable. Based on these findings, *He*WT was selected for scale-up reactions in continuous flow.

Table 3| *Pf*TA mediated conversion of small cyclic prochiral ketones (3a-6a) to the corresponding amines.



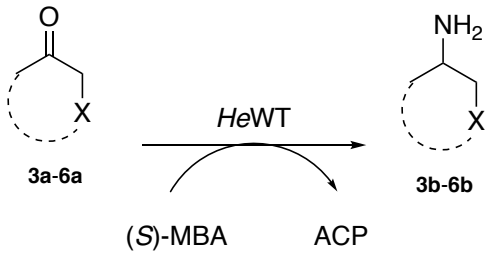
		1 eq. amino donor		*2 eq. amino donor*	
Entry	**Substrate**	**M.c. (%)**	***ee* (%)**	**M.c. (%)**	***ee* (%)**
3a		57.9	20 (*S*)	55.2	66 (*S*)
4a		48.6	42 (*S*)	66.5	70 (*S*)
5a		5.8	n.d.	5.2	n.d.
6a		17.6	>99 (*S*)	9.6	>99 (*S*)

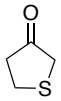
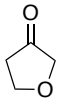
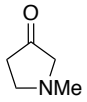
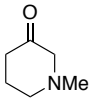
Molar conversions (m.c.), and enantiomeric excess (*e.e.)* for wild-type *Pf*TA towards tetrahydrothiophene-3-one (**3a**), tetrahydrofuran-3-one (**4a**) 1-methylpyrrolidin-3-one (**5a**) and 1-methyl-piperidin-3-one (**6a**). Final Conversions were determined after 24 h of reaction. Biotransformations were performed with 10 mM ketones, 1-2 equiv. (*S*)-(-)-α-methylbenzylamine, 0.1 mM PLP, 1 mg/mL enzyme in 50 mM phosphate buffer pH 8 at 37 °C (See experimental) 10 % (*v/v*) DMSO was used in the case of **3a** to improve solubility. All experiments were conducted in triplicate. Shown are an average of the three experiments which were within 5 %.

4.2.3 Biocatalytic performance of *He*WT at high substrate loading

Despite the attractive scope of the reactions described above, a major limitation of many transaminase enzymes is their insufficient operational stability at high substrate concentrations. To test the catalytic performance of *He*WT at higher substrate loadings, biotransformations were carried out on a 50 mM scale. Again excellent conversions to the corresponding amines **3b**-**6b** could be achieved using 1 equivalent of (*S*)-MBA as the amino donor and either 25 or 50 mM of the ketone substrate at 37 ^{o}C. (Table 4). Precipitation of the biocatalysts was observed in the case of ketones **5a** and **6a** when concentrations >25 mM were applied which suggests that these substrates, at high concentrations, may have a destabilizing effect on the protein quaternary structure. Nevertheless, these results prompted the intensification and scale-up of the reaction. Specifically, the effect of enzyme immobilization and its impact on the biocatalytic reaction under continuous flow conditions was examined.

Table 4| *He*WT mediated conversion of small cyclic prochiral ketones (3a-6a) to the corresponding amines.

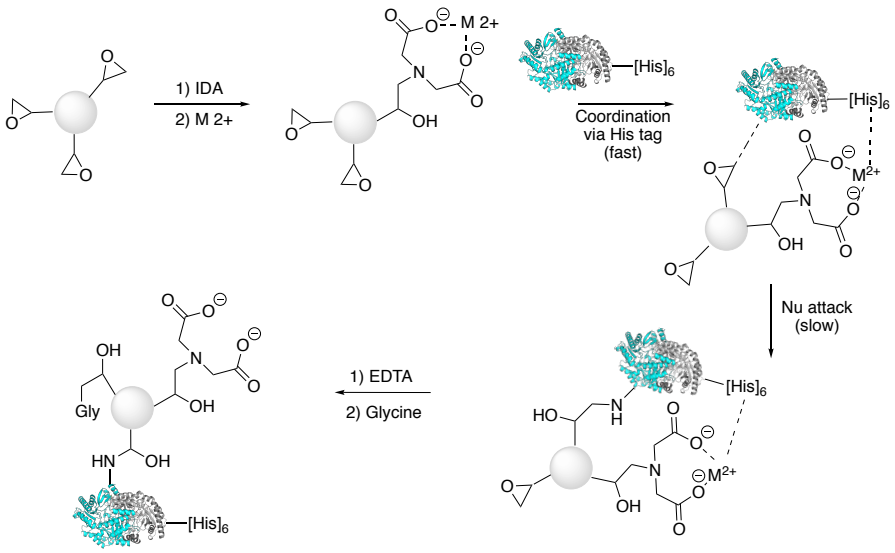


Entry	Substrate	Conc. (mM)	Reaction time (min)	M.c. (%)	*e.e.* (%)
3a		50	30	>99	66 (*S*)
4a		50	120	>99	70 (*S*)
5a		25	120	94	90 (*S*)
6a		25	120	98	90 (*S*)

Molar conversions (m.c.), and enantiomeric excess (*e.e.)* for wild-type *He*WT towards tetrahydrofuran-3-one (**3a**), tetrahydrothiophene-3-one (**4a**), 1-methylpyrrolidin-3-one (**5a**) and 1-methyl-piperidin-3-one (**6a**). Final conversion was obtained within 2 h of reaction. Biotransformations were performed with 25-50 mM ketones, 1 equiv. (*S*)-(-)-α-methylbenzylamine, 0.1 mM PLP, 1 mg/mL enzyme in 50 mM phosphate buffer pH 8 at 37 °C (See experimental) 10 % (*v/v*) DMSO was used in the case of **4a** to improve solubility. All experiments were conducted in triplicate. Shown are an average of the three experiments which were within 5 %.

4.2.4 Immobilization of *He*WT

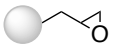
The immobilization of ω-transaminases, including *He*WT, has been reported in a number of studies.[11,12] For example, in a recent publication, our group reported on the application of *He*WT in continuous flow for the transformation of a series of aldehydes into the corresponding amines.[13] Most impressive however, was the rapid reaction time and high conversions achieved compared to those in batch. For example, the system allowed for complete conversion of *para*-nitro-benzaldehyde to *para*-nitro-benzylamine in 2 min under continuous flow conditions whereas the corresponding batch conditions required 210 min to achieve the same conversion. An immobilization strategy, first reported by the group of Guisan, was adopted for the covalent immobilization of *He*WT.[14] As shown in Scheme 2, this strategy exploits the poly-histidine tag fused to the enzyme for a selective interaction with a metal derivatized epoxy-resin. Nucleophilic residues on the surface of the protein (Lys, Cys or Ser) then react with unreacted epoxy groups on the resin to give a successful covalent immobilization. To minimize toxicity on the enzyme, the metal ion was removed by washing with a EDTA solution. Finally, the beads were treated with glycine as a capping agents to ensure that no reactive epoxides remained.



Scheme 2| General scheme for the covalent immobilization of *He*WT on epoxy-resins.

In this study, *He*WT was successfully immobilized onto a commercially available epoxy resin (Table 5), using the immobilization strategy described above. The use of non-swelling resins, such as Sepabeads EC-EP/S, are particularly suited to flow processes because they minimize back pressure and their volume remains constant. A high loading of the biocatalyst (5mg/g resin) afforded a recovered activity of 30 % (5.2 U/g resin) which is consistent with previously published data.[12]

Table 5| *He*WT immobilization onto commercially available epoxy resin.

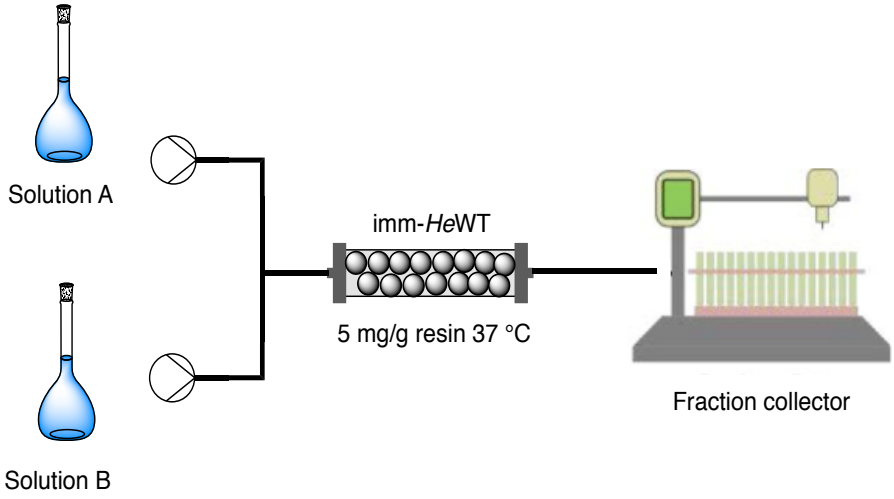
	Structure and functional group	Resin name[a]	Pore size
Covalent immobilization		Sepabeads EC-EP/S	10 -20 nm

[a] The resin had a methacrylate matrix and a particle size in the range of 100-300 µm. Data was provided by the supplier in the Product Technical Data Sheet (PTDS).

4.2.5 Flow synthesis of small cyclic amines

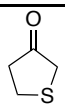
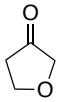
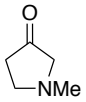
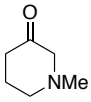
The resulting biocatalyst was subsequently applied for the synthesis of the target amines (**3b**-**6b**). To perform the reactions, an Omnifit glass column (6.6 mm i.d. x 100 mm length) was filled with the immobilized biocatalyst and attached to an R2+/R4 flow reactor commercially available from Vaportec. Aqueous reaction solutions containing the substrate, amino donor and an exogenous supply of PLP were mixed in a T-tube and flowed through the packed-bed reactor as depicted in Scheme 3. Using the same reaction conditions applied in batch, the amines were prepared with excellent molar conversions (84->99%) and moderate to excellent *ee* (26-90%) (Table 6). Notably, a loss in *ee* was observed in the case of **3b** and **4b**, however the enzyme still showed selectivity for the (*S*)-enantiomer. Structural changes following immobilisation are considered to be the main reason for this unusual loss in *ee*. Subtle changes in the orientation of the substrate in the catalytic active site may make it more challenging for the enzyme to differentiate between the α- and α′-moieties flanking the carbonyl function. The introduction of a protein linker in the immobilization strategy, as

described by Planchestainer *et al*., may be beneficial in this case as it is likely to minimise the rigidification imposed upon covalent immobilisation and prevent distortion of the catalyst.[15]



Scheme 3| Schematic of a packed bed reactor (PBR) containing the immobilized *He*WT for the continuous production of small cyclic amines (3c-6c).

Table 6| Continuous flow synthesis of small cyclic amines 3b-6b.

Entry	Amine substrate	Residence time (min)	M.c. (%)	*e.e.* (%)
3a		10	94	26 (*S*)
4a		5	98	30 (S)
5a		30	>99	90 (*S*)
6a		45	84	90 (*S*)

Reactions were performed in the presence of 25-50 mM ketone substrate, 1 equiv. (*S*)-MBA and 0.1 mM PLP in phosphate buffer (50 mM, pH 8.0).

4.2.6 Acyltransferase substrate scope evaluation

In an effort to enhance the enantiomeric excess of the small cyclic amines discussed in the previous section, it was envisaged that a second biocatalyst could be applied to produce the corresponding enantiopure amides by kinetic resolution. An example of this strategy is the highly enantioselective acylation of (*R,S*)-1-phenethylamine using a lipase from *Burkholderia sp*, (Figure 3).[16] In this process, the (*R*)-amide is separated from the (*S*)-amine by distillation or extraction, and the free (*R*)-amine is obtained through basic hydrolysis.

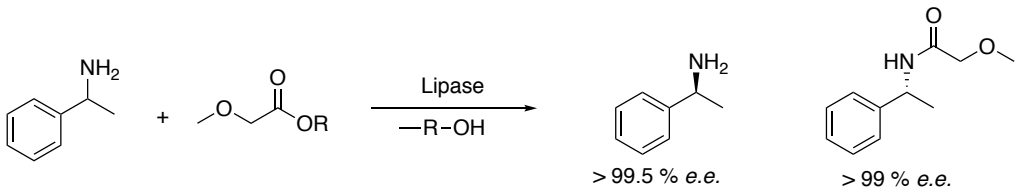


Figure 3| Lipase-catalysed kinetic resolution of amines.

The acyltransferase from *Mycobacterium smegmatis* (*Ms*AcT) was proposed as a suitable candidate, owing to its ability to catalyse the acyl transfer between a range of primary amines in aqueous solution. Within this context, the substrate scope and enantioselectivity of *Ms*AcT was probed with a panel of commercially available racemic amines (**3b**-**6b**). As demonstrated earlier, these amines can be generated from the corresponding prochiral ketones using the ω-transaminase from *Halomonas elongata* (*He*WT). To establish the optimum reaction conditions, a range of pH values and temperatures were first evaluated using **6b** as a model substrate. *Ms*AcT performed well across the range of pH values screened, however the optimal conversion was achieved when the reaction was performed at pH 8.0. (Figure 4a). A screen of different temperatures indicated that the enzyme performed better a lower temperatures, which is in agreement with current literature (Figure 4b).

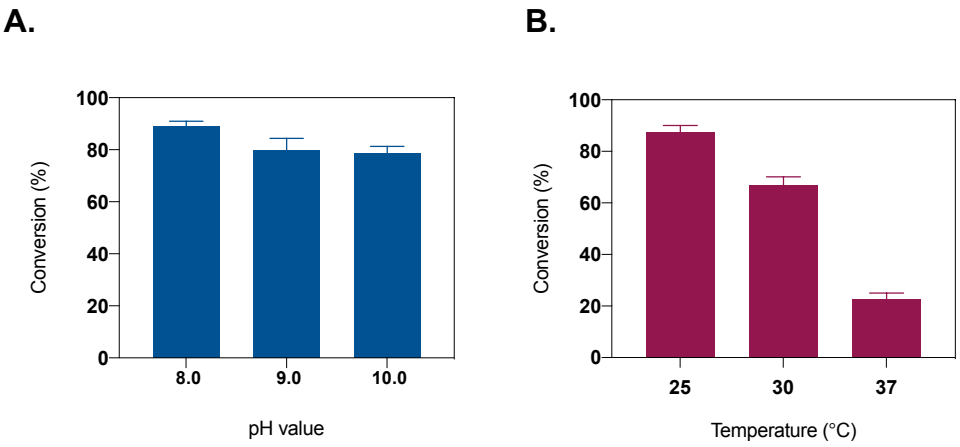
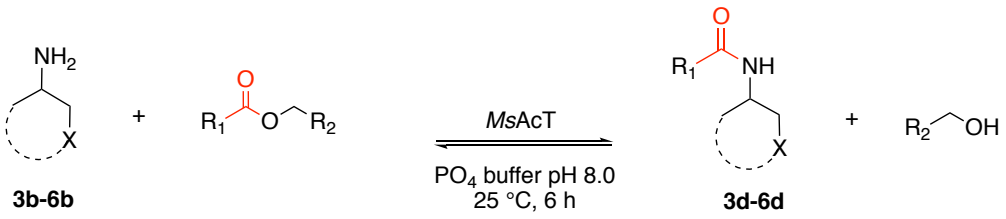
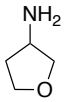
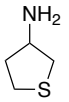
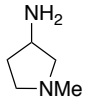
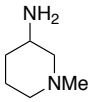


Figure 4| pH (a) and temperature (b) profile for the *Ms*AcT catalysed amidation of 6c using methyl methoxyacetate as acyl donor.

Next, coupling of **3b**-**6b** with a variety of acyl donors was examined. Purified *Ms*AcT was applied at 1 mg/mL while the amine concentration and acyl donor loading were kept constant at 20 mM and 10% v/v respectively. Table 7 shows the results of the biotransformations performed. Rapid conversion of the amine to amide product was observed in all cases. Notably, higher conversions were achieved when methyl methoxyacetate was used as the acyl donor.

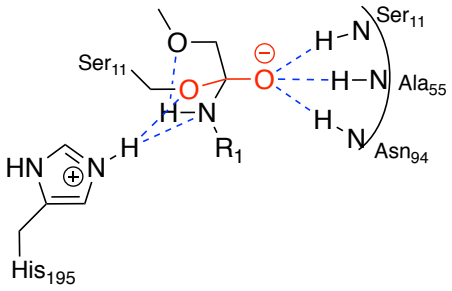
Table 7| *Ms*AcT mediated conversion of small cyclic amines 3b-6b to the corresponding amides.



		Acyl donor 10 % (v/v)		
Entry	**Amine substrate**	**Ethyl acetate M.c. (%)**	**Vinyl acetate M.c. (%)**	**Methyl methoxyacetate M.c. (%)**
3b		70.1	79.2	91.1
4b		79.6	84.7	89.5
5b		>99	>99	>99
6b		80.9	90.2	92.1

Biotransformations were performed with 20 mM amine substrate, 10 % v/v acyl donor and 1 mg/mL enzyme in potassium phosphate buffer (100 mM, pH 8.0) at 25 °C. Conversions were determined after 6 h. Longer reaction times did not yield higher conversions. All experiments were conducted in triplicate. Shown are an average of the three experiments which were within 5%.

Methoxyacetates are commonly used as acyl donors in the biocatalytic amidation of amines.[17,18] The reason for this is the formation of an internal hydrogen bond between the β-oxygen atom of methoxyacetate and the hydrogen atom of the amine which stabilises the transition state and increases the rate of reaction (Scheme 4). This makes the amine a better competitor against water and favours the formation of the amide over hydrolysis. Nevertheless, these results demonstrate a clear overlap between the product scope of the transaminase and the substrate scope of the acyltransferase.

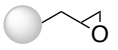
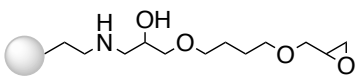


Scheme 4| Proposed conformation of the tetrahedral intermediate for the *Ms*AcT catalysed amidation showing the β-oxygen atom of methoxyacetate interacting with the hydrogen atom of the amine.

4.2.7 Acyltransferase immobilization and optimization

For application in continuous flow, a highly robust immobilization strategy for the acyltransferase was developed. To date, *Ms*AcT has been immobilized onto carbon-nanotubes to fulfil its perhydrolase activity and siliceous monolithic microreactors for the transesterification of neopentylglycol.[19,20] While continuous flow microchannel reactors can be efficient, the synthesis of silica monoliths is tedious, requiring the use of nitric acid, high temperatures, an inert atmosphere and long reaction times. As *Ms*AcT is a large molecule, an octamer, with dimensions of 72 x 72 x 60 Å, formed though tight association of pairs of dimers, it needs to be tightly bound to the carrier to ensure its long term use. Strategies forming a covalent bond between the enzyme and the highly porous methacrylate resins functionalized with epoxy groups (Table 8) were initially screened.

Table 8| List of commercially available resins for enzyme immobilization.

	Structure and functional group	Resin name[a]	Pore size
Covalent immobilization		Relizyme EP403	40-60 nm
		Relizyme HFA403	40-60 nm

[a] All resins had a methacrylate matrix and a particle size in the range of 100-300 µm. Data was provided by the supplier in the Product Technical Data Sheet (PTDS).

An additional level of complexity is associated with the extensive hydrophobicity of the enzyme (Figure 5) which could lead to non-specific hydrophobic interactions between the enzyme and hydrophobic regions of the carrier. These non-specific hydrophobic interactions determine close packing of *Ms*AcT molecules onto the carrier surface and potentially the hydrophobic catalytic site. Consequently the attached *Ms*AcT molecules would have limited flexibility and their strong interaction with the surface via hydrophobic-hydrophobic interactions would reduce the substrate accessibility to the active site and this the enzyme activity.

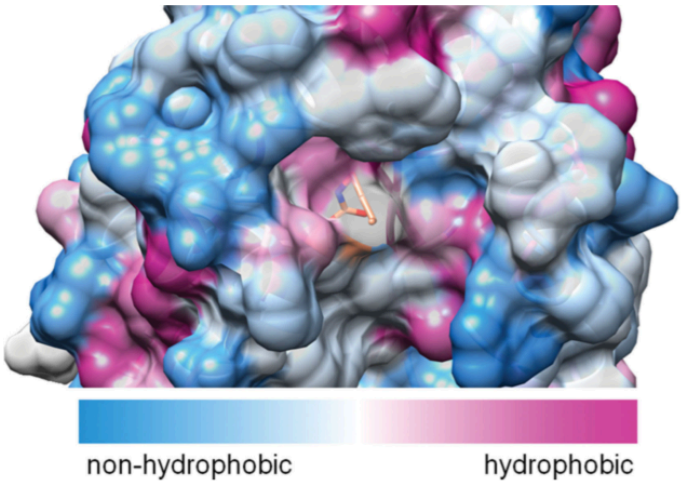


Figure 5| Tunnel leading to the active site of *Ms*AcT. The amino acids are coloured according to their hydrophobicity. [21]

As seen in Table 9, complete immobilization of the acyltransferase was achieved in both cases. However, the resin bearing a short length functional group, Relizyme EP403, yielded a biocatalyst with a slightly better recovered activity, This result was in fact surprising, as enzyme carriers with longer functional groups have been shown to minimize the loss of activity commonly observed in immobilization processes. It was assumed that Relizyme HFA403 would help reduce rigidification of the enzyme upon immobilization, allowing easier access of the substrate to the active site and thus improved activity. As this was not the case

Relizyme EP403 was selected as the most appropriate carrier for our application.

Table 9| *Ms*AcT immobilization onto epoxy resins.

Resin name	Enzyme loading (mg/g $_{resin}$)	Immobilization yield (%)	Specific activity (U/g $_{resin}$)	Recovered activity (%)
Relizyme EP403	1	>99	38.1	32.3
Relizyme HFA403	1	>99	25	21.2

Different enzyme loadings were subsequently investigated (1, 2 and 5 mg/g resin) to assess the loading capacity of the resin, and whether the recovered activity could be further improved. The highest recovered activity was obtained with an enzyme loading of 1 mg/g resin. Higher enzyme loadings resulted in a decrease in recovered activity possibly due to surface overloading (Figure 6).

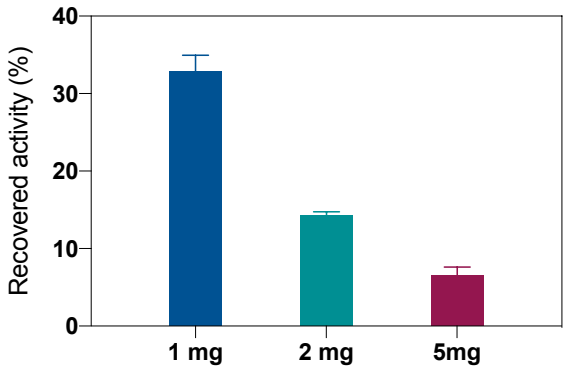
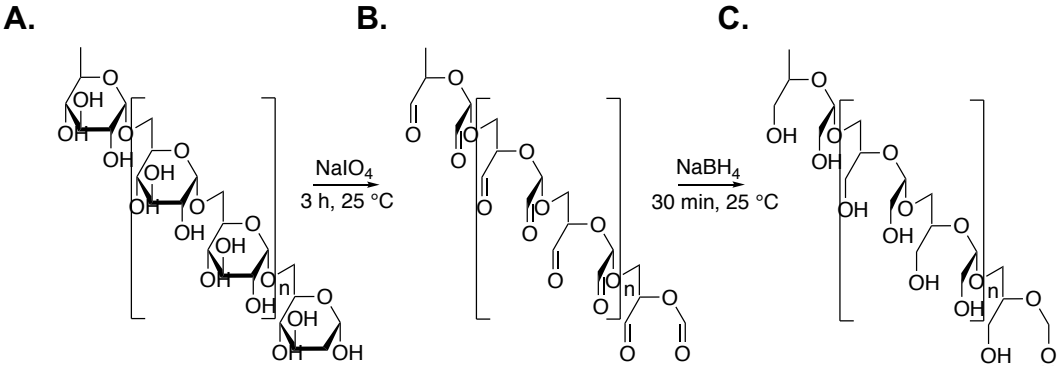


Figure 6| The effect of different enzyme loadings on the recovered activity.

The ability to re-use a biocatalyst for a number of reaction cycles in continuous flow is instrumental in the development of any immobilization procedure. Within this context, it is important to note that immobilisation is not always enough to fully stabilise the quaternary structure of multimeric enzymes.[22] In these cases, the enzyme can still release subunits to the reaction medium and become easily deactivated. Considering that *Ms*AcT requires tight association of dimer pairs to work, additional stabilization strategies were taken into consideration to

prevent subunit dissociation under continuous flow conditions. Several post-immobilization techniques have been used to complement enzyme immobilization, resulting in biocatalysts that very often possess improved catalytic properties, particularly in terms of activity and stability. These techniques include enzyme surface coating with polymers such as dextran aldehyde.[23] Dextran is a polymer with a backbone of α-1-6-glycosidic linkages between glucose molecules. Aldehyde dextran is obtained by oxidation with $NaIO_4$ (Scheme 5).



Scheme 5| Dextran polymer with different modifications. A) An unmodified dextran polymer, which consists of α-1-6-glycosidic linkages between glucose molecules. (**B**). An fully oxidized dextran polymer which consists of aldehyde groups. (**C**). A reduced dextran polymer which consists of hydroxyl groups.

In this study, we investigated the effect of inter-subunit crosslinking by exploiting the reactivity of nucleophilic groups on the surface of the immobilized acyltransferase with the aldehyde groups on the oxidized dextran polymer (Figure 7). In this case, the dextran polymer was modified to 50 % aldehyde groups. A reduction step with borohydride was subsequently carried out in which Schiff bases between the amino and aldehyde groups were converted into secondary amino bonds. At this point, all remaining aldehyde groups were converted into inert hydroxyl groups. By comparison, the chemically modified immobilized preparation yielded a slightly lower recovered activity (30%). The loss in activity may be the result of a structural distortion induced by covalent cross-linking or the use of borohydride in the reduction step, which is known to adversely affect the structure of immobilized enzymes.[24,25]

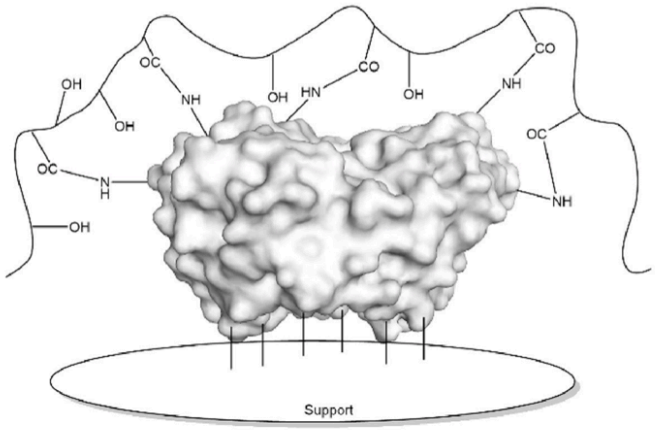


Figure 7| Graphical representation of enzyme surface coating with dextran.[26]

To evaluate whether the coating step had any additional benefits, the operational stability of both immobilized preparations were assessed in continuous flow. With a residence time of 30 min, the conversion of **6c** (20 mM) into the corresponding amide, using ethyl acetate (10% v/v) as the acyl donor, was monitored over the course of 8 reaction cycles. In both cases, the reaction was performed in potassium phosphate buffer (100 mM, pH 8.0) at 25 ^{o}C . A maximum molar conversion of 37.5% was obtained at the end of the first cycle using the non-coated biocatalyst. However, with each subsequent reaction cycle a clear decline in conversion was observed (Figure 8a). The results were less prominent for the modified biocatalyst, which achieved a maximum conversion of 16.3%. However, the conversion remained consistent across each reaction cycle, which suggests an excellent retention of activity compared to the non-coated preparation.

To further access the stabilization of the quaternary structure, both immobilisation preparations were boiled at 99 ^{o}C for 30 minutes sodium dodecyl sulfate (4 %) and mercaptoethanol (10 %). In this way, any protein subunits not covalently attached to the support were released into the medium and visible following analysis of the supernatant by SDS-

PAGE.[REF] As seen in Figure 8b, the surface coated biocatalyst did not appear to release subunits under these conditions. These results suggest that all protein subunits were covalently attached to the surface of the support, indicating that the additional coating step plays a key role in achieving full quaternary structure stabilization.

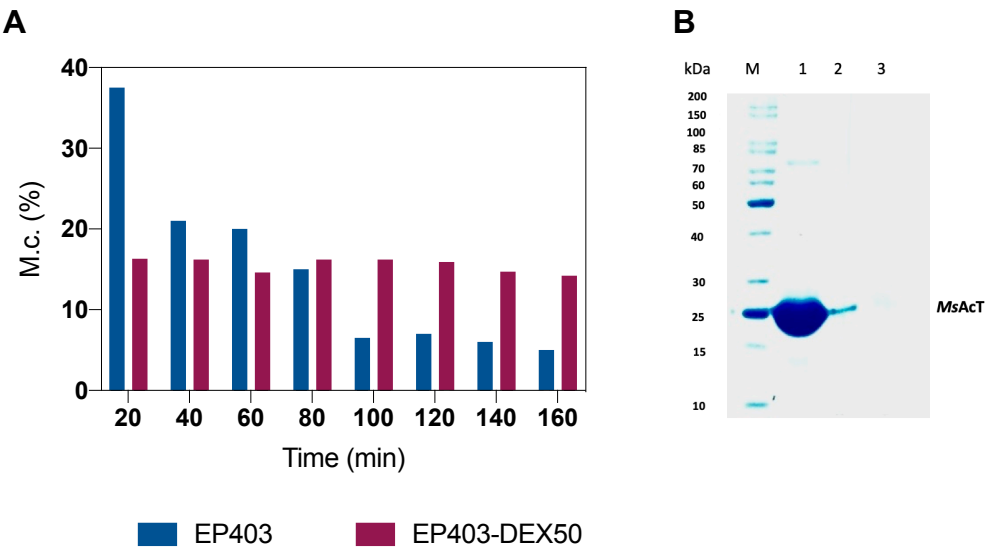
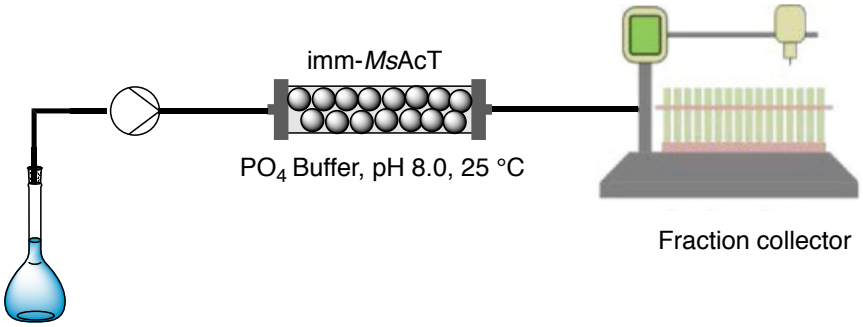


Figure 8| (A). Operational stability of the immobilized MsAcT in continuous flow. **(B).** SDS-PAGE analysis of different *Ms*AcT preparations. **M.** Unstained Protein Standard Broad Range (10 -200 kDa); **1.** Soluble *Ms*AcT; **2.** *Ms*AcT immobilized on Relizyme EP403; **3.** *Ms*AcT immobilized on Relizyme EP403 followed by surface coating with DEX50.

4.2.8 Flow synthesis of small cyclic amides

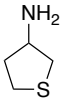
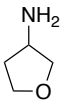
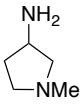
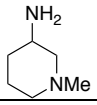
A continuous flow system using the immobilized *Ms*AcT was subsequently set up and optimized for the preparation of small cyclic amides. Based on the excellent results achieved in batch, methyl methoxyacetate (10% v/v) was selected as the optimal acyl donor. To perform the reactions, *Ms*AcT was immobilized onto Relizyme EP403 (1 mg g^{-1} resin) and chemically modified with dextran aldehyde (50% oxidized) as discussed above. The resulting biocatalyst was packed into an Omnifit glass column as described for the transaminase system. A reaction buffer containing 20 mM of the amine and 10% v/v of the acyl donor was pumped through the column as shown in Scheme 6. All reactions were performed at 25 ^{o}C and the residence time was varied for

each substrate to achieve the maximum conversion. The desired amides (3d-6d) were produced with very good molar conversions (Table 10) using a residence time of 10 min. Prolonged reaction times did not afford better results.



Scheme 7| Schematic of a packed bed reactor (PBR) containing the immobilized *Ms*AcT for the continuous production of small cyclic amides (3d-6d).

Table 10| Continuous flow synthesis of small cyclic amides (3d-6d).

Entry	Amine substrate	Residence time (min)	M.c. (%)
3b		10	70
4b		10	89
5b		10	76
6b		10	78

Reactions were performed in the presence of 20 mM amine substrate and 10% v/v methyl methoxyacetate in phosphate buffer (100 mM, pH 8.0).

In order to match the conversions achieved in batch, shorter residence times ought to be considered. While it is generally thought that the longer the substrate is in contact with the biocatalyst, the higher the conversion will be, in this particular cas, longer reaction times are likely to promote hydrolysis of the acyl donor leading to the formation of methoxyacetic acid and concomitant drop in pH.[21,27] These conditions are not optimal for the biocatalyst. The key to achieving high conversions in flow is therefore finding the optimal residence time for maximum substrate conversion while avoiding hydrolysis of the acyl donor.

4.3 Conclusion

In this chapter, we have developed a novel route for the preparation of a series of valuable small cyclic molecules using the ω-transaminase from *Halomonas elongata* and the acyltransferase from *Mycobacterium smegmatis*. Using a robust immobilization strategy, the respective enzymes have successfully been applied in continuous flow for the overall scale-up and intensification of the process, leading to excellent molar conversions and unapparelled reaction times. While this work delivers a more efficient and sustainable process compared to traditional chemical methods, the use of immobilized enzymes in packed bed reactors paves the way for the development of a ‘plug and play’ enzymatic system that can be used to assemble in vitro cascade reactions.

References

1. Devine, P. N. *et al.* Extending the application of biocatalysis to meet the challenges of drug development. *Nat. Rev. Chem.* **2**, 409–421 (2018).

2. Sun, Z. *et al.* Catalytic Asymmetric Reduction of Difficult-to-Reduce Ketones: Triple-Code Saturation Mutagenesis of an Alcohol Dehydrogenase. *ACS Catal.* **6**, 1598–1605 (2016).

3. Elzein, E. *et al.* N6-Cycloalkyl-2-substituted adenosine derivatives as selective, high affinity adenosine A1 receptor agonists. *Bioorganic Med. Chem. Lett.* **17**, 161–166 (2007).

4. Liang, J. *et al.* Highly enantioselective reduction of a small heterocyclic ketone: Biocatalytic reduction of tetrahydrothiophene-3-one to the corresponding (R)-Alcohol. *Org. Process Res. Dev.* **14**, 188–192 (2010).

5. Ma, S. K. *et al.* A green-by-design biocatalytic process for atorvastatin intermediate. *Green Chem.* **12**, 81–86 (2010).

6. Contente, M. L. *et al.* Stereoselective reduction of aromatic ketones by a new ketoreductase from Pichia glucozyma. *Appl. Microbiol. Biotechnol.* **100**, 193–201 (2016).

7. Hyde, A. M. *et al.* General Principles and Strategies for Salting-Out Informed by the Hofmeister Series. *Org. Process Res. Dev.* **21**, 1355–1370 (2017).

8. Leipold, L. *et al.* The identification and use of robust transaminases from a domestic drain metagenome. *Green Chem.* **21**, 75–86 (2019).

9. Roura Padrosa, D. *et al.* Enhancing PLP-binding capacity of class-III ω-transaminases by single residue substitution. *Front. Bioeng. Biotechnol. 2019* (2019).

10. Schätzle, S., Höhne, M., Redestad, E., Robins, K. & Bornscheuer, U. T. Rapid and sensitive kinetic assay for characterization of ω-transaminases. *Anal. Chem.* **81**, 8244–8248 (2009).

11. Neto, W., Schürmann, M., Panella, L., Vogel, A. & Woodley, J. M. Immobilisation of ω-transaminase for industrial application: Screening and characterisation of commercial ready to use enzyme carriers. *J. Mol. Catal. B Enzym.* **117**, 54–61 (2015).

12. Böhmer, W. *et al.* Highly efficient production of chiral amines in batch and continuous flow by immobilized ω-transaminases on controlled porosity glass metal-ion affinity carrier. *J. Biotechnol.* **291**, 52–60 (2019).

13. Planchestainer, M. *et al.* Continuous flow biocatalysis: Production and in-line purification of amines by immobilised transaminase from Halomonas elongata. *Green Chem.* **19**, 372–375 (2017).

14. Mateo, C. *et al.* One-step purification, covalent immobilization, and additional stabilization of poly-his-tagged proteins using novel heterofunctional chelate-epoxy supports. *Biotechnol. Bioeng.* **76**, 269–276 (2001).

15. Planchestainer, M., Padrosa, D. R., Contente, M. L. & Paradisi, F. Genetically fused t4l acts as a shield in covalent enzyme immobilisation enhancing the rescued activity. *Catalysts* **8**, (2018).

16. Balkenhohl, F., Ditrich, K., Hauer, B. & Ladner, W. Optisch aktive amine durch lipase-katalysierte methoxyacetylierung. *J. fur Prakt. Chemie - Chem. - Zeitung* **339**, 381–384 (1997).

17. Cammenberg, M., Hult, K. & Park, S. Molecular basis for the enhanced lipase-catalyzed N-acylation of 1-phenylethanamine with methoxyacetate. *ChemBioChem* **7**, 1745–1749 (2006).

18. Veld, M. A. J. et al. Fast DKR of amines using isopropyl 2-methoxyacetate as acyl donor. *European J. Org. Chem.* 5416–5421 (2007).

19. Dinu, C. Z. et al. Enzyme-based nanoscale composites for use as active decontamination surfaces. *Adv. Funct. Mater.* **20**, 392–398 (2010).

20. Szymańska, K. *et al.* MsAcT in siliceous monolithic microreactors enables quantitative ester synthesis in water. *Catal. Sci. Technol.* **6**, 4882–4888 (2016).

21. de Leeuw, N. *et al.* Ester Synthesis in Water: Mycobacterium smegmatis Acyl Transferase for Kinetic Resolutions. *Adv. Synth. Catal.* **360**, 242–249 (2018).

22. Guisán, J. M. *Immobilization of enzymes and cells*. (Human Press, 2000).

23. Pessela, B. C. *et al.* Stabilization of the quaternary structure of a hexameric alpha-galactosidase from Thermus sp. T2 by immobilization and post-immobilization techniques. *Process Biochem.* **43**, 193–198 (2008).

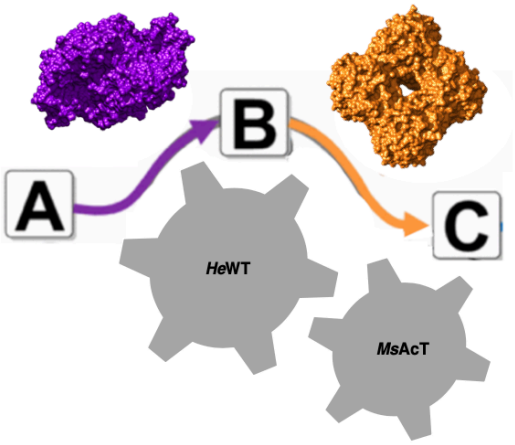
24. Bolivar, J. M. et al. Stabilization of a highly active but unstable alcohol dehydrogenase from yeast using immobilization and post-immobilization techniques. *Process Biochem.* **47**, 679–686 (2012).

25. Orrego, A. H. et al. Stabilization of enzymes by multipoint covalent attachment on aldehyde-supports: 2-picoline borane as an alternative reducing agent. *Catalysts* **8**, (2018).

26. Romero-Fernández, M. et al. Preparation of a robust immobilized biocatalyst of β-1,4-endoxylanase by surface coating with polymers for production of xylooligosaccharides from different xylan sources. *N. Biotechnol.* **44**, 50–58 (2018).

27. Boros, Z. et al. Stereoselective Hydrolase-Catalyzed Processes in Continuous-Flow Mode. *Cascade Biocatal.* 199–230 (2014).

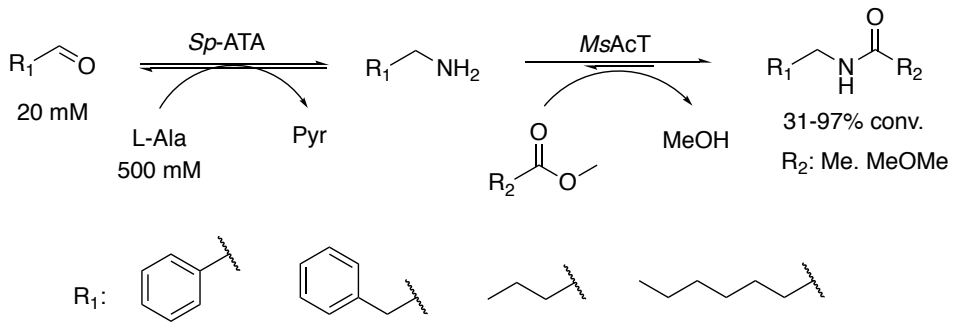
Chapter 5: The Development of a Biocatalytic Cascade for the Synthesis of Small Cyclic Amides



5.1 Introduction

As demonstrated in the previous chapter, the ω-transaminase from *Halomonas elongata* (*He*WT) and the acyltransferase from *Mycobacterium smegmatis* (*Ms*AcT) are synthetically useful biocatalysts for the synthesis of chiral amines and amides respectively.[1,2] While there are numerous examples of cascades involving ω-transaminases, there have been few reports of ω-transaminase cascades where the reductive amination is followed by amidation.[3–5]

In a recent publication, Berglund and co-workers were the first to describe the preparation of a series of amides from the corresponding aldehydes and ketones using the ω-transaminase from *Silicibacter pomeroyi* (*Sp*-ATA) in combination with the acyltransferase from *Mycobacterium smegmatis* (*Ms*AcT) (Scheme 1).[6] To avoid competition with the amine product in the second step of the cascade, L-alanine, which is not accepted as a substrate for amidation by the acyltransferase, was employed as the amine donor for the transaminase in the first step. Under optimized conditions, a preparative scale synthesis of *N*-benzyl-2-methoxyacetamide was performed, in which 134 mg of the desired amide was synthesized from benzaldehyde with 92 % conversion and 75% isolated yield.



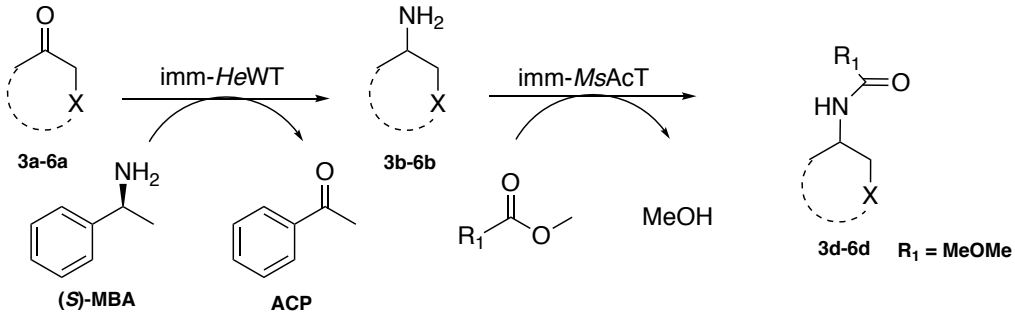
Scheme 1| Transamination followed by amine acylation. The transaminase from *Silicibacter pomeroyi* (*Sp*-ATA) and the acyl transferase from *Mycobacterium smegmatis* (*Ms*AcT) enabled the transformation of benzyaldehyde into N-benzylacetamide using either methyl acetate or methyl methoxyacetate as acyl donor.

Given the widespread occurrence of amides in biologically active compounds, an efficient biocatalytic route to their synthesis, starting from inexpensive ketones in aqueous media is highly desirable.[7] Building on the work presented in the previous chapter, herein a versatile multienzymatic cascade reaction that combines the ω-transaminase from *Halomonas elongata* (*He*WT) with the acyltransferase from *Mycobacterium smegmatis* (*Ms*AcT) for the continuous flow synthesis of small cyclic chiral amides is described.

5.2 Results and discussion

5.2.1 One-pot cascade in batch

In order to test the feasibility of a one-pot cascade, batch reactions were initially performed with the small cyclic ketone substrates (**1a**-**4a**) (Scheme 2). Although one-pot cascades can be advantageous, their success relies on the compatibility of the individual reaction steps within the sequence.[8] For example, reaction conditions such as pH and temperature must be suitable for all enzymes involved. In the previous chapters, the optimal pH for both transamination and transamidation reactions was found to be pH 8, however these reactions were carried out at notably different temperatures. Taking into consideration that *Ms*AcT operates better a lower temperatures, the cascade was performed at 25 °C as a compromise.



Scheme 2| Proposed reaction scheme for the aminotransferase and acyltransferase cascade.

The combination of *He*WT and *Ms*AcT in a one-pot cascade presented the additional challenge of competition between the enzymes for the amino donor. In theory, the amino donor for the transamination reaction can also be used as a substrate for transamidation. To avoid any unwanted side products, it was therefore necessary to select an amino donor that was not readily accepted by *Ms*AcT. Fortunately, *Ms*AcT does not accept (*S*)-MBA as a substrate for amidation which makes it well suited for application in the cascade.[2] High concentrations of methyl methoxyacetate could also induce significant loss in transaminase activity, however, in the case of this study, *He*WT showed excellent stability in the presence of this acyl donor (Figure 1).

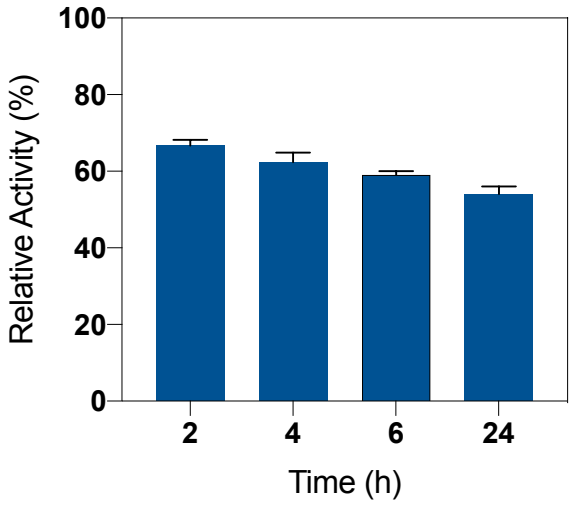
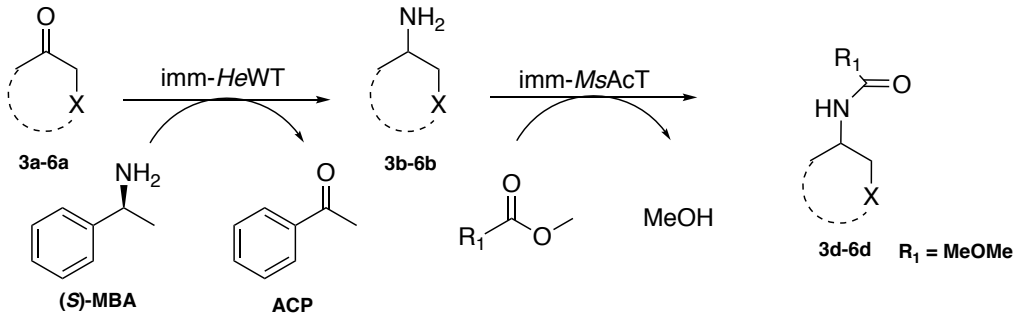
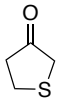
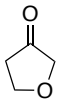
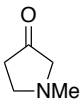
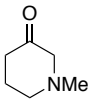


Figure 1| Stability of *He*WT in the presence of 10% v/v methyl methoxyacetate. The stability of *He*WT was investigated by storing the enzyme in the presence of methyl methoxyacetate at 4 °C. For up to 24 h. The residual activity was determined using the standard acetophenone assay.[9]

The cascade was subsequently performed on a 20 mM scale using 1 eq. of (*S*)-MBA as amino donor and 10 % v/v methyl methoxyacetate as acyl donor. A buffer concentration of 100 mM was used to help stabilize the pH in the event of hydrolysis of the acyl donor. All reactions were monitored at different time points over the course of 24 h. The optimal molar conversions, which were determined by GC, are presented in Table 1.

Table 1| Preparation of small cyclic amides from the corresponding ketones via a one-pot mutli-enzyme cascade.



Entry	Substrate (20 mM)	Reaction time (h)	M.c. (%)
3a		6	54.3
4a		6	37.2
5a		6	40.8
6a		6	39.5

Reactions were performed in the presence of 20 mM ketone substrate, 1 equiv. (*S*)-MBA, 10 % v/v methyl methoxyacetate and 0.1 mM PLP in phosphate buffer (100 mM, pH 8.0). Reactions were performed at 25 °C . All biotransformation were performed in triplicate. Shown are an average of the three experiments which were within 5 %. 10% DMSO was used to increase solubility of 1a.

It is noteworthy to mention that precipitation was visible very early on in the reaction and a significant drop in pH was also observed (from pH 8 to pH 4). Although the transamidation reaction is clearly observed in buffer, hydrolysis is still a major side reaction, particularly when the enzyme is applied at high concentrations.[10] The formation of

methoxyacetic acid within the system contributed to the drop in pH and is also thought to have promoted precipitation. SDS-PAGE analysis of the precipitate indicated that *He*WT was highly unstable under these reaction conditions which would explain the low conversions (Figure 2). No further conversion was observed after 6 h in all cases.

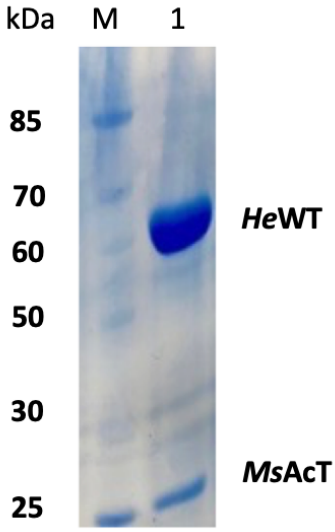


Figure 2| SDS-PAGE Analysis of protein precipitate. L1: Unstained Protein Standard Broad Range (10-200 kDa); L2: Sample of precipitate extracted from biotransformation reaction mixture.

To improve on these results, further reaction optimisation was carried out using **4a** as substrate. In this case, the loading of *Ms*AcT was reduced from 1 mg/mL to 0.1 mg/mL to minimise hydrolysis of the acyl donor. With better control over the pH, the first step of the reaction preceded favourably achieving 76 % m.c., however, further conversion of the amine to the corresponding amide was negligible at such low catalyst loading. Increasing the buffer concentration from 100 mM to 400 mM also failed to stabilise the pH at high *Ms*AcT loading (1mg/mL).

In an effort to overcome the challenges encountered above, the possibility of performing the reactions in a stepwise fashion rather than simultaneously was next explored. In this instance, the transamination reaction was first carried out at its optimal temperature of 37 ^{o}C, while the substrate, amino donor and enzyme loadings where kept the same

as described before. When the reaction had reached completion (after 2 h), *Ms*AcT and methyl methyoxyacetate were added at the desired concentrations (1 mg/mL and 10 % v/v respectively). The second step was performed at 25 °C and the reaction progress was monitored at different time points for up to 24 h. By performing the individual reaction steps sequentially, the cascade consistently afforded the desired amide (**2d**) with 67 % m.c.

5.2.2 Optimization of a stepwise cascade in continuous flow

To circumvent incompatibilities within the different steps, flow concepts are particularly suitable when compartmentalisation is required. With immobilisation strategies for both enzymes already well established, a natural progression was to perform the cascade in continuous flow mode. To this aim, the immobilized biocatalysts were assembled into two contiguous bioreactors. The tunability of the flow system allowed for the use of different optimal temperatures in the two bioreactors (37 °C for the transamination step catalysed by *He*WT, and 25 °C for the subsequent reaction catalysed by *Ms*AcT). Based on the work carried out in chapter 4, a substrate loading of 50 mM was first trialled. Using a residence time of 5 min, the first continuous step afforded 98 % conversion of **4a** to the corresponding amine, which was consistent with previous results. However, after 3 consecutive reaction cycles in flow, a significant drop in conversion was observed. A subsequent activity assay revealed that the immobilized biocatalyst had lost approximately 90 % of its original activity during the course of the reaction. Extensive washing with an exogenous supply of PLP failed to recover any activity. It was hypothesized that the ketone had an inactivating effect on the activity of the enzyme. Consequently, the substrate concentration flowed through the packed bed reactor was reduced from 50 mM to 20 mM. Despite this measure, no further improvement in enzyme stability was observed. A clear decrease in conversion was observed across the 6 cycles performed (Figure 1).

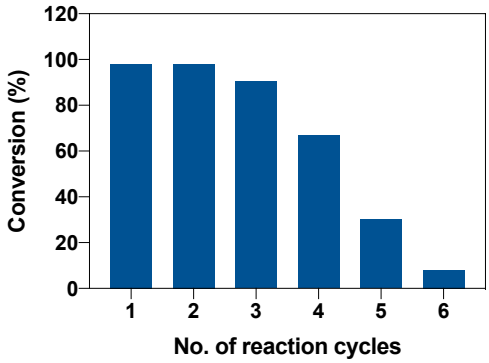
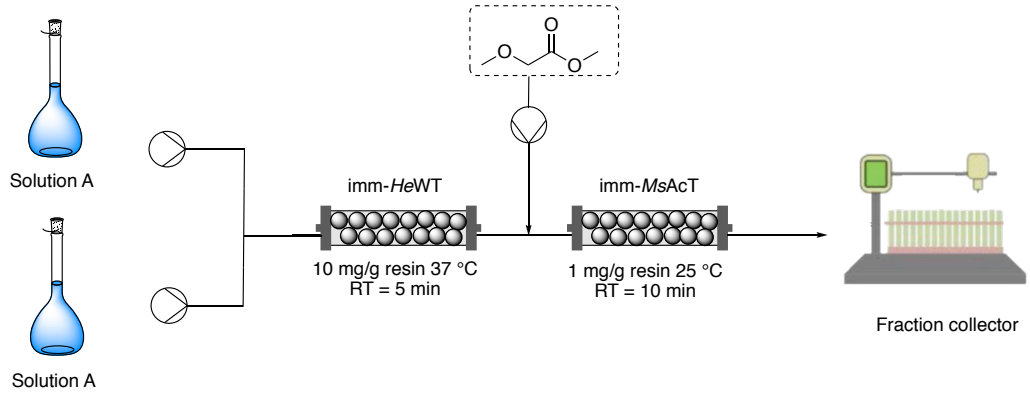


Figure 1| Operational stability of *He*WT-EC-EP/S under continuous flow conditions. Reactions were performed at 37 °C in the presence of 20 mM tetrahydrofuran-3-one (**4a**), 1 equiv. (*S*)-MBA in 50 mM phosphate buffer pH 8.0 containing 0.1 mM PLP and 2.5% DMSO. A residence time of 5 min was used for each reaction cycle.

While the immobilization of *He*WT has to date always been performed with methacrylate resins such as Sepabeads EC-EP/S[11–14], it is possible that alternative conditions or different supports may give even better results, yielding a more active enzyme which may be capable of better efficiency and stability under continuous conditions. Therefore, the next logical step was to revisit the immobilization of the biocatalyst. To further improve the performance of the immobilized biocatalyst, higher catalyst loading on Sepabeads EC-EP/S was tested. With a loading of 10 mg/g of resin, the resulting biocatalyst displayed an activity of 18.5 U/g of resin. However, under flow conditions the performance of the enzyme was only marginally better. The full cascade was carried out in any case as illustrated in Scheme 2. The acyl donor was introduced downstream of the first column via an inlet which generated a liquid-liquid phase composed of buffer and methyl methoxyacetate (90:10).

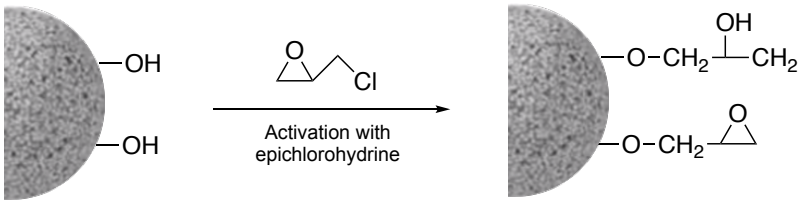


Scheme 2| Flow assembly for the synthesis of 2-methoxy-N-(tetrahydro-3-furanyl)acetamide. Solution A: 40 mM tetrahydrofuran-3-one (2a) in phosphate buffer (50 mM, pH 8.0) containing 0.1 mM PLP. Solution B: 40 mM (*S*)-MBA in phosphate buffer (50 mM, pH 8.0) containing 0.1 mM PLP, 5% (v/v) DMSO. Methyl methyoxyacetate (10 % v/v) was added downstream of the first column using a peristaltic pump.

By applying the optimized conditions for each individual step, as reported in chapter 4, 47 % m.c. of **4a** to the corresponding amide was achieved**.** Notably, the acyltransferase did not perform as well as expected, achieving a m.c. of just 65 %, compared to 89 % when the reaction was performed as a single step, starting from the commercially available amine substrate. It is hypothesized that insufficient the mixing of the acyl donor with the substrate flow stream may have contributed to these lower yields. One possible solution would be to combine the acyl donor with the amino donor solution upstream of the first column. Different reaction conditions in terms of residence times and reaction temperatures were also trialled with the aim of improving the overall molar conversion. Not surprisingly, longer residence times (10, 20 and 30 min respectively) led to the inactivation of *He*WT very early on in the reaction, despite higher catalyst loading. Prolonged reaction times also had a negative effect on the transamidation reaction. As little or no conversion could be detected, it is thought that residence times longer than 10 min promoted cleavage of the desired amide product.[15] Increasing the temperature of this step from 25 °C to 30 °C also afforded no additional benefits.

5.2.3 Immobilization of *He*WT on epoxy activated agarose

While the use of methacrylate resins, such as Sepabeads EC-EP/S, are particularly suited to flow processes, some enzymes are less stable in hydrophobic environments.[16] Taking this into consideration, agarose was proposed as an alternative carrier for the immobilization of *He*WT. To retain the same immobilization chemistry, the agarose was functionalized with epoxy groups using epichlorohydrine as outlined in Scheme 3).[17] The efficiency of the derivatization however was limited by the hydrolysis of a large number of epoxy groups to glycerol groups. This was promoted by the strong alkaline conditions required for activation. In all batches, the number of glycerol groups was quantified to be approximately 60% of the total number of epoxide groups initially activated.



Scheme 3| Functionalization of agarose with epoxy groups.

Different loadings of the biocatalyst were investigated and directly compared to previous immobilization studies using Sepabeads EC-EP/S (Table 1). By simply increasing the hydrophilicity of the matrix, a biocatalyst with more than twice the activity was obtained. Interestingly, agarose also yielded a more active biocatalyst at higher enzyme loadings.

Table 1. Immobilization of *He*WT on different enzyme carriers

Resin name	Enzyme loading (mg/g $_{resin}$)	Immobilization yield (%)	Specific activity (U/g $_{resin}$)	Recovered activity (%)
Sepabeads	1	>99	1.9	51.4
EC-EP/S	15	>99	14.0	25.6
Epoxy	1	>99	4.9	138.9
Agarose	15	>99	23.1	42.5

Encouraged by these excellent results, 10 mM scale reactions using **4a** as a model substrate were carried out in batch mode to study the operational stability of *He*WT when immobilized onto epoxy agarose (enzyme loading; 15mg/g resin). After 1 h of reaction, the molar conversion was determined by HPLC and the resin was washed extensively with phosphate buffer (50 mM, pH 8.0) containing 0.1 mM of PLP. A fresh substrate solution was applied and the cycle was repeated. Remarkably the biocatalyst remained very stable after 6 hours of continuous reaction (Figure 3).

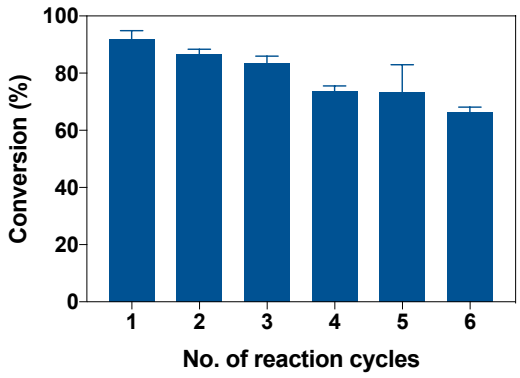
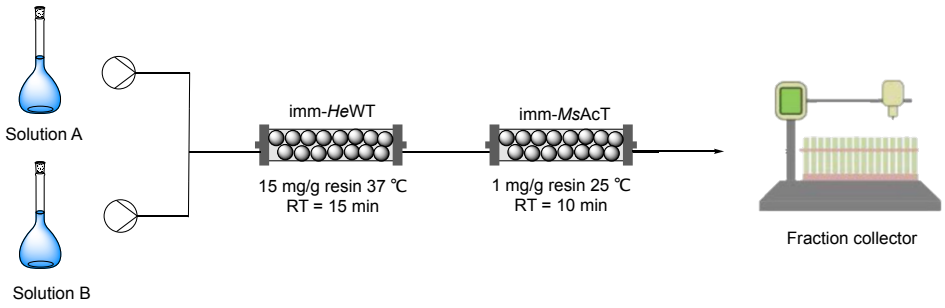


Figure 3| Operational stability of *He*WT immobilized on epoxy agarose. Reactions were performed in batch in the presence of 10 mM tetrahydrofuran-3-one (**4a**), 1 equiv. (*S*)-MBA in 50 mM phosphate buffer pH 8.0 containing 0.1 mM PLP and 2.5 % DMSO. After 1 h, the conversion was analysed by HPLC. The resin was washed extensively with 50 mM phosphate buffer pH 8.0 containing 0.1 mM PLP and fresh substrate added.

5.2.4 Continuous flow synthesis of a model small cyclic amide

Considering the excellent operational stability demonstrated in batch, the newly generated biocatalyst was incorporate into the continuous flow system. However, given that agarose is less mechanically robust than methacrylate resins when exposed to high flow rates, a lower flow rate leading to a longer residence time of 15 min was employed for the transaminase reaction. The concentration of the ketone was increased again to 20 mM in the reactor. The second step was carried out without further modification. Using this approach, the cascade afforded the desired amide with 63 % m.c. and 33% *e.e*. While the overall conversion had significantly improved, the *e.e.* was not satisfactory. Given the poor selectivity of *Ms*AcT, the chirality was introduced only by *He*WT in the first step of the cascade, and retained throughout.



Scheme 4| Modified flow assembly for the synthesis of 2-methoxy-N-(tetrahydro-3-furanyl)acetamide. Solution A: 40 mM tetrahydrofuran-3-one in phosphate buffer (50 mM, pH 8.0) containing 0.1 mM PLP. Solution B: 40 mM (*S*)-MBA in phosphate buffer (50 mM, pH 8.0) containing 0.1 mM PLP, 5 % (v/v) DMSO and 20 % v/v methyl methyoxyacetate.

While this work highlights the synthetic potential of immobilised *He*WT and *Ms*AcT for the continuous production of small cyclic amides, further optimisation of the system is required in order to meet current industrial demands. Further engineering of *He*WT is required to enhance the stereoselectivity of the enzyme for asymmetric synthesis. Strategies such as triple-code saturation mutagenesis (TCSM) are particularly attractive and have been used to great effect by the group of Manfred Reetz to fine-tune the stereoselectivity of a limonene epoxide hydrolase (LEH) and an alcohol dehydrogenase (ADH).[18,19] This approach utilizes

three properly chosen amino acids as building blocks in saturation mutagenesis at a large randomisation site lining the enzyme's binding pocket.[20] The system could also benefit from more robust immobilisation strategies. For example, to help minimise the distortion of the biocatalyst upon immobilisation, the use of a protein linker should be considered.[21] Using this approach, covalent bonds between the sacrificial protein and the support may be useful in shielding the biocatalyst and enhancing the recovered activity. The incorporation of an in-line purification step would also be a valuable addition to the system. It is envisaged that the use of a benzylamine supported scavenger, upstream of the second reactor, would trap any unwanted acetophenone produced during the first step of the reaction.[11] The desired amide product could be recovered in the organic phase using a Zaiput liquid/liquid separator downstream of the second reactor, while the recovered waste water, containing any unreacted amine, could be re-circulated in the system.[13] Finally, evaporation of the organic phase would allow for the recovery of the acyl donor.[22] The addition of these simple steps would significantly simplify and accelerate the work-up procedure, while also implementing a closed-loop strategy.

5.3 Conclusion

In summary, a versatile and efficient multienzymatic cascade for the synthesis of small cyclic amides using an ω-transaminase and acyltransferase was developed and applied in continuous flow. The cascade was fully optimized for the synthesis of 2-methoxy-N-(tetrahydro-3-furanyl)acetamide with relatively high molar conversion and excellent residence times. Considering the low enantioselectivity of the final product, efforts are currently focussed on the engineering of *He*WT for the asymmetric reduction of tetrahydrofuran-3-one, which would allow for the preparation of an enantiopure product. Nevertheless, this methodology has the potential to be applied for the efficient and sustainable synthesis a broad range of valuable amides.

References

1. Cerioli, L. et al. Characterization of a novel amine transaminase from Halomonas elongata. *J. Mol. Catal. B Enzym.* **120**, 141–150 (2015).

2. Contente, M. L. et al. Biocatalytic N-Acylation of Amines in Water Using an Acyltransferase from Mycobacterium smegmatis. *Adv. Synth. Catal.* **360**, 4814–4819 (2018).

3. O'Reilly, E. et al. A regio- and stereoselective ω-transaminase/monoamine oxidase cascade for the synthesis of chiral 2,5-disubstituted pyrrolidines. *Angew. Chemie - Int. Ed.* **53**, 2447–2450 (2014).

4. Martínez-Montero, L. et al. Stereoselective amination of racemic sec-alcohols through sequential application of laccases and transaminases. *Green Chem.* **19**, 474–480 (2017).

5. Erdmann, V. et al. Enzymatic and Chemoenzymatic Three-Step Cascades for the Synthesis of Stereochemically Complementary Trisubstituted Tetrahydroisoquinolines. *Angew. Chemie - Int. Ed.* **56**, 12503–12507 (2017).

6. Land, H. et al. One-pot biocatalytic amine transaminase/acyl transferase cascade for aqueous formation of amides from aldehydes or ketones. *Catal. Sci. Technol.* **6**, 2897–2900 (2016).

7. Dunetz, J. R., Magano, J. & Weisenburger, G. A. Large-Scale Applications of Amide Coupling Reagents for the Synthesis of Pharmaceuticals. *Org. Process Res. Dev.* **20**, 140–177 (2016).

8. Gandomkar, S., Żądło-Dobrowolska, A. & Kroutil, W. Extending Designed Linear Biocatalytic Cascades for Organic Synthesis. *ChemCatChem* **11**, 225–243 (2019).

9. Schätzle, S. et al. Rapid and sensitive kinetic assay for characterization of ω-transaminases. *Anal. Chem.* **81**, 8244–8248 (2009).

10. Kazemi, M. et al. Computational Study of Mycobacterium smegmatis Acyl Transferase Reaction Mechanism and Specificity. *ACS Catal.* **8**, 10698–10706 (2018).

11. Planchestainer, M. et al. Continuous flow biocatalysis: Production and in-line purification of amines by immobilised transaminase from Halomonas elongata. *Green Chem.* **19**, 372–375 (2017).

12. Contente, M. L. et al. Highly Efficient Oxidation of Amines to Aldehydes with Flow-based Biocatalysis. *ChemCatChem* **9**, 3843–3848 (2017).

13. Contente, M. L. & Paradisi, F. Self-sustaining closed-loop multienzyme-mediated conversion of amines into alcohols in continuous reactions. *Nat. Catal.* **1**, 452–459 (2018).

14. Contente, M. L. & Paradisi, F. Transaminase-Catalyzed Continuous Synthesis of Biogenic Aldehydes. *ChemBioChem* 1–5 (2019).

15. de Leeuw, N. et al. Ester Synthesis in Water: Mycobacterium smegmatis Acyl Transferase for Kinetic Resolutions. *Adv. Synth. Catal.* **360**, 242–249 (2018).

16. Zucca, P., Fernandez-Lafuente, R. & Sanjust, E. Agarose and its derivatives as supports for enzyme immobilization. *Molecules* **21**, 1–25 (2016).

17. Guisan, J. M. et al. Improvement of Enzyme Properties with a Two-Step Immobilizaton Process on Novel Heterofunctional Supports. *Biomacromolecules* **11**, 3112–3117 (2010).

18. Sun, Z. et al. Structure-Guided Triple-Code Saturation Mutagenesis: Efficient Tuning of the Stereoselectivity of an Epoxide Hydrolase. *ACS Catal.* **6**, 1590–1597 (2016).

19. Sun, Z. et al. Catalytic Asymmetric Reduction of Difficult-to-Reduce Ketones: Triple-Code Saturation Mutagenesis of an Alcohol Dehydrogenase. *ACS Catal.* **6**, 1598–1605 (2016).

20. Sun, Z., Lonsdale, R., Li, G. & Reetz, M. T. Comparing Different Strategies in Directed Evolution of Enzyme Stereoselectivity: Single- versus Double-Code Saturation Mutagenesis. *ChemBioChem* 1865–1872 (2016).

21. Planchestainer, M. et al. Genetically fused t4l acts as a shield in covalent enzyme immobilisation enhancing the rescued activity. *Catalysts* **8**, (2018).

22. Contente, M. L. et al. Flow-based enzymatic synthesis of melatonin and other high value tryptamine derivatives: A five-minute intensified process. *Green Chem.* **21**, 3263–3266 (2019).

Conclusions & Future Outlook

Conclusions & Future Outlook

The results obtained during the course of this research project showcase how enabling technologies such as high-throughput screening, enzyme immobilisation and continuous flow can successfully be applied to develop robust biocatalytic strategies for the synthesis of molecules that are inherently difficult to access using traditional synthetic approaches.

In chapter 3, the validity of a newly developed solid-phase screening method for detecting the activity of aminotransferases was evaluated by applying it to an ω-TA from *Halomonas elongata* (*He*WT), evolved through rounds of random mutagesis twoards a series of prochiral ketones. The library was first screened towards *para*-nitro-acetophenone which is a poor substrate for *He*WT. After 2 rounds of screening, variant B2 was identified which displayed a 2.5 fold increase in activity and conversion increase from 14% to 22%. Repeating this exercise with *para*-cyano-acetophenone revealed an impressive 60-fold improvement in activity but again only marginal improvement in conversion (from 9% to 14%). A series of 4 small cyclic ketones were then studied leading to the identification of variant C1, which again displayed modest improvements in activity towards the target substrates (ca. 2-fold). While this work effectively demonstrates the power of the screening methodology in aminotransferase evolution towards target substrates, the chapter also highlights the application of *He*WT in the synthesis of synthetically useful chiral amines starting from simple prochiral ketone percurosors.

In chapter 4, enzymes from a diverse range of classes, with different reaction chemistries, cofactor requirements and reaction coditions were accessed for activity towards the same panel of small cyclic prochiral ketones. While the ketoreductase from *Pichia glucozyma* (KRED1-*Pglu*) did not show a marked enantiopreference in the reduction of tetrahdrofuran-3-one, *He*WT was found to be the preferred biocataysts for the reductive amination of the target substrates, capable of achieving high molar conversions and enantioselectivities compared to the ω-TA from *Psudomonas fluorescence* (*Pf*TA). To further extend the utility of

this work, it was envisaged that the newly synthesised chiral amines could be combined with different acyl donors using the acyltransferase from *Mycobacterium smegmatis* (*Ms*AcT) for the synthesis of optically active amides in aqueous solution. For this purpose the enzyme was screened for activity towards the comercially available amines. Excellent molar conversions (70.1% to 92.1%) were achieved in all cases. Robust immobilisation strategies were then applied to facilitate the transfer of this methodology into continuous flow.

Finally, building on the work carried out in chapter 4, the application of multiple enzymes within one-pot was accessed for the synthesis of optically active amides by combining *He*WT with *Ms*AcT. However, an incompatibility between the two enzymatic systems resulted in severe precipitation of the biocatalysts when combined together under the same reaction conditions. To overcome this challenge, the cascade was applied in continuous flow, which allowed for the compartmentalisation of the immobilised enzymes in separate bioreactors. Following optimisation of the flow conditions, the system afforded 2-methoxy-N-(tetrahydro-3-furanyl) acetamide with relatively high molar conversion and excellent residence time.

While this work highlights the feasibility of complex multi-enzyme systems in continuous flow, there are still a number of limitations that need to be addressed in order to develop an efficient biocatalytic cascade for the assembly of small cyclic chiral amides. To meet this constraint, a deeper studey of the active site of *He*WT, together with subsequent engineering efforts, such as TCSM, would be required to fine-tune the stereoselectivity of the enzyme. Once the properties of the biocatalyst have been fully optimised for asymmetric synthesis, the system would also benefit from more robust immobilisation strategies. For example, to minimise distortion of the catalyst upon immobilistation, it could be useful to fuse a sacrificial protein to the target enzyme which would form covalent bonds with the support, thereby shielding the biocatalyst and preserving its catalytic activity Furthermore, the

possibility to perform an in-line purification step, through the use of a Zaiput Flow technology liquid-liquid separator and polymer supported benzylamine would significantly streamline the overall process and provide a means of recycling any unreacted substrate, leading to an ultra-efficient, zero-waste process. To conclude, the results presented within this thesis will no doubt help pave the way towards more sustainable and cost-effective manufacturing processes for high-value molecules.

Exploring the Production of Enzymes of Industrial Interest in *Haloferax volcanii*

Introduction

1.1 The discovery of Archaea

The discovery of the Archaea as a distinct domain of life, came to light in the late 1960's following studies led by Carl Woese, which aimed to determine how cellular life had evolved to the forms presently existing on Earth. Until that time biologists had assumed that all life on Earth belonged to one of two primary lineages, the eukaryotes and the prokaryotes. Woese discovered however that there were in fact three primary lineages.[1]

At that time, organisms were classified based on morphology and physiology. However, these methods did not establish meaningful evolutionary relationships. Using the emerging techniques of nucleic acid sequencing, Woese proposed that the small-subunit (SSU) ribosomal-RNA nucleotide sequence could be used as a 'molecular chronometer'.[2] In his findings, Woese found that a group of anaerobic bacteria, which had been well studied for a number of years owing to their ability to generate methane, were not bacteria at all. The rRNA phylogeney revealed that they are no more related to bacteria then they are to eukaryotes.[2] This led to the belief that the prokaryotes are much more diverse that previously assumed, and that the phylogenetic structure of this domain should be reassessed. As a result of this work, Woese renamed this group of microorganism Archaebacteria. In a succeeding paper published in 1990, he shortened the name to Archaea and proposed that this domain should be considered a domain of equal primacy to Bacteria and Eukarya.[2] Despite initial resistance, it is now widely accepted that there are three primary divisions of living systems – the Eukarya, the Bacteria and the Archaea (Figure 1.1).

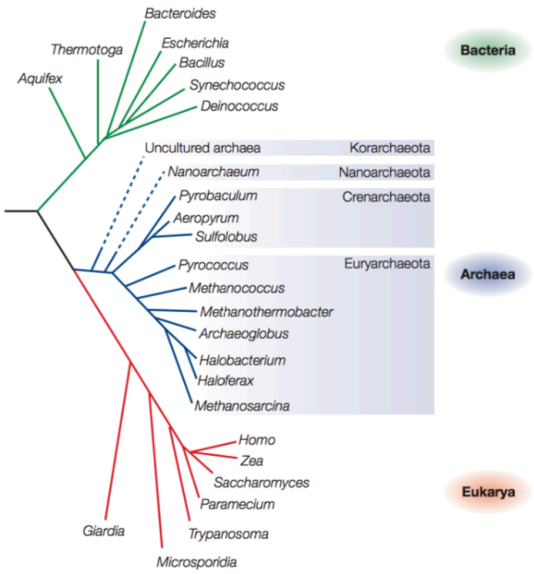


Figure 1.1| The Tree of Life. Universal phylogenetic tree showing the tree domains of life. Branching order and branch lengths are based upon rRNA sequence comparison.[2]

The domain Archaea comprises of two main phyla: the Euryarchaeota, which include all known halophiles and methanogens in addition to thermophilic and psychrophilic species, and the Crenarchaeota, members of which are renowned hyperthermophiles.[2] Of the remaining phyla, Nanoarchaeota has one known member (*Nanoarchaeum equitans*)[3], and thus far *Korarchaeota* are represented only by environmental DNA sequences.[4] Owing to the limited number of identified species, the position of these phyla on the tree remain unclear.

1.2 Characteristics of Archaea

The archaea are well known for inhabiting the most hostile environments on the planet. They thrive under conditions that few bacteria and no eukaryotes would tolerate. For example, the Methanogens are strict anaerobes that inhabit anoxic habitats such as sewage plants and swamps. They also have the ability to generate methane from carbon dioxide.[5] Halophilic archaea readily grow in hypersaline bodies of water such as the Dead Sea. Unlike Bacteria, which maintain an osmotic balance using organic solutes, archaea accumulate inorganic salts, primarily K^+ in the cytoplasm. While this allows them to grow in saturating

NaCl solutions, it also means that proteins of haloarchaea need to be adapted to function in high salt environments.[6] Acidophiles and alkaliphiles, as their name suggest grow at extremes of pH: acidophiles are often thermophiles and a significant fraction of alkaliphiles are also halophiles. Thermophiles such as *Pyrolobus fumarii* are found near deep sea hydrothermal vents, where temperatures exceed 100 ^{o}C, and *Sulfolobus solfataricis* populates hot springs such as those in Yellowstone National Park.[2] At the opposite end of the spectrum, psychrophilic archaea thrive in permanently cold conditions such as seawater or dry lakes in the Antarctic.[7] However, it is misleading to believe that all archaea are extremophiles. Archaea are in fact widely distributed in nature and are common in much less extreme habitats, such as the ocean, soil and even the human gut.[1]

1.3. *Haloferax volcanii*

Haloferax volcanii (H. volcanii) was isolated form the Dead Sea in 1975 by Benjamin Elazari Volvani, who was the first to determine that the Dead Sea, in spite of its name, contains many microorganisms.[8] *H. volcanii* is a moderate halophile and is able to grow in the presence of molar concentration of salt at an optimum temperature of 45 ^{o}C. It has a versatile metabolism and can be grown on simple synthetic media with a variety of sugars, amino acids, glycerol, pyruvate or acetate as the sole carbon and energy source. In addition to aerobic growth, it can also grow anaerobically using nitrate or DMSO as an electron acceptor.[9]

The genome of *Haloferax volcanii* is composed of five circular genetic elements: a 2.848 Mb main chromosome, three smaller chromosomes (the 636 kb pHV4, the 438 kb pHV3 and the 85.1 kb pHV1) as well as 1 plasmid (the 6.35 kb pHV2).[9] The GC content of the genome is relatively high at 65 %, however this is in keeping with other haloarchaea.[10]

To survive in a hypersaline environment, halophilic Archaea like *H. volcanii* rely on a variety of strategies manifested at the molecular level. For example, haloarchaeal proteins have much more acidic residues

compared to their non-halophilic homologs.[11] This allows haloarchaeal proteins to fold and function properly in the presence of molar amounts of salt, however a modified amino acid composition does not allow these proteins to adapt to fluctuations in their surroundings. Instead, post-translational modifications offer proteins a route to respond to changing environmental conditions. In the case of the *H. volcanii* S-layer glycoprotein, changes in environmental salinity are reflected in a modified N-glycosylation profile.[12]

A wide range of genetic tools have been developed for *H. volcanii*, many of which revolve around introducing DNA into *H. volcanii* cells. For example, a typical shuttle vector, such as the pTA230 vector (Figure 1.2), uses the origin from pHV2, the naturally occurring 6.4 kb *H. volcanii* plasmid.[13] As this is a non-essential plasmid, *H. volcanii* could be cured of pHV2 using ethidium bromide, generating the widely used laboratory strain WFD11.[14] A strain that was cured without ethidium bromide, the DS70 strain, has since been isolated.[15] Furthermore, Cline and Doolitle demonstrated an efficient polyethylene glycol-mediated transformation method for *H. volcanii*.[16] This was the first example of high-efficiency transformation of archaea. Significant improvements of transformation protocols have since been developed by generating strains deficient in the Mrr restriction endonuclease.[17] Mrr cleaves foreign DNA that is methylated at 5'-GATC and reduces the transformation efficiency by 50-fold. The Δ*mrr* strains allow direct and efficient transformation of *H. volcanii*.

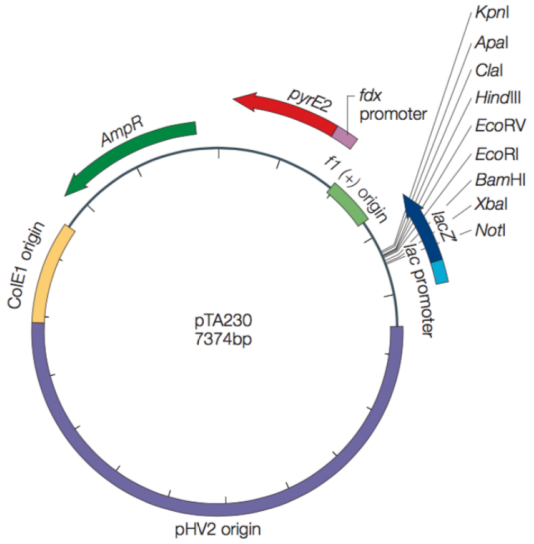


Figure 1.2| The pTA230 plasmid. A typical shuttle vector for *Haloferax volcanii* showing all relevant features. (Plasmid map was kindly provided by Prof. Thorsten Allers, University of Nottingham).

The genetic toolbox for *H. volcanii* also includes a wide range of selectable markers. Although most bacterial antibiotics are ineffective in archaea, several exceptions have been exploited to develop selectable markers for *H. volcanii.* Antibiotic markers include novobiocin, which inhibits DNA gyrase, and mevinolin, a HMG-CoA reductase inhibitor.[13,18] However both of these antibiotic resistance markers share homology with essential genes, which is a problem when using homologous recombination to integrate a DNA fragment containing either of the markers onto the chromosome. This has been circumvented by developing auxotrophic mutants, to allow the use of auxotrophic markers to select for the presence of DNA transformed into *H. volcanii*.[19] These include uracil, tryptophan, leucine, thymidine, histidine and methionine.

1.4 Overexpression and purification of halophilic proteins in *Haloferax volcanii*

Several strategies have been applied to develop a system for the over expression and purification of halophilic proteins in *H. vlocanii*. This has resulted in a highly engineered host strain and a corresponding plasmid for the inducible overexpression of His-tagged proteins.

In the host strain, *H. volcanii* 1209, the *pitA* gene has been replaced with its orthologue from *Natronomonas pharaonic*.[17] PitA is a fusion of chlorite dismutase-like and monooxygenase-like domains. It is unique to haloarchaea and in almost all species features a histidine rich linker.[5] Owing to this histidine rich region, PitA is a major contaminant of His-tagged recombinant proteins purified from *H. volcanii* by immobilized metal affinity chromatography. Attempts to delete the *pitA* gene proved unsuccessful indicating that it is essential. Instead this gene was replaced with its orthologue from the haloalkaliphile *N. pharaonic*, which does not feature a high number of histidine residues in the central linker region. The resulting strain exhibits no contamination by PitA, thus improving protein yield and purity of recombinant proteins.[17]

The pTA963 overexpression vector (Figure 1.3) utilizes the P.tnaA tryptohanase promoter of *H. volcanii*. Genes under control of the P.tnaA promoter show strong and rapid induction of expression upon addition of ≥ 1 mM tryptophan. For the expression of proteins with an N-terminal hexahistidine tag, a $(CAC)_6$ tract was incorporated in the expression vector and a polylinker ensures that cloning is facile. The vector is based on the pHV2 replicon that maintains the plasmid at a copy number of ~ 6 per genome equivalent.[19] Selection is based on the *pyr*E2 and *hdr*B markers which allow growth of the host strain on media lacking uracil and thymidine respectively. The latter marker allows the plasmid to be maintained in rich media (*Hv*-YPC), maximizing protein overexpression.

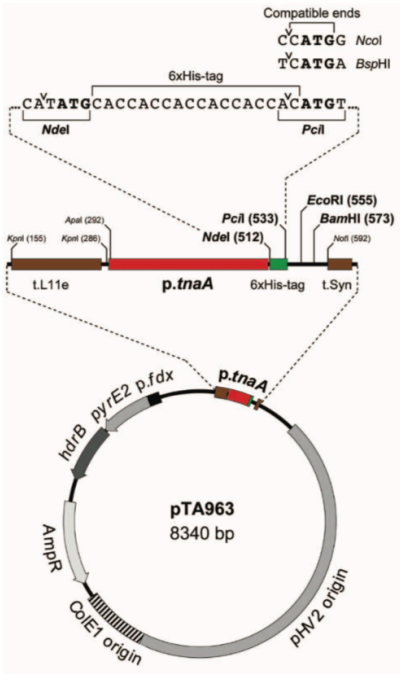


Figure 1.3| The pTA963 conditional overexpression vector. The pTA963 expression vector has been utilized for the successful overexpression of halophilic proteins in *Haloferax volcanii.*[14]

1.5 Common expression systems in the biotechnological industry

The challenge of producing high quality recombinant proteins at the scale required for commercial and therapeutic applications has led to the development of a variety of methods for heterologous protein production. Bacteria, yeast, insect and mammalian are among the main cell based expression systems that are widely used and well established across the biotechnological industry, each of which have their own inherent strengths and weaknesses.

- **Bacterial Expression Systems**

  The Gram-negative bacterium *E. coli* is routinely used for the overexpression of recombinant proteins in academic and industrial settings. The advantage of using bacterial expression systems stems from its cost effectiveness, as *E. coli* has minimal technical requirements and is able to grow rapidly on inexpensive

culture media. In addition, *E. coli* is amendable to a variety of genetic manipulations and there are a wealth of modified host strains available which enhance protein yield and reduce proteolytic degradation.[20]

While the bacterial expression system has been the workhorse in protein expression studies for several decades, this system has many limitations when it comes to the expression of eukaryotic proteins. *E. coli*, being a prokaryote has a very different cell structure than eukaryotes and its simpler machinery is unable to fold foreign proteins correctly or perform posttranslational modifications that commonly occur in naturally expressed eukaryotic proteins.[21] As a result eukaryotic proteins expressed by *E. coli* are often produced in an insoluble form. In some cases, these limitations can be circumvented by the use of genetically modified bacterial expression strains or by performing an additional protein refolding step. Moreover, *E. coli* can produce endotoxins. This is a major limiting factor if the target enzyme if intended for industrial processes as the removal of bacterial endotoxin form recombinant proteins is both challenging and expensive.[22]

- **Yeast Expression Systems**

  Expression of proteins in yeast is a common alternative to bacterial expression systems. Yeast cells offer many advantages as they share the complex biology of multicellular organisms and are able to produce proteins that carry out post translational modifications (PTMs) such as lipidation and proteolytic processing. Similar to bacteria, yeast are easy to manipulate genetically, have a rapid growth rate, and achieve high cell densities in culture, delivering up to several milligrams of protein. The most commonly used strains include *Pichia pastoris*, *Saccharomyces cerevisiae* and *Kluyveromyces lactis* and a growing number of engineered strains are becoming available for

improved protein expression.[23] For example, protease deficient *Pichia pastoris* is becoming one of the most popular yeast expression systems. Yeast cells are however limited by their inability to produce complex *N*-linked glycans. In addition, both *S. cerevisiae* and *K. lactis* produce hypermannosylated *N*-linked glycans which raises the risk of immunogenicity, particularly for therapeutic products.[24]

- **Insect Cell Expression Systems**

  Baculoviral expression systems are widely used to produce large quantities of recombinant proteins in insect host cells.[25] These systems are particularly well suited for proteins that are difficult to express in bacteria due to size, complexity, or posttranslational modifications that occur in mammalian cells. However, the *N*-linked glycosylation in insect cells results in glycoproteins having only simple oligo-mannose sugar chains with little sialyation.[26] This is a major imitation because *N*-glycans contribute to the functionality of the glycoprotein in many ways. Attempts to address this problem have resulted in the development of an insect cell line that expresses the genes for the enzymes required for producing the mammalian glycosylation patterns that were lacking in the parent insect cell line.[27] The glyco-engineered insect cells coupled with the baculovirus expression vectors can produce recombinant glycoproteins with complex terminally sialyated *N*-glycans.

- **Mammalian Expression System**

  Given that a substantial part of protein research focusses on mammalian and human proteins, the mammalian system is the most desirable for many research and industrial projects. This system delivers fully functional proteins with the most relevant biological modifications. These PTMs include, but are not limited to glycosylation, phosphorylation, acetylation and methylation.[28] These PTMs are important because they directly relate to the

functionality of the recombinant protein being produced. However, mammalian expression systems typically produce very low protein yields and require laborious scale-up processes.[29] Consequently, they are the least economical systems among those mentioned.

It is clear to see that a diverse range of heterologous hosts are available for the production of therapeutic and commercial proteins. However, in spite of these resources there is currently no universal system that provides every protein in a high yield, functional and scalable fashion. Furthermore, the absence of an archaeal expression system is immediately recognized from this list.

1.6 The application of *H. volcanii* as an alternative expression system for enzymes of industrial interest

To date, the *H. volcanii* expression system has been successfully applied for heterologous protein expression on a shaker-flask scale.[30] However, the tendency of *H. volcanii* to form biofilm prevented the use of this halophilic expression system in stirred tank bioreactors because biofilm interferes with sensors during the fermentation process.[31a] The genes Hvo_1033 and Hvo_1034, which encode an ATPase and an integral membrane protein of the pilus assembly system are necessary for biofilm formation.[32] Knockout of these genes has successfully eliminated the attachment of *H. volcanii* to surfaces of any kind while leaving the cells motile. The resulting H1895 strain is therefore an ideal host for the expression of halophilic proteins in a stirred tank bioreactor. Given these advancements, one asks the question whether the *H. volcanii* expression system could be used as an alternative host for the high-level expression of enzymes of industrial interest.

Aims & Objectives

In keeping with industry's desire to move away from traditional expression systems such as *E. coli*, a non-conventional system for the expression of biocatalysts will be investigated using the halophilic archeon *Haloferax volcanii*. *H. volcanii* is an attractive host for this purpose as several strategies have already been put in place to engineer a strain amendable for heterologous protein expression. Exploiting these features, the genes encoding the *Halomonas elongatea* ω-transaminase and a mesophilic alcohol dehydrogenase from horse liver will be subcloned into a suitable expression vector. Protein expression will then be investigated and optimised accordingly.

Materials & Methods

2.1 Reagents, strains and culture conditions

All chemical reagents, unless otherwise stated, were purchased from Sigma Aldrich. Restriction enzymes were purchased from New England Biolabs. *E. coli* XL10 Gold electro-competent cells were prepared in house using the procedure outlined in 2.5.2. Phusion U Multiplex PCR Master Mix (Thermo Scientific) was used for PCR amplification. T4 DNA ligase (New England Biolabs) was used for DNA ligation. *H. volcanii* strains were grown at 45 ^{o}C on *Hv*-YPC or *Hv*-Min agar or in *Hv*-YPC broth as described previously.[33] Transformation of *H. volcanii* was carried out as previously described.[16] All *H. volcanii* strains (H1895 and H1325) and vectors (pTA963) were kindly donated by Prof. Thorsten Allers (University of Nottingham).

2.2 Construction of the pTA963-*spuC* expression vector

The *spuC* gene, encoding the ω-transaminase from *H. elongata* (*He*WT) was initially isolated from the pRSETb (Thermo Scientific) expression vector using *NotI* and *NdeI* restriction sites. As pRSETb does not naturally contain a *NotI* restriction site, this site was generated using the QuikChange Lighting Multi Site Directed Mutagenesis Kit (Agilent Technologies) following the manufacturers procedures.

The product of digestion, corresponding to the expected molecular weight of 1504 bp was gel purified and ligated with the pTA963 expression vector following the manufacturers procedures. Prior to ligation the pTA963 vector was digested at *NotI* and *NdeI* restriction sites to create compatible ends for cloning. The ligation mixture was then used to transform *E. coli* XL10 Gold electro-competent cells directly. Plasmid DNA was isolated from candidate clones and screened by restriction digest using *NotI* and *NdeI* restriction enzymes. Successful cloning was confirmed by DNA sequencing (Eurofins Genomics, Germany).

As an alternative approach, the *H. elongata spuC* gene was PCR amplified from plasmid DNA using two unique primers (Table 2.1). These

primers were designed to incorporate *EcoRI* and *BamHI* restriction enzyme sites, respectively. The 1417 bp PCR product was digested with *EcoRI* and *BamHI* restriction enzymes and ligated with the pTA963 expression vector. Prior to ligation the pTA963 vector was also digested at *EcoRI* and *BamHI* restriction sites to generate the compatible ends required for cloning. The ligation mixture was subjected to an ethanol precipitation step and then used to transform *E. coli* XL10 Gold electro-competent cells. Plasmid DNA isolated from candidate clones was screened by *EcoRI/BamHI* restriction digest and verified by DNA sequencing (Eurofins Genomics, Germany).

Table 2.1| Forward and reverse primers used to amply the *spuC* gene

Primer Name	Sequence
SPUC_FW	GACGATAAGAATTCGATGCAAACCCAAGACTATCAGGC
SPUC_RV	ATCAAGCTTCGGATCCTCATGCGGTTGGC

2.3 Transformation of *H. volcanii* H1895

H. volcanii H1895 was transformed using the standard PEG-mediated transformation protocol previously outlined.[16] *Hv*-Min agar plates, plated with the transformation mixture were placed in a humidity controlled environment and incubated at 45 ^{o}C. Colony formation became apparent after 5 days of incubation.

2.4 Expression of *He*WT in *Haloferax volcanii* H1895

Starter cultures (5 mL) of *H. volcanii* H1895 transformed with the pTA963-*spuC* plasmid were used to inoculate 50 mL *Hv*-YPC broth. After 16 h of growth, protein expression was induced with the addition of L-tryptophan to a final concentration of 5 mM. The cells were cultured for up to 8 h following induction. Cells were harvested by centrifugation at 4,000 rpm, for 15 min at 4 ^{o}C. The wet cell pellet was weighed and routinely stored at -20 ^{o}C.

The pellets were thawed and resuspended in two variant lysis buffers; 50 mM potassium phosphate buffer, pH 8.0, containing 0.1 Mm pyridoxal 5'-phosphate (PLP) and 50 mM potassium phosphate buffer, pH 8.0, containing 0.1 Mm pyridoxal 5'-phosphate (PLP) and 3 M KCL. 1 mL of buffer was used to resuspend 100 mg of cell pellet. Cells were disrupted by sonication at 6 W, 4 ^{o}C at intervals of 30 s on and 30 s off until the lysate appeared transparent. After centrifugation (14,000 rpm, 4 ^{o}C , 30 min) the supernatant was assayed for *He*WT activity (see section 2.6.2 in the general materials and methods). Samples of the pellet and crude supernatant were analysed by SDS-PAGE employing a 12% polyacrylamide gel and stained with Instant Blue. A broad range protein marked (10-200 kDa) was used for determination of relative molecular weight.

2.5 Purification of *He*WT from *H. volcanii* H1895

The supernatant resulting from *H. volcanii* cells transformed with pTA963-*spuC* was purified by affinity chromatography using a 10 mL gravity column filled with Ni-NTA resin. In brief, the column was equilibrated with loading buffer (50 mM potassium phosphate buffer, pH 8.0, containing 100 mM NaCl, 0.1 mM PLP and 30 mM imidazole) and the sample loaded. The column was washed three times with the same buffer. Two elution steps were then carried out with elution buffer (50 mM potassium phosphate buffer, pH 8.0, containing 100 mM NaCl, 0.1 Mm PLP and 300 mM imidazole). Samples of the crude supernatant and collected fractions were analysed by SDS-PAGE using a 12% polyacrylaminde gel and stained with Instant Blue. A broad range protein marker (10-200 kDa) was used for determination of relative molecular weight. Fractions showing the presence of a band corresponding to the molecular weight of the His-tagged protein (54 kDa) were dialyzed overnight against 50 mM potassium phosphate buffer, pH 8.0, containing 0.1 mM PLP. The purified sample was then assayed for transaminase activity using methods outlined in section 2.6.2 in the general materials and methods.

2.6 Synthetic gene design and syntheses

Codon optimized genes for expression in *H. volcanii* were designed by substituting suboptimal codons with those preferentially used in *H. volcanii*. In addition, the genes were designed to feature *EcoRI* and *BamHI* restriction enzyme sites for facile cloning. Once designed, these genes were synthesised chemically by Eurofins Genomics (Ebersberg, Germany) All synthetic genes were received in a standard cloning vector: pEX-K4.

2.7 Construction of the pTA963-HLADH expression vector

The gene encoding horse liver alcohol dehydrogenase (HLADH), optimized for expression in *H. volcanii* was isolated from pEX-K4 using *EcoRI* and *BamHI* restriction sites. The product of digestion, corresponding to the molecular weight of the synthetic gene (1135 bp) was gel purified and ligated with the pTA963 expression vector. Prior to ligation, pTA963 was digested with *EcoRI* and *BamHI* restriction enzymes to generate compatible ends for cloning. The resulting ligation mixture was subjected to ethanol precipitation and then used to transform *E. coli* XL10 Gold electro-competent cells. Plasmid DNA isolated from candidate clones was screened by *EcoRI*/*BamHI* restriction digest and then verified by DNA sequencing.

2.8 Expression of HLADH in *H. volcanii* H1895 and H1325

H. volcanii strains H1895 and H1325 were transformed with the pTA963-HLADH plasmid using the standard protocol for PEG mediated transformation as previously described by Allers et al.[33] Protein expression was investigated under two different conditions:

1. Starter cultures (5 mL) of the respective strains transformed with pTA963-HLADH were used to inoculate 50 mL *Hv*-YPC broth. Cultures were grown for 24 h at 45 ^{o}C, 200 rpm and then diluted into 270 mL of *Hv*-YPC broth. After 16 h of growth, protein expression was induced with the addition of L-tryptophan to a final concentration of 5 mM. The cells were cultured for 8 h following

induction. The cells were harvested by centrifugation at 4,000 rpm, for 15 min at 4 °C. Wet cell pellets were weighed and stored routinely at -20 °C.

2. Starter cultures (5 mL) of *H. volcanii* H1895 and H1325 strains transformed with pTA963-HLADH were used to inoculate 50 mL *Hv*-YPC broth. Again the cultures were grown for 24 h at 45 °C, 200 rpm and then diluted into 333 mL of *Hv*-YPC broth. Following incubation at 45 °C, 200 rpm for 16 h, protein expression was induced with the addition of L-tryptophan to a final concentration of 3 mM. After 1 h, additional tryptophan was added to a final concentration of 4.5 mM. The cultures were incubated for an additional hour at 45 °C, 200 rpm. Cells were harvested by centrifugation at 4,000 rpm, for 15 min at 4 °C. Wet cell pellets were weighted and stored at -20 °C.

Pellets were thawed and resuspended in two variant lysis buffers; 20 mM Na_2HPO_4-NaH_2PO_4 buffer, pH 7.4, containing 0.5 M NaCl and 0.02 M imidazole, and 20 mM Na_2HPO_4-NaH_2PO_4 buffer, pH 7.4, containing 3 M NaCl, 0.02 M imidazole. 1 mL of buffer was used to resuspend 100 mg of cells. Cells were disrupted by sonication as previously described in section 3.3. After centrifugation (14,000 rpm, 4 °C, 30 min) the supernatant was assayed for HLADH activity (see section 3.8). Samples of the pellet and crude extract were also analysed by SDS-PAGE using 12% polyacrylamide gels stained with Instant Blue. A broad range protein marker was used for determination of relative molecular weight.

2.9 Alcohol Dehydrogenase activity assay

Enzymatic activity was investigated spectrophotometrically using a kinetic assay previously described by Quaglia et al.[34] The reaction was carried out in a microcuvette at 25 °C. The reaction mixture for the oxidative step contained NAD^+ (1 mM), ethanol (4 mM), an appropriate amount of the enzyme and up to 1 mL of 50 mM phosphate buffer , pH

8.8. Activity was based on the production of NADH (ε_{340} = 6.2 mM^{-1} cm^{-1}) during the first five minutes of reaction at 340 nm.

2.10 Construction of the pTA963-*spuC* expression vector

The *spuC* gene, optimized for expression in *H. volcanii*, was isolated form the pEX-K4 plasmid using *Eco*RI and *BamHI* restriction sites. The product of digestion, corresponding to the molecular weight of the synthetic gene (1394 bp) was gel purified and ligated with the pTA963 expression vector. Prior to ligation, pTA963 was digested with *EcoRI* and *BamHI* restriction enzymes to create compatible ends for cloning. The resulting ligation mixture was subjected to an ethanol precipitation step and then used to transform *E. coli* XL10 Gold electro-competent cells. Plasmid DNA isolated from candidate clones was screened by *EcoRI*/*BamHI* restriction digest and verified by DNA sequencing.

2.11 Expression of *He*WT in *H. volcanii* H1895 and H1325

H. volcanii strains H1895 and H1325 were transformed with the pTA963-*spuC* plasmid using the standard protocol for PEG mediated transformation as described by Allers et al.[33] Protein expression was investigated under two different conditions:

1. Starter cultures (5 mL) of the respective strains transformed with pTA963-*spuC* were used to inoculate 50 mL *Hv*-YPC broth. Cultures were grown for 24 h at 45 ^{o}C, 200 rpm and then diluted into 270 mL of *Hv*-YPC broth. After 16 h of growth, protein expression was induced with the addition of L-tryptophan to a final concentration of 5 mM. The cells were cultured for up to 8 h following induction. The cells were then harvested by centrifugation at 4,000 rpm, for 15 min at 4 ^{o}C. Wet cell pellets were weighed and routinely stored at -20 ^{o}C.

2. Starter cultures (5 mL) of *H. volcanii* H1895 and H1325 strains transformed with pTA963-HLADH were used to inoculate 50 mL *Hv*-YPC broth. The cultures were grown for 24 h at 45 ^{o}C, 200 rpm

and then diluted into 333 mL of *Hv*-YPC broth. Following incubation at 45 ^{o}C, 200 rpm for 16 h, protein expression was induced with the addition of L-tryptophan (3 mM). After 1 h, additional tryptophan was added to a final concentration of 4.5 mM. The cultures were incubated for an additional hour at 45 ^{o}C, 200 rpm. Cells were harvested by centrifugation at 4,000 rpm, for 15 min at 4 ^{o}C. Wet cell pellets were weighted and stored at -20 ^{o}C.

Pellets were thawed and resuspended in two variant lysis buffers; 50 Mm potassium phosphate buffer, pH 8.0, containing 0.1 Mm pyridoxal 5'-phosphate (PLP) and 50 Mm potassium phosphate buffer, pH 8.0, containing 0.1 mM pyridoxal 5'-phosphate (PLP) and 3 M KCl. 1 mL of buffer was used to resuspend 100 mg of cell pellet. Cells were disrupted by sonication at 6 W, 4 ^{o}C at intervals of 30 s on and 30 s off until the lysate appeared transparent. After centrifugation (14,000 rpm, 4 ^{o}C , 30 min) the supernatant was assayed for HEWT activity (see section 3.7). Samples of the pellet and crude supernatant were analysed by SDS-PAGE employing a 12% polyacrylamide gel, stained with Instant Blue. A broad range protein marked (10-200 kDa) was used for determination of relative molecular weight.

2.12 Purification of *He*WT from *Haloferax volcanii*

Purification of *He*WT was carried out by affinity chromatography using an ÄKTA Start chromatography system. A 1 mL HisTrapTM FF column pre-packed with Ni Sepharose 6 Fast Flow resin and precharged with 0.1 M $NiSO_4$ was employed for the purification. In brief, the system was equilibrated with loading buffer (50 mM phosphate buffer, pH 8.0 containing 100 mM NaCl, 0.1 mM PLP and 30 mM imidazole) and the filtered cellular extract loaded. The column was washed with 20 column volumes of the same buffer at a flow rate of 1 mL/min followed by an intermediate step with 10% of elution buffer (50 mM phosphate buffer, pH 8.0 containing 100 mM NaCl, 0.1 mM PLP and 300 mM imidazole) to remove non-specifically bound proteins. An isocratic elution step using

elution buffer was then applied to collect the His-tagged protein. Samples of the pellet, crude extract and fractions collected were analysed by SDS PAGE using a 12% polyacrylamide gel stained with Instant Blue. A broad range protein marker was used to determine relative molecular weight. The fractions showing the presence of a band corresponding to the expected molecular weight of the His-tagged protein (50.4 kDa) were pooled and dialyzed overnight against 50 mM potassium phosphate buffer, pH 8.0 and 0.1 mM PLP and stored at 4 ^{o}C . The purified protein was then assayed form transaminase activity using methods outlined in section 2.6.2 in the general materials and methods.

Results & Discussion

3.1 Expression of *He*WT in *H. volcanii*

To investigate the expression of *He*WT in *H. volcanii*, the native *spu*C gene was subcloned into the pTA963 expression vector using *NotI* and *NdeI* restriction sites. To achieve this, a *NotI* restriction site first had to be incorporated upstream of the gene of interest in pRSETb. For this purpose two point mutations were incorporated at positions 1601 and 1606 using the QuikChange Multi Site-Directed Mutagenesis Kit. Successful incorporation of the *NotI* restriction site was confirmed by DNA sequencing. Next, an overnight restriction enzyme digest, using *NotI* and *NdeI* restriction enzymes, was carried out to isolate the *spu*C gene from pRSETb. The destination vector, pTA963 was also subjected to an overnight digest with *NotI* and *NdeI*, thereby creating the compatible ends required for cloning. As seen in Figure 3.1, linear bands corresponding to the molecular weight of the *spu*C gene and the pTA963 vector backbone were obtained. Negative controls, to which no DNA was added, were carried out in parallel to ensure complete digestion was achieved.

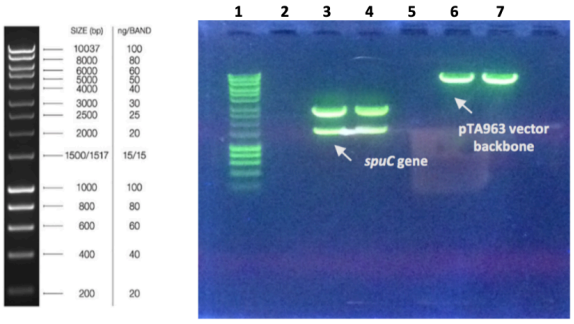


Figure 3.1| Agarose gel electrophoresis following a double digest with *NdeI* and *NotI.* Lane 1: Bioline Hyperladder 1 kb, **Lanes 3-4:** pRSET B-*spuC* following digestion with *NdeI* and *NotI*, **Lanes 6-7**, pTA963 expression vector following digestion with *NdeI* and *NotI*. Molecular weight in base pairs are indicated on the left. An arrow indicates the position of the *spuC* gene and pTA963 vector backbone.

Overnight ligations were carried out at 4 °C and 16 °C using vector:insert molar ratios of 1:3, 1:6 and 1:9. Between 1-5 µL was used directly to transform *E. coli* XL10 Gold electro-competent cells. However, after several attempts, no transformants were obtained. This called for a comprehensive review of DNA preparation and handling techniques.

Given that numerous studies have reported poor ligation and transformation efficiencies after prolonged exposure of DNA to ultraviolet light, initial considerations pointed towards the integrity of the DNA used in these downstream cloning protocols.[35] In an effort to minimize DNA damage and enhance cloning efficiencies, a blue light transilluminator was employed for the visualisation of DNA to be purified from gel fragments.

Next, the viability of the cells used for transformation was investigated by transforming an appropriate amount of the common laboratory plasmid, pUC19. The transformation efficiency of the cells was calculated to be 2.8×10^6 CFU/µg of DNA, which is below the recommended value of 10^8 CFU/µg of DNA. A fresh batch of electro-competent cells was prepared yielding a 10-fold increase in transformation efficiency. The size of the vector backbone was also taken into consideration. At 8340 bp, it was found that the amount of insert added to the ligation mixture was insufficient for successful ligation to occur. An unconventional method for ligation, previously reported by Allers and co-workers was thus investigated.[36] This required half the volume of vector and all of the insert eluted from the gel purification to be included in the ligation mixture. After an overnight incubation at 16 °C, 1 µL of the resulting mixture was incubated with *E. coli* XL10 Gold electro-competent cells for up to 30 min. The incubation period was carried out to allow the DNA come in close proximity with the cells. Electroporation was subsequently carried out a 18,000 V. Colony formation was apparent the next morning and random colonies were screened by restriction digest with *NotI* and *NdeI*

restriction enzymes (Figure 3.2). The sequence of the native *spu*C gene was later confirmed with 100% identity by DNA sequencing.

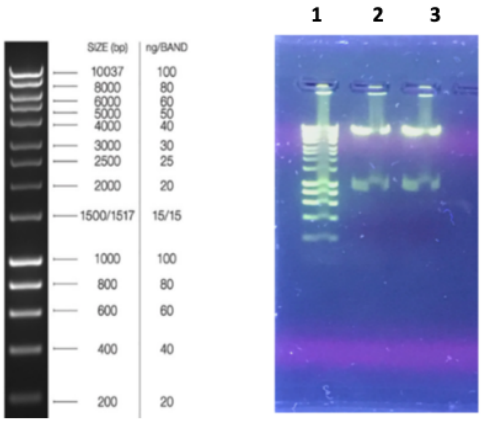


Figure 3.2| Random colonies were screened for positive clones by restriction digest with *NotI* and *NdeI*. Lane 1: Bioline Hyperladder 1 kb, **Lanes 2-3:** Random colonies screened by restriction digest with *NotI* and *NdeI*. Relative molecular weight in base pairs are indicated on the left. In each case a band corresponding to the size of the *spuC* gene (1504 bp) was observed.

As outlined above, the challenges encountered during this preliminary cloning experiment can be attributed to a number of factors, however it is noteworthy to mention that DNA fragments digested with *NdeI* type generally exhibited poor ligation efficiency with respect to other restriction enzymes commonly used within the laboratory.

Expression of the His-tagged ω-TA was investigated in *H. volcanii* H1895. This strain was selected based on the deletion of two genes encoding key components of the flagella assembly system. Knockout of these gene allows for the efficient growth of *H. volcanii* in a stirred biotank reactor without biofilm formation.[32] This feature makes it particularly interesting from an industrial point of view. Expression was performed on *Hv*-YPC medium according to methods previously described by Timspon *et al*.[37]

Two different lysis buffers were compared: 50 mM potassium phosphate buffer pH 8.0 containing 0.1 mM PLP and 50 mM potassium phosphate buffer, pH 8.0 containing 0.1 mM PLP and 3 M KCl. Buffers were selected

based on the knowledge that halophilic archaea avoid osmotic shock by increasing the ion concentration of their cytoplasm. Thus, the addition of 50 mM phosphate buffer pH 8.0, containing 0.1 mM PLP and no salt resulted in partial lysis of the cells. An obvious difference in the clarity and colour of the cell suspension was noted. 5 cycles of sonication at intervals of 30 s was sufficient to obtain a completely transparent lysate. In contrast, cells responded in buffer containing 3 M KCl required at lease 10 cycles of sonication before a completely clear lysate could be obtained.

To remain biologically active and folded at high intracellular concentrations of salt, proteins native to *H. volcanii* have evolved towards a biased amino acid composition. It was therefore thought that many of these proteins would precipitate out of solution in an environment containing no salt. However, analysis of the crude extracts by SDS-PAGE revealed that this was not the case. As seen in Figure 3.3, similar profiles were obtained following resuspension in the two variant buffers. Concentration measurements of each samples also revealed no significant variations (Table 3.1). Expression of the His-tagged transaminase was also difficult to interpret. A quick purification of the crude extract was therefore carried out using gravity chromatography. The purified fractions were also analysed by SDS-PAGE and compared to a sample of the His-tagged ω-TA previously purified from *E. coli* BL21(DE3). As seen in Figure 3.3, bands corresponding to the molecular weight of the *He*WT were obtained, indicating successful expression of the *spu*C gene in *H. volvanii* H1895. From the purification it was possible to obtain 0.12 mg/L cell culture.

To test for transaminase activity, a spectrophotometric assay previously described by Schätzle et al was carried out.[38] Despite the expression of soluble protein, transaminase activity could not be detected.

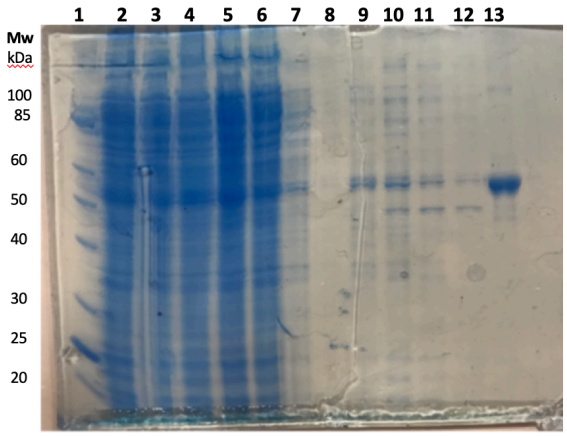


Figure 3.3| SDS-PAGE visualization of *He*WT following expression and purification from *H. volcanii* H1895. Lane 1: Unstained Protein Standard, Broad Range (10-200 kDa), **Lanes 2-3**: *H. volcanii* H1895 *He*WT supernatant (resuspended in buffer containing no salt), **Lanes 4-5**: *H. volcanii* 1895 *He*WT supernatant (resuspended in buffer containing 3 M KCl), **Lane 6**: Purification flow through, **Lane 7-8**: Eluate following 2 wash steps with 50 mM potassium phosphate buffer, pH 8.0 containing 100 mM NaCl, 0.1 mM PLP and 30 mM imidazole, **Lane 9-12**: Fractions collected following elution with 50 mM potassium phosphate buffer, pH 8.0, containing 100 mM NaCl, 0.1 mM PLP nd 300 mM imidazole. **Lane 13**: Purified *He*WT following expression in *E.coli* BL21 (DE3). Molecular masses in kDa are indicated on the left. An arrow indicates the position of *He*WT.

Table 3.1| Concentration measurements of crude extracts following resuspension in different lysis buffers

Crude Extract	Buffer	Concentration (mg/mL)
H. volcanii H1895 pTA963-*spu*C	PO_4 Buffer (50 mM, pH 8.0) containing 0.1 mM PLP	8.5
H. volcanii H1895 pTA963-*spu*C	PO_4 Buffer (50 mM, pH 8.0) containing 0.1 mM PLP and 3M KCl	10.0

3.2 Codon optimization of genes

Genetic codes comprise 64 nucleotide triplets (codons) encoding 20 amino acids and 3 stop codons. The frequencies of codon usage among organisms differ considerably. Moreover highly expressed genes are biased towards codons that are recognized by the most abundant tRNA species in the host organism. A potential obstacle to optimal expression of the target genes in the *H. volcanii* host may be the differences in codon usage between the host organism, *Equus caballus* (*E. caballus*) and *H. elongata.* A study of the genomic content of these three organisms was

therefore undertaken which revealed a GC content of 65% for *H. volcanii*, compared to 41% for *E. caballus* and 63% for *H. elongata*. In an effort to improve heterologous protein expression in *H. volcanii* codon-optimized genes for the target proteins were designed and chemically synthesized by Eurofins genomics using suitable codons for the host cell without altering the amino acid sequences.

Codon Bias for *Haloferax volcanii* main chromosome

Relative percentage per amino acid

	T				C				A				G			
T	TTT	Phe	F	7.75%	TCT	Ser	S	3.55%	TAT	Tyr	Y	8.04%	TGT	Cys	C	36.72%	T
	TTC	Phe	F	92.25%	TCC	Ser	S	22.78%	TAC	Tyr	Y	91.96%	TGC	Cys	C	63.28%	C
	TTA	Leu	L	1.07%	TCA	Ser	S	2.73%	TAA	***	*	22.95%	TGA	***	*	59.22%	A
	TTG	Leu	L	3.97%	TCG	Ser	S	44.59%	TAG	***	*	17.83%	TGG	Trp	W	100.00%	G
C	CTT	Leu	L	4.16%	CCT	Pro	P	1.94%	CAT	His	H	6.22%	CGT	Arg	R	4.42%	T
	CTC	Leu	L	67.15%	CCC	Pro	P	41.31%	CAC	His	H	93.78%	CGC	Arg	R	54.34%	C
	CTA	Leu	L	1.21%	CCA	Pro	P	3.48%	CAA	Gln	Q	17.69%	CGA	Arg	R	11.85%	A
	CTG	Leu	L	22.45%	CCG	Pro	P	53.27%	CAG	Gln	Q	82.31%	CGG	Arg	R	25.34%	G
A	ATT	Ile	I	14.50%	ACT	Thr	T	3.39%	AAT	Asn	N	6.51%	AGT	Ser	S	4.34%	T
	ATC	Ile	I	80.56%	ACC	Thr	T	46.04%	AAC	Asn	N	93.49%	AGC	Ser	S	22.01%	C
	ATA	Ile	I	4.93%	ACA	Thr	T	3.43%	AAA	Lys	K	26.99%	AGA	Arg	R	2.40%	A
	ATG	Met	M	100.00%	ACG	Thr	T	47.15%	AAG	Lys	K	73.01%	AGG	Arg	R	1.64%	G
G	GTT	Val	V	4.50%	GCT	Ala	A	3.41%	GAT	Asp	D	5.55%	GGT	Gly	G	9.73%	T
	GTC	Val	V	70.73%	GCC	Ala	A	45.39%	GAC	Asp	D	94.45%	GGC	Gly	G	64.57%	C
	GTA	Val	V	1.89%	GCA	Ala	A	4.67%	GAA	Glu	E	31.45%	GGA	Gly	G	7.54%	A
	GTG	Val	V	22.88	GCG	Ala	A	46.53%	GAG	Glu	E	68.55%	GGG	Gly	G	18.16%	G

Figure 3.4| Codon usage table for *H. volcanii* main chromosome.[39]

3.3 Construction of the pTA963-HLADH expression vector

The synthetic gene encoding HLADH was subsequently cloned into the pTA963 expression vector using *EcoRI* and *BamHI* restriction sites. Again, cloning was not a straightforward process and a significant amount of laboratory time was invested before positive clones were obtained. In this case, transformants could only be obtained when an ethanol precipitation step was carried out prior to ligation with T4 DNA ligase. Random colonies screen by a restriction digest with *EcoRI* and *BamHI* revealed a band corresponding to the size of the HLADH synthetic gene (1135 bp). The sequence was later confirmed by DNA sequencing with 100% identity.

3.4 Construction of the pTA963-*spuC-Opt* expression vector

Construction of the pTA963-*spuC-Opt* expression vector also presented some challenges, with initial cloning experiments resulting in an empty plasmid. To gain a better understanding as to why this was occurring, random colonies were sent for DNA sequencing. From these results, it became apparent that *BamHI* was cleaving at a non-specific site upstream if the *EcoRI* site. Double cleavage by *BamHI* resulted in re-circularization of the vector backbone. To overcome this problem single digests were carried out. This involved an initial 15 min digest with *EcoRI* followed by a 5 min digest with *BamHI.* Using this approach positive clones were obtained.

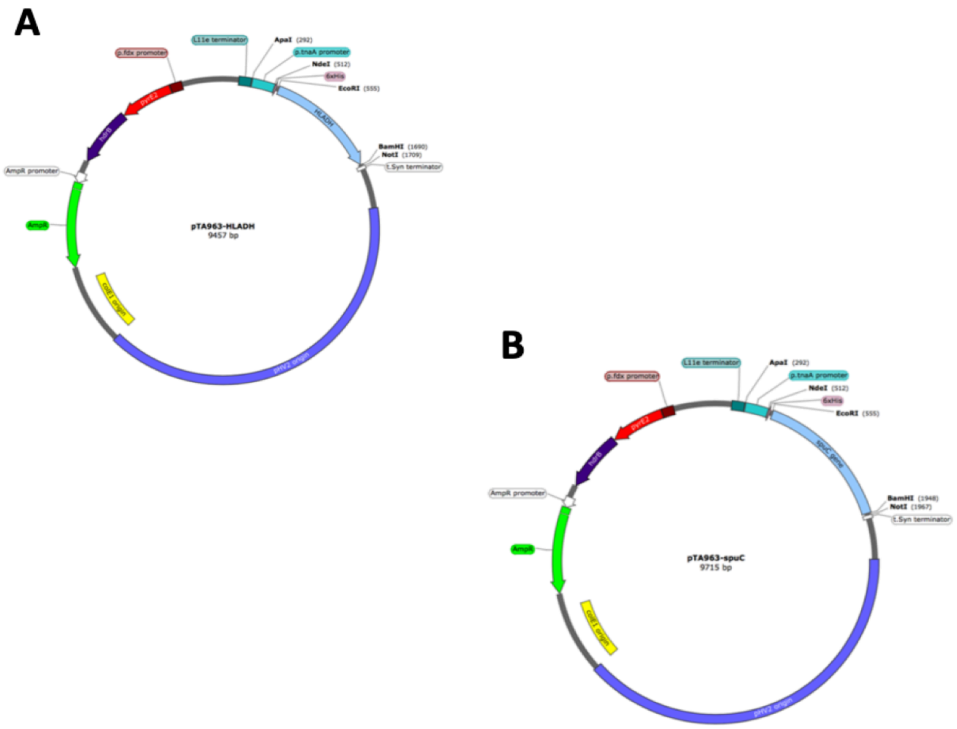


Figure 3.5| Resulting constructs from cloning experiments.
(A). Plasmid construct containing the codon optimised HLADH gene under the *tna*A promoter; (B) Plasmid construct containing the codon optimised *spu*C under the *tna*A promoter.

3.5 Expression of synthetic genes in *H. volcanii*

Two *H. volcanii* expression systems were investigated for the soluble expression of HLADH and *He*WT: *H. volcanii* H1895 and *H. volcanii* H1325. In the case of HLADH, both expression systems yielded insoluble protein. This is evident in Figure 3.6, which compares the expression profile of both systems directly the wild type strains. In order to improve the solubility of the expressed protein, different expression strategies were investigated. Previous publications outlining conditions for optimal gene expression under control of the *tna*A promoter served as a starting point.[15] Based on these reports it was found that the induction of protein expression using L-tryptophan induces concomitant expression of the native tryptophanase gene *tna*A in *H. volcanii*. Hence, *H. volcanii* is able to metabolise the added L-tryptophan over time[40]. This lead to an optimized two-step induction protocol, which involved the addition of L-tryptophan (3 mM) when the cells reached and OD_{600} of 0.5. After 60 min of incubation 45 °C, 200 rpm, a second induction was carried out with the addition of L-tryphophan to a final concentration of 4.5 mM. The cultures were incubated under the same conditions for an additional 60 min and the cells were harvested by centrifugation at 4,500 rpm for 15 min at 4 °C. Despite these efforts, soluble protein expression was not obtained.

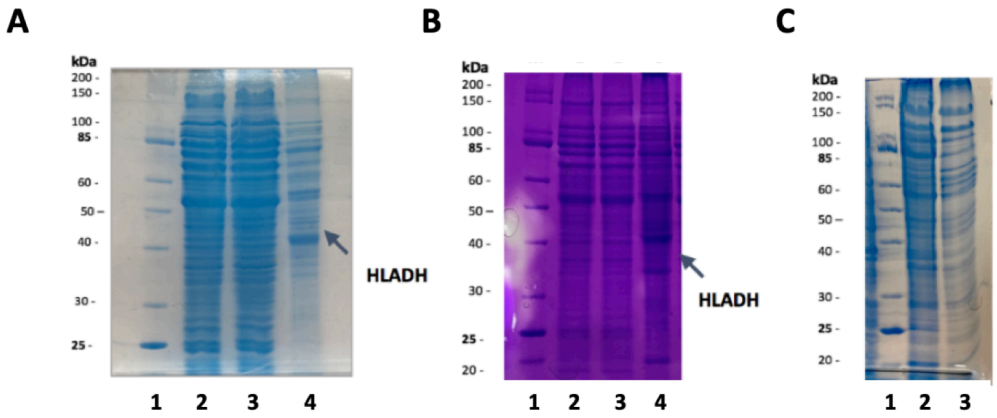


Figure 3.6| SDS-PAGE visualization of HLADH following expression in *H. volcanii* H1895 (A). Lane 1: Unstained Protein Standard, Broad Range (10-200 kDa), **Lane 2:** *H. volcanii* H1895 HLADH supernatant (cells resuspended in buffer containing no salt), **Lane 3:** *H. volcanii* H1895 HLADH supernatant (cells resuspended in buffer containing 3 M KCl), **Lane 4:** *H. volcanii* H1895 HLADH pellet. **SDS-PAGE visualization of HLADH following expression in *H. volcanii* H1325 (B)**. **Lane 1:** Unstained Protein Standard, Broad Range (10-200 kDa), **Lane 2:** *H. volcanii* H1325 HLADH supernatant (cells resuspended in buffer containing no salt), **Lane 3:** *H. volcanii* H1325 HLADH pellet (resuspended in buffer containing 3 M KCl) **Lane 4:** *H.x volcanii* H1325 HLADH pellet. **SDS-PAGE visualization of pellets resulting for *wild type* strains (C) Lane 1:** Unstained Protein Standard, Broad Range (10-200 kDa**), Lane 2:** *H. volcanii* H1895 supernatant, **Lane 3:** *H. volcanii* pellet H1325 supernatant. Molecular masses in kDa are indicated on the left..

In contrast, the expression of *He*WT in both *H. volcanii* expression systems yielded more favourable results. Analysis of the resulting crude extracts by SDS-PAGE proved difficult to interpret due to the high level of native protein expression exhibited by the host strains. The crude extracts were therefore tested for transaminase activity using the standard kinetic assay, in which the production of acetophenone was detected during the first five minutes of reaction. These results indicated successful expression of the target enzyme in a soluble and biologically active form. To further confirm these results, the enzyme was purified by affinity chromatography using a 1 mL HisTrap FF column. Starting from approximately 3.3 g of wet cell pellet it was possible to obtain 0.2 mg (0.7 mg/L cell culture) of pure protein.

A comparative study was subsequently carried out in which the expression of the native *spuC* gene in *E.coli* BL21(DE3) was directly compared to expression in the *H. volcanii* expression system. Expression was routinely carried out in auto induction media according to procedures previously described by Cerioli *et al*. and the enzyme was purified by affinity chromatography, again using a 1 mL HisTrap FF column.[41] Starting from approximately 4 g of wet cell pellet it was possible to obtain 16.5 mg (50 mg/L cell culture) of pure protein. Based on these results it is evident that *E.coli* BL21(DE3) is a superior host for the high level production of *He*WT.

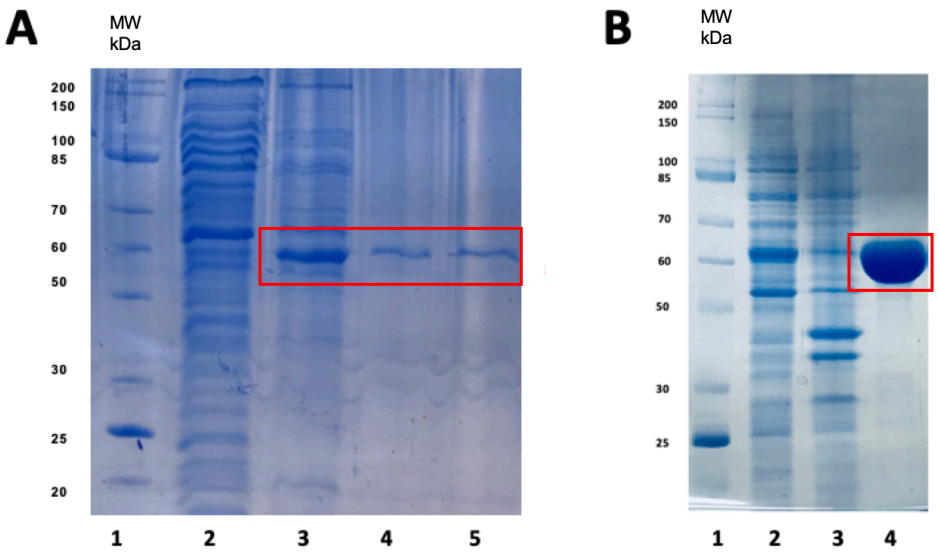


Figure 3.7 SDS-PAGE visualization of *He*WT following expression in *Haloferax volcanii* H1895 (A). Lane 1: Unstained Protein Standard, Broad Range (10-200 kDa), **Lane 2:** *H. volcanii* H1895 *He*WT supernatant (cells resuspended in buffer containing no salt), **Lane 3:** *H. volcanii* H1895 *He*WT pellet **Lane 4-5:** Purified fractions showing the presence of a band corresponding to the molecular weight of *He*WT (~50.4 kDa). **SDS- PAGE visualization of *He*WT following expression in *E.coli* BL21(DE3) (B) Lane 1:** Unstained Protein Standard, Broad Range (10-200 kDa), **Lane 2:** *E.coli* BL21(DE3)Star *He*WT supernatant **Lane 3:** *E.coli* BL21(DE3)Star *He*WT pellet **Lane 4-6:** Purified fractions showing the presence of a band corresponding to the molecular weight of *He*WT (~54 kDa). Molecular masses in kDa are indicated on the left.

4.0 Conclusions

The use of *H. volcanii* as a non-conventional host for the high-level expression of enzymes used in biocatalytic processes was investigated. For this purpose two enzymes of industrial, an ω-transaminase from *H. elongata* and an alcohol dehydrogenase from Horse Liver, were selected for expression trials.

Preliminary expression of the native *spuC* gene, encoding the *H. elongata* ω-transaminase, resulted in the production of an inactive enzyme. Attention then focussed on the design of synthetic genes encoding the target enzymes. Codon optimization was performed by choosing only codons preferentially used in *H. volcanii*. These genes were synthesized chemically and cloned into the pTA963 expression vector. The resulting constructs were used to transform *H. volcanii* H1895 and H1325 strains and protein expression was carried out under different conditions. In the case of HLADH an insoluble and inactive protein was expressed. More significant results were obtained following the expression of the optimized *spuC* gene in *H. volcanii*. The protein was obtained (0.7 mg/L cell culture) in a soluble and biologically active (1.3 U/mg) form following a one-step purification using Nickel Affinity Chromatography. While these results are significant, the expression of *He*WT in *H. volcanii* is not comparable to the high levels of recombinant protein obtained from the *E.coli* BL21(DE3) expression system.

Before embarking on this study, it was predicted tha*t H. volcanii* cells would lyse by osmotic shock upon the addition of a lysis buffer containing no salt. In such an environment, it was expected that native halophilic proteins would precipitate out of solution leaving the target enzyme active and in solution. Such features are invaluable from an industrial perspective as they would eliminate the need for cell disruption and time-consuming purification steps. Surprising, these features were not observed during the study. In spite of the use of a lysis buffer containing no salt, *H. volcanii* cells required disruption by means of sonication. Moreover, the majority of proteins native to *H. volcanii* remained in

solution even in the absence of molar concentrations of salt. Based on these findings, the use of *H. volcanii* as an alternative host for the production of enzymes of industrial interest presents no significant advantages over traditional expression systems such as *E.coli*. As a result, further development of *H. volcanii* as a platform for the expression of recombinant proteins will no longer be considered within the scope of this thesis.

References

1. Woese, C. R. & Fox, G. E. Phylogenetic structure of the prokaryotic domain: The primary kingdoms. **74**, 5088–5090 (1977).

2. Allers, T. & Mevarech, M. Archaeal genetics - The third way. *Nat. Rev. Genet.* **6**, 58–73 (2005).

3. Barns, S. M. et al. Perspectives on archaeal diversity, thermophily and monophyly from environmental rRNA sequences. **93**, 9188–9193 (1996).

4. Deppenmeier, U. The unique biochemistry of methanogenesis. *Prog. Nucleic Acid Res. Mol. Biol.* **71**, 223–283 (2002).

5. Oren, A. Diversity of halophilic microorganisms: Environments, phylogeny, physiology, and applications. *J. Ind. Microbiol. Biotechnol.* **28**, 56–63 (2002).

6. Oren, A. & Ventosa, A. Benjamin Elazari Volcani (1915-1999): sixty-three years of studies of the microbiology of the Dead Sea. *Int. Microbiol.* **3**, 195–198 (1999).

7. Wheelis, M. L., Woese, C. R. & Kandler, O. Towards a natural system of organisms: proposal for the domains Archaea, Bacteria, and Eucarya. *Proc. Natl. Acad. Sci. U. S. A.* **87**, 4576–4579 (1990).

8. Soppa, J. Ploidy and gene conversion in archaea. *Biochem. Soc. Trans.* **39**, 150–154 (2011).

9. Hartman, A. L. et al. The complete genome sequence of Haloferax volcanii DS2, a model archaeon. *PLoS One* **5**, (2010).

10. Fukuchi, S. et al. Unique amino acid composition of proteins in halophilic bacteria. *J. Mol. Biol.* **327**, 347–357 (2003).

11. Eichler, J. & Maupin-Furlow, J. Post-translation modification in Archaea: Lessons from Haloferax volcanii and other haloarchaea. *FEMS Microbiol. Rev.* **37**, 583–606 (2013).

12. Guan, Z. et al. Protein glycosylation as an adaptive response in Archaea: Growth at different salt concentrations leads to alterations in Haloferax volcanii S-layer glycoprotein N-glycosylation. *Environ. Microbiol.* **14**, 743–753 (2012).

13. Lam, W. L. & Doolittle, W. F. Mevinolin-resistant mutations identify a promoter and the gene for a eukaryote-like 3-hydroxy-3-methylglutaryl-coenzyme A reductase in the archaebacterium Haloferax volcanii. *J. Biol. Chem.* **267**, 5829–5834 (1992).

14. Allers, T. et al. Improved strains and plasmid vectors for conditional overexpression of His-tagged proteins in Haloferax volcanii. *Appl. Environ. Microbiol.* **76**, 1759–1769 (2010).

15. Allers, T. Overexpression and purification of halophilic proteins in Haloferax volcanii. *Bioeng. Bugs* **1**, 288–290 (2010).

16. Cline, S. W. et al. Transformation methods for halophilic archaebacteria. *Can. J. Microbiol.* **35**, 148–152 (1989).

17. Holmes, M. L. & Dyall-Smith, M. L. A plasmid vector with a selectable marker for halophilic archaebacteria. *J. Bacteriol.* **172**, 756–761 (1990).

18. Allers, T. & Ngo, H. P. Genetic analysis of homologous recombination in Archaea: Haloferax volcanii as a model organism. *Biochem. Soc. Trans.* **31**, 706–709 (2003).

19. Bitan-Banin, G., Ortenberg, R. & Mevarech, M. Development of a Gene Knockout System for the Halophilic Archaeon. *J. Bacteriol.* **185**, 772–778 (2003).

20. Rosano, G. L. & Ceccarelli, E. A. Recombinant protein expression in Escherichia coli: Advances and challenges. *Front. Microbiol.* **5**, 1–17 (2014).

21. Mamat, U. et al. Detoxifying Escherichia coli for endotoxin-free production of recombinant proteins. *Microb. Cell Fact.* **14**, 1–15 (2015).

22. Romanos, M. A., Scorer, C. A. & Clare, J. J. Foreign gene expression in yeast: a review. *Yeast* **8**, 423–488 (1992).

23. Buckholz, R. G. & Gleeson, M. A. G. Yeast systems for the commercial production of heterologous proteins. *Bio/Technology* **9**, 1067–1072 (1991).

24. The, S. H., Fong, M. Y. & Mohamed, Z. Expression and analysis of the glycosylation properties of recombinant human erythropoietin expressed in Pichia pastoris. *Genet. Mol. Biol.* **34**, 464–470 (2011).

25. Berger, I., Fitzgerald, D. J. & Richmond, T. J. Baculovirus expression system for heterologous multiprotein complexes. *Nat. Biotechnol.* **22**, 1583–1587 (2004).

26. Hollister, R. J. & Jarvis, D. L. Engineering lepidopteran insect cells for sialoglycoprotein production by genetic transformation with mammalian 1,4-galactosyltransferase and 2,6-sialyltransferase genes. *Glycobiology* **11**, 1–9 (2001).

27. Hacker, D. L. & Balasubramanian, S. Recombinant protein production from stable mammalian cell lines and pools. *Curr. Opin. Struct. Biol.* **38**, 129–136 (2016).

28. Fernandez, J. M. & Hoeffler, J. . . *Gene Expression Systems. Using nature for the art of expression*. (Academic Press, San Diego 1999, 1999).

29. Gomes, A. R., Byregowda, S. M., Veeregowda, B. M. & Balamurugan, V. An Overview of Heterologous Expression Host Systems for the Production of Recombinant Proteins. *Adv. Anim. Veterynary Sci.* **4**, 346–356 (2016).

30. Tripepi, M. et al. Haloferax volcanii cells lacking the flagellin FlgA2 are hypermotile. *Microbiol. (United Kingdom)* **159**, 2249–2258 (2013).

31. Albers, S. V. & Pohlschröder, M. Diversity of archaeal type IV pilin-like structures. *Extremophiles* **13**, 403–410 (2009).

32. Strillinger, E. et al. Production of halophilic proteins using Haloferax volcanii H1895 in a stirred-tank bioreactor. *Appl. Microbiol. Biotechnol.* **100**, 1183–1195 (2016).

33. Allers, T. et al. Development of Additional Selectable Markers for the Halophilic Archaeon. *Appl. Environ. Microbiol.* **70**, (2004).

34. Quaglia, D. et al. His-tagged Horse Liver Alcohol Dehydrogenase: Immobilization and application in the bio-based enantioselective synthesis of (S)-arylpropanols Dedicated to Prof. Gianfranco Cainelli on the occasion of his 80th birthday. *Process Biochem.* **48**, 810–818 (2013).

35. Camps, M. & Loeb, L. A. Use of Pol I-Deficient E. coli for Functional Complementation of DNA Polymerase. in *Directed Enzyme Evolution* 11–18 (Humana Press).

36. Timpson, L. M. et al. Characterization of alcohol dehydrogenase (ADH12) from Haloarcula marismortui, an extreme halophile from the Dead Sea. *Extremophiles* **16**, 57–66 (2012).

37. Timpson, L. M. et al. A comparison of two novel alcohol dehydrogenase enzymes (ADH1 and ADH2) from the extreme halophile Haloferax volcanii. *Appl. Microbiol. Biotechnol.* **97**, 195–203 (2013).

38. Schätzle, S. et al. Rapid and sensitive kinetic assay for characterization of ω-transaminases. *Anal. Chem.* **81**, 8244–8248 (2009).

39. Soppa, J. Compilation of Halobacterial Protein Coding Genes, the Halobacterial Codon Usage Table and its Use. *Syst. Appl. Microbiol.* **16**, 725–733 (1993).

40. Large, A. et al. Characterization of a tightly controlled promoter of the halophilic archaeon Haloferax volcanii and its use in the analysis of the essential cct1 gene. *Mol. Microbiol.* **66**, 1092–1106 (2007).

41. Cerioli, L. et al. Characterization of a novel amine transaminase from Halomonas elongata. *J. Mol. Catal. B Enzym.* **120**, 141–150 (2015).

Acknowledgements

First and foremost, I would like to thank my supervisor, Professor Francesca Paradisi, for giving me the opportunity to be a part of an incredible team over the last three years. Under your guidance, I have overcome so many challenges, both personally and professionally, that up until a few year ago I really didn't think were possible. You have always encouraged to be strong and believe in my work and for that I will be forever grateful.

To my amazing colleagues, David, Martina, Maria, Lidia, Ana, Valentina, Chirs, Nourah and Matteo. Working in the Paradisi group has been, without a doubt, one of the most valuable and enjoyable of experiences. It has been honour to work with such a talented group of people in an environment that has always encouraged me to reach my goals, no matter what obstacles were in the way. Thank you all for sharing this journey with me, for your unconditional support, and most importantly for making me smile each and every day. A special thanks also to the members of the O'Reilly group who have been so accommodating with the use of their equipment during the course of my PhD.

To Vera and Zé, thank you for making my time in Nottingham so enjoyable. This journey would have been a lot more challenging without you. A special thanks also to my friends in Ireland for putting up with my absence over the last few months.

Finally, I would like to thank my Mum & Dad, who have been with me every step of way. None of this would have been possible without you both!